

ALERT Geomaterials

Alliance of laboratories in Europe for Research and Technology

Aussois, September 28 – 30, 2026

37th ALERT Workshop / POSTER SESSION



Booklet of abstracts

Editors: Nadia Benahmed
Antoine Wautier

(INRAE, France)

The Alliance of Laboratories in Europe for Education, Research and Technology

37th ALERT Workshop

Poster Session

Aussois 2026

Editors:

Nadia Benahmed
Antoine Wautier

(INRAE, Aix-en-Provence – France)

ISBN: 978-2-9584769-6-0

Welcome Address

Dear colleagues,

We are pleased to welcome you to Aussois and to our 37th ALERT Workshop and School. As always, it is an exciting time for us to continue to meet and bring together inspired people for fruitful days with interesting, stimulating discussions, exchange of knowledge and experience on Geomechanics. Presentations of recent advances offer the chance to get up-to-date and to remain at the cutting edge.

We would like to express our thanks to all of you who contributed to the success of this poster session. The number of confirmed posters this year reached a new record with 66 contributions!

We wish you a good workshop and school experience and a pleasant stay in Aussois! Kind regards,

Antoine Wautier and *Nadia Benahmed*

Contents

Fractal Characterization of Sand-Geomaterial Interface Response: Material Geometry Effects **2**

Abdulmuttalip Ari, Suat Akbulut

The Role of the Subgrade Soil in the Road of the Future **4**

Sebastian Ullmann, Ivo Herle

Advancing Thermo-Chemo-Mechanical Modelling of swelling clays within a double structure framework **6**

Han Ming Lai, Lidija Zdravkovic, David M. Potts, Matthew Kirby

Impact-loading debris avalanches in unsaturated slopes: modelling the cascading processes via MPM **8**

Raffaele Orazzo, Sabatino Cuomo, Rita Ciaglia, Mario Martinelli, Rosa Maria Stefania Maiorano, Stefano Aversa

Numerical modelling of centrifuge tests on flow-like landslides using MPM **10**

Rita Ciagla, Sabatino Cuomo, Angela Di Perna, Mariagiovanna Moscariello, Mario Martinelli

Interaction of flowslides with fixed and movable barriers: centrifuge tests on Baskarp and Vesuvian soils **12**

Mariagiovanna Moscariello, Sabatino Cuomo, Angela Di Perna, Rita Ciaglia, Mario Martinelli

Interplay between Pore and Solid Tortuosities of Synthetic Rocks **14**

Alexandre Sac-Morane, Maria Olarte-Garzon, Jean-Michel Pereira, Philipp Braun

Shifted interface approach for nonsmooth frictional and hydraulically conductive interfaces in porodynamic media **16**

David Riley, Guglielmo Scovazzi, Ioannis Stefanou

Modeling the Morphological Evolution of Railway Ballast Using a Core–Shell Bonded-Cell Approach **18**

Jitinun Prommarin, Peerapong Jitsangiam, Mathieu Renouf, Emilien Azéma

A shifted interface approach for fully coupled 3D poroelastodynamics with non-smooth frictional discontinuities **20**

Clément Rey, David Riley, Ioannis Stefanou

Discrete Compliant-Element Method **22**

Mukesh Singh Bisht, Vincent Richefeu

Influence of particle gradation on the surface erosion resistance of MICP-treated soils **24**

Angelo Giuseppe Tarullo, Michele Calvello, Tae-Hyuk Kwon, Marcopolo Alcantara Fuentes, Juyeon Jeong

Reservoir-Induced Hydromechanical Response in a Homogeneous Earth Dam from Coupled MASW-ERT In-situ Measurements **26**

Yogarish Narasinga Raja, Sourav Sarkar, P Anbazhagan

An integrated analytical framework for the thermo-mechanical response of groups of energy piles subjected to multi-axial **28**

Rosario Mattia Moniaci, Tomáš Mladý, Gianvito Scaringi

Robotic Automated Specimen Preparation (RASP): Specimen Homogeneity and Reproducibility in Centrifuge Physical Modelling **30**

Faith Abimaje, Luis Mugele, Tristan Quinten, Miguel Cabrera, Hans Stutz

Terrain Interaction Mechanics of Off-road Heavy-duty Vehicles **32**

Alejandro Secades, Wolfgang Fellin, Manuel Ferdik

Influence of potassium sulfate on the mineralogical and physicochemical properties of an expansive clay **34**

Alan Ribeiro-Santos, Benjamin Dardé, Anh-minh Tang

Fabric Orientation and Liquefaction Susceptibility of Granular Materials **36**

Carolina Castro-Malaver, Manuel Cárdenas-Barrantes, Mathieu Renouf, Emilien Azéma, Carlos Ovalle

Active geogrids – a new approach to controlling earthquake wave propagation **38**

Lutf Al-Subari, Ali Akbar, Raul Fuentes

Numerical Simulation of CPT in sands using Finite Element Analysis ... **40**

Ana Karine Santos Dantas, Arash Alimardani Lavasan

Permeability Assessment of Weathered and Poorly Graded Rockfill: Experimental Testing and Numerical Validation **42**

Carlos Laina Gómez, Diego Escudero-Merino, Mario Caballero-Ezquerro, Enrique Asanza-Izquierdo

Assessment of inclined dry soil cover systems for reactive mine waste in boreal climatic conditions **44**

Abdalla Saafan, Jasmina Toromanovic, Jan Laue, Christian Maurice

Grain morphology effects on liquefaction-driven submarine landslide **46**

Govind Mishra, Vanessa Magnanimo, Stefan Luding, Hongyang Cheng

Modeling of the poro-viscoplastic behavior of the Callovo-Oxfordian claystone **48**

Corentin Donius, Philipp Braun, Maxime Pierre, Carlos Plúa, Siavash Ghabezloo

A coordinate-free elliptic general interface model for geomaterial interphases **50**
Alexandros Stathas, Matthias Neuner

Investigation of Air Fluidization during Intruder Penetration in Sand ... **52**
Bowen Wang

Paths to critical state under partial drainage **54**
Jochen Zürn, Luis Mugele, Hans Henning Stutz

Hybrid DLVO/CGMD approach for THM modelling of clay particles in COx formation **56**
Alissar Alrifai, Alice Di Donna, Majdouline Laanaiya

On the control of Groningen's induced seismicity: stochastic and discrete-time extensions **58**
Diego Gutiérrez-Oribio, Ioannis Stefanou

Extending the H-model to Mechanics of Permafrost **60**
Vincent Guigonnet, Jérôme Aubry, François Nicot

Increase in granular drag forces near boundaries **62**
Mahsa Azizi, Pierre Rognon, François Guillard

Testing the validity of a nonlinear kinematic hardening model with data-driven identification **64**
Ludovic Druette, Jérémy Bleyer, Siavash Ghabezloo, Goustan Bacquaert

Numerical exploration for feasibility of heat storage in the ground via energy piles **66**
Mattia Garza, Ritesh Gupta, Alice Di Donna

Neural constitutive models under hard thermodynamic constraints and differentiable finite-element solvers **68**
Edoardo Fabbrini, Vincent Acary, Filippo Masi

Modeling of sorption-induced deformations of porous materials **70**
Jingyi Leng, Patrick Dangla, Laurent Brochard, Matthieu Vandamme

Implementation of rough contact models in modelling the direct shear behaviour of Crushed Waste Glass **72**
Xinran Zhang, Yi Pik Helen Cheng

Crushing behavior of sand grains with Voronoi-based heterogeneous initial damage: a peridynamics investigation **74**
Guangzhi Li, Takashi Matsushima

Deterioration and Damage Features of Rock Masses within the Fluctuating Zone of Three Gorges Reservoir Area under Complex Dynamic Water Conditions **76**
Zhiqiang Yi, Yueping Yin, Gonghui Wang, Shouding Li, Tianqiao Mao, Xuebing Wang

Geobattery: a dimensionless criterion for seasonal heat storage in flooded mine workings **78**
Ali Ahmadi

Grain morphological effects on the pullout response of soil-geogrid interface **80**
Amrisha Khandelwal, Debayan Bhattacharya, J.T. Shahu, Manoj Datta

THCM Feedbacks In Volcanic Edifices: Bridging Transport-Driven Alteration To Mechanical Factor Of Safety **82**
Jens Niclaes, Poulet Thomas, Delmelle Pierre, Rattez Hadrien

Gravity-driven granular rheology with cloned particles and its impact behaviour with safety measures **84**
Prity Dhanai, Debayan Bhattacharya

Bio-Inspired Cone Pressuremeter propulsion as active soil-structure interface problem in planetary regolith exploration **86**
Harsha Vardhan Kurugodu, Debayan Bhattacharya, Prashanth Vangla, David Frost

A data-driven machine learning approach for decision-making in the context of abandoned underground mines **88**
Fernan Villanueva Zavala, Lina Maria Guayacan Carrillo, Nathalie Conil, Jean Sulem, Jean-Michel Pereira

Scaling-Law-Based Design of a Laboratory Model for Fluid Injection-Induced Earthquakes **90**
Yubao Zhou, Ioannis Stefanou

Spontaneous imbibition and pore throat size distribution in volcaniclastic rocks: implications for UGS **92**
Gimena Biene, Sandra Orlandi, Diego Manzanal

Adaptive Mesh Refinement for Phase-Field Fracture **94**
Prince Kitembo, Philipp Braun, Ana Loyola, Diego Manzanal, Jean-Michel Pereira, Miguel Stickle

Development and Verification of Coupled OpenFOAM–YADE CFD–DEM Solvers for Particle–Fluid Systems **96**
Manikandan Valliappan, Eleni Gerolymatou

Geomechanical Heterogeneity of a Volcaniclastic Formation: Potential Effects on Geological CO_2 Storage **98**
Maximiliano Cortés, José Allard, Sandra Orlandi, Diego Manzanal

A proposed Tuffaceous Index (Gs-Z) for evaluating volcaniclastic reservoirs **100**
Pablo Vidal, Jose Allard, Diego Manzanal

Normal–tangential coupling in elastoplastic contacts enables stress recovery in cyclically sheared granular materials **102**
Min Deng, Yi Pik Cheng, Lianheng Zhao

A Hydromechanical eTANN Macroelement for Translational Slides in Partially Saturated Slopes **104**
Andres Macias-Gutierrez, Jean Vaunat, Yeudy Felipe Vargas-Alzate

Multiscale Experimental and Analytical Validation of a DEM Framework for Compressibility of Rockfill **106**
Cristian Maurer, Carlos Ovalle, Esteban Saez

From Clay to Tailings: Evaluation of the Terracota Model for Liquefiable Iron Ore Tailings **108**
Pablo Dos Santos Cardoso Coelho, Fangzhou Liu, Gordon Ward Wilson, Paul Simms, Gonzalo Zambrano Narvaez

Learning Thermo-Hydro-Mechanical Coupled Fracture Permeability Evolution via Physics-Informed Generative AI in Geotherma **110**
Jiangmei Qiao, Mengwei Liu, Xi Hua, Shengzong Xu, Xuhai Tang

Geomechanical Characterization of Biopolymer-Treated Kaolinite: Plasticity and Undrained Shear Strength Evolution **112**
Milad Jabbarzadeh, Arash Alimardani Lavasan

Experimental and Numerical Study of Erosion in Chalk Reservoirs **114**
Tatsuki Komatsubara, Alexandre Lavrov, Euripides Papamichos, Roar Egil Flatebø

New aspects of inclined surface flows of photoelastic disks **116**
Fu-Ling Yang

Enhancing the Soil–Anchor Interface of Screwed Pile Anchors in Loose Sand through MICP Treatment **118**
Xuanyi Chen, Frank Mcdermott, Shane Donohue, Budi Zhao

A new interface shear method for investigation of the influence of lateral stress components **120**
Sabine Gehring, Hans Henning Stutz

Effect of contact friction variability on granular behavior **122**
Nabil Younes, Saeid Nezamabadi, Franck Radjai

DEM Modeling of Crack Formation and Propagation in Fine-Grained Soils **124**
Zahra Mousavi, Arash Alimardani Lavasan

Modelling Wetting–Drying Effects in Unsaturated Soils: The Role of Expressions in Predicting Relative Permeability. **126**
Qinghexing Kong, Catherine O'Sullivan, Katerina Tsiampousi, Hao Wang

The role of geological uncertainties in the modelling of deep-seated gravitational slope deformations **128**
Maria Honisch, Barbara Schneider-muntau

Characterisation of drying-induced cementation and shearing behaviour of biopolymer-treated sand using X-ray tomography **130**
Mhlengi Khaya Luke Masango, Hui Zhang, Budi Zhao

Integrated multi-method assessment of rainfall-induced debris flows 132
Giulia La Porta, Marina Pirulli, Giuseppe Bausilio, Diego Di Martire, Ascanio Rosi, Elisa Saler, Luca Badin, Andrea Gennaro, Francesca Da Porto, Carlo Esposito

Fractal Characterization of Sand-Geomaterial Interface Response: Material Geometry Effects

Abdulmuttalip Ari[1], Suat Akbulut[1]
[1] Yildiz Technical University
talipari@yildiz.edu.tr

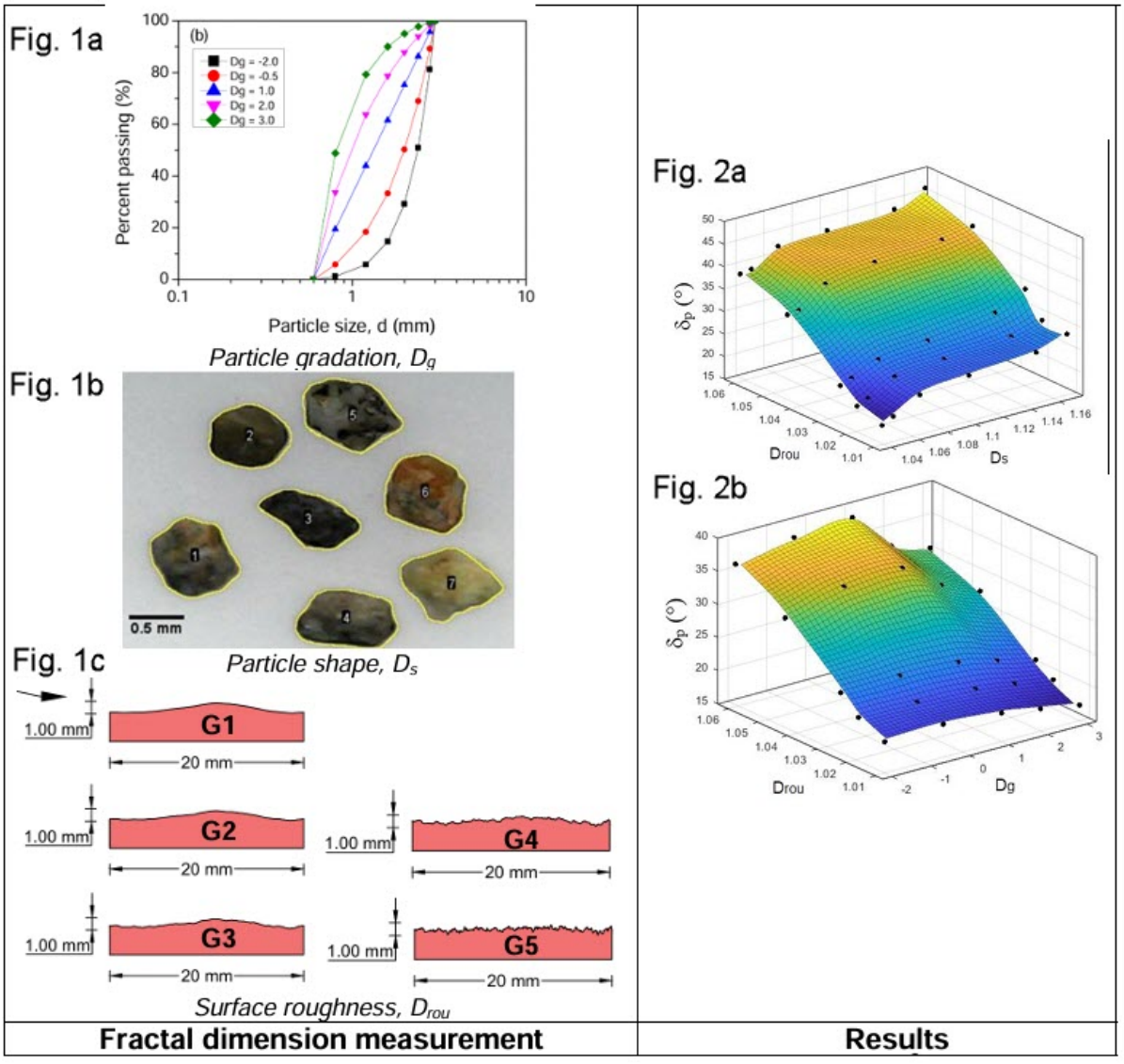
1. Motivation: The mechanical response of sand-geomaterial interfaces is a governing factor in the design of critical geotechnical structures. In practice, both sand particles and structural surfaces exhibit inherent geometric irregularities across multiple scales [1,2]. Furthermore, the varying gradations of sand assemblies introduce additional complexity to the interface fabric [3]. This study employs fractal theory as a mathematical framework to quantify these multi-scale irregularities. By implementing fractal descriptors for shape, gradation, and roughness, this research establishes a link between fundamental material geometry, macroscopic interface behavior, and the evolution of micro-mechanical fabric [4].

2. Approach: Interface shear tests were conducted using the Discrete Element Method (DEM), calibrated against experimental results from a custom-made transparent interface shear box. The study utilizes three distinct fractal dimensions to characterize the interface: - Dg (Gradation): Measures the complexity of the particle size distribution (Fig. 1a) - Ds (Shape): Quantifies the overall angularity and irregularity of sand particles (Fig. 1b). - Drou (Roughness): Characterizes the irregularity of the geomaterial surface (Fig. 1c). The analysis focuses on the evolution of internal variables during shearing, specifically the coordination number (Cn) and contact normal anisotropy (an), to provide a micro-mechanical explanation for the observed interface shear strength.

3. Results: The findings demonstrate that fractal geometry provides a robust framework for predicting interface response. The DEM results reveal that increasing Ds and Drou significantly enhances the friction angle by promoting higher levels of contact anisotropy (Fig. 2a). A significant result is the bell-shaped relationship identified between the gradation fractal dimension (Dg) and the interface friction angle, indicating that an optimal range of gradation complexity exists for maximum shear strength (Fig. 2b).

References

[1] A. Fatin, M. R. Coop, and V. N. Georgiannou. "Effect of particle shape on the mechanical behavior of natural sands." Journal of Geotechnical and Geoenvironmental Engineering 142.12 (2016): doi.org/10.1061/(ASCE)GT.1943-5606.000156904016071.
[2] W. Jianfeng, J. E. Dove, and M. S. Gutierrez. "Anisotropy-based failure criterion for interphase systems." Journal of geotechnical and geoenvironmental engineering 133.5 (2007): doi.org/10.1061/(ASCE)1090-0241(2007)133:5(599)
[3] C. Wei-Bin, et al. "Metaheuristic model for the interface shear strength between granular soil and structure considering surface morphology." Computers and Geotechnics 135 (2021): doi.org/10.1016/j.compgeo.2021.104141
[4] A. Abdulmuttalip, and S. Akbulut. "Investigation of sand-geomaterial interface response using fractal theory: particle shape, gradation and surface roughness effects." Advanced Powder Technology 36.11 (2025): doi.org/10.1016/j.apt.2025.105072



Simulation of fractal geometry of materials

The Role of the Subgrade Soil in the Road of the Future

Sebastian Ullmann[1], Ivo Herle[1]
[1] TU Dresden, Institute of Geotechnical Engineering
sebastian_pierre.ullmann@tu-dresden.de

The stiffness of the subgrade soil significantly governs the load-bearing capacity and the deformation behavior of pavements. It is strongly influenced by the state of the subgrade soil such as the stress condition, density, fabric and hydraulic conditions. Within the development of a digital twin of the road (Collaborative Research Centre Transregio 339), one research objective is to capture the nonlinear and inelastic behavior of the subgrade soils using advanced constitutive models. A prerequisite for this is a detailed understanding of how the subgrade soil is loaded under heavy truck traffic.

Preliminary numerical investigations indicate that the subgrade soil beneath highway pavements experiences vertical stress variations in the range of 10 to 15 kPa under heavy truck loading. Moreover, the structural response is predominantly controlled by the near-surface subgrade soil, extending to approx. 1m below the subgrade soil surface. As a consequence, the near-surface subgrade soil remains at a low stress level, governed by the overburden pavement, while simultaneously subjected to high-cyclic loading. However, the soil behavior under such low stress levels, especially for mixed-grained soils, remains poorly understood and requires further investigation.

To address this, a sand-fines mixture was investigated through drained triaxial tests under initial confining pressures ranging from 20 to 300 kPa. Remarkably, the friction angle and the dilatancy angle were found to be largely independent of the confining pressure in the low stress range. This unexpected behavior is attributed to the soil fabric. Computed tomography (CT) imaging of the initial state reveals that fine particles form bridge-like structures between coarser grains rather than acting merely as filler. It is hypothesized that these fines, actively provide a lubrication-like effect during loading, explaining the observed stress insensitivity of the macroscopic parameters.

Advanced constitutive models must be both calibrated and validated. While element tests provide a basis for calibrating constitutive model parameters, they are limited in representing the complex soil–structure interaction, which is required for a meaningful validation of the constitutive models and their parameters. To address this issue, a large-scale model test has been developed at the Geotechnical Laboratory of TU Dresden. The experimental setup consists of a cylindrical soil column with a diameter of $D = 1.2$ m, and a height of $H = 1.0$ m, which can be subjected to both monotonic and cyclic loading while allowing to change the groundwater conditions. Comprehensive instrumentation enables the measurement of earth pressures, settlements, pore water pressures, and moisture content.

Advancing Thermo-Chemo-Mechanical Modelling of swelling clays within a double structure framework

Han Ming Lai[1], Lidija Zdravkovic[1], David M. Potts[1], Matthew Kirby[2]
[1] Imperial College London
[2] Nuclear Waste Services (NWS) UK
h.lai23@imperial.ac.uk

The long-term performance of engineered clay barriers in deep geological disposal facilities (GDFs) for radioactive waste depends on the coupled interaction between thermal, hydraulic, mechanical, and chemical processes occurring over geological timescales of radioactive decay. Compacted bentonite, as a highly swelling clay, is widely selected as a buffer material for safe storage of radioactive waste due to its low permeability, swelling capacity, and self-sealing behaviour. However, uncertainties remain regarding its performance under combined thermo-hydro-mechanical-chemical (THM-C) loading, particularly in highly saline groundwater environments, for repository settings close to coastal regions or with evaporite formations. Experimental studies [1] have shown that salinity significantly influences the mechanical, hydraulic, and thermal properties of bentonite, particularly reducing its swelling capabilities and increasing its permeability.

This research presents the development of a chemically coupled constitutive and numerical framework capable of simulating THM-C interactions governing bentonite behaviour important for performance assessment and safe design. The work extends an existing double-structure constitutive formulation, the Imperial College Double Structure Model (ICDSM) [2], by incorporating chemical effects within a continuum framework in which chemical variables influence material response through internal variables representing microstructural behaviour. The principal novelty lies in embedding physico-chemical mechanisms into the microstructural effective stress definition.

Chemical coupling is achieved by linking solute concentration to osmotic suction through the van't Hoff equation, which is subsequently transformed into an equivalent osmotic pressure acting on the microstructural stress state. This approach enables chemical loading to influence mechanical response through modification of microstructure, and subsequently the micro–macro structural interaction. The framework therefore establishes a consistent pathway connecting chemical environment, microstructural evolution, and macroscopic swelling behaviour.

Numerical predictions in this research, obtained from simulations of bentonite swelling tests, demonstrate the capability of the proposed framework to reproduce key experimentally observed trends: (i) increased salinity leading to suppressed swelling pressure, attributed to altered microstructure behaviour. Analysis of the microstructural parameters shows that increasing salinity reduces the void factor (VF), or proportion of microstructure within the clay fabric, indicating decreased interlayer hydration and suppressed microswelling. Model predictions show good agreement with available experimental datasets (e.g. [3]) across a range of dry densities and bentonite types, indicating that chemically induced microstructural stress modification provides a physically meaningful mechanism for representing chemo-mechanical coupling.

This research contributes toward reducing key uncertainties associated with the design and safety assessment of geological disposal systems. This is achieved through introduction of a physically grounded chemo-mechanical coupling embedded within a validated double-structure constitutive framework suitable for finite element implementation. The developed modelling capability underpins evaluation of engineered barrier performance

under complex THM-C boundary conditions, supporting optimisation of buffer design parameters and improving confidence in long-term containment strategies for radioactive waste disposal.

This research receives funding from the Nuclear Waste Services UK and the Imperial College Skempton Scholarship.

References

[1] Dixon, D.A., 2019. Review of the THMC Properties of MX-80 Bentonite. Nuclear Waste Management Organization: Toronto, ON, Canada.

[2] Ghiadistri, G.M., 2019. Constitutive modelling of compacted clays for applications in nuclear waste disposal. PhD Thesis, Imperial College London, UK.

[3] Lloret, A., Romero, E., and Villar, M. V. (2004). FEBEX II Project Final report on thermo-hydro-mechanical laboratory tests.

Impact-loading debris avalanches in unsaturated slopes: modelling the cascading processes via MPM

Raffaele Orazzo[1], Sabatino Cuomo[2], Rita Ciaglia[2], Mario Martinelli[3], Rosa Maria Stefania Maiorano[1], Stefano Aversa[2]

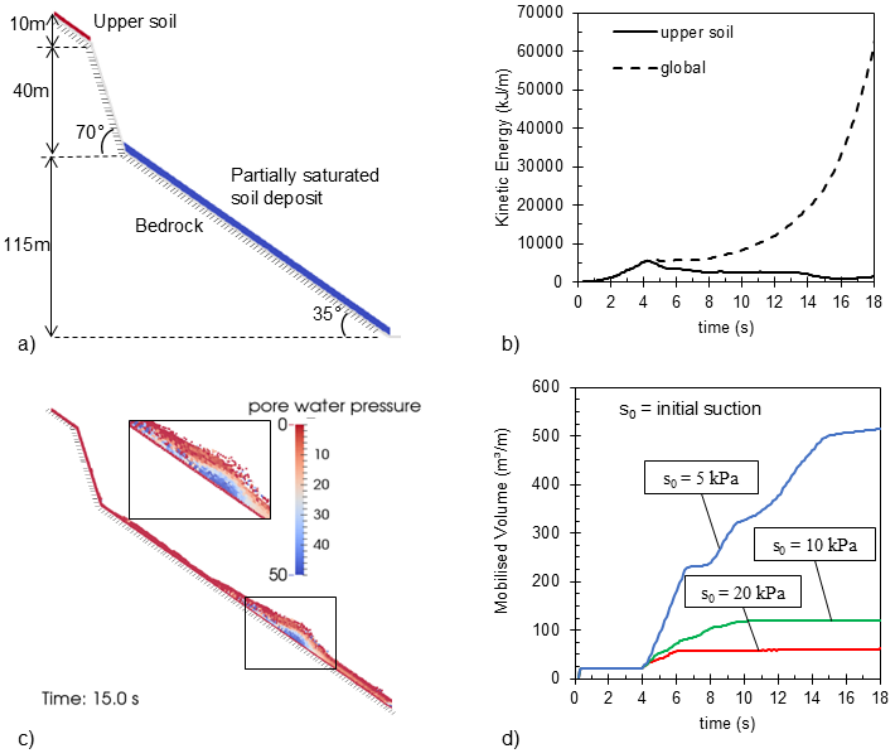
[1] University of Naples Parthenope
[2] University of Salerno
[3] SPERI S.p.A.

raffaele.orazzo001@studenti.uniparthenope.it

Keywords: Modelling, Material Point Method, unsaturated soil, hydro-mechanical coupling, kinetic energy

Debris avalanches (DA) are rapid mass movements which involve partially or fully saturated debris on a steep slope, propagating downslope without lateral confinement [1]. They are among the most destructive geological events, posing severe hazards in urbanized piedmont areas due to their long runout and potential volume increase through bed entrainment. Significant events occurred in May 1998 in the Campania Region in Southern Italy and have been extensively documented. In particular, [2] identified different triggering mechanisms for both debris flows and debris avalanches: among the DAs studied some phenomena occurred at the base of bedrock scarps in correspondence to karst springs, while others were triggered by impact-loading mechanisms at base of bedrock outcrops leading to cascading slope failures. Regarding the latter context, the conditions determining whether a small initial instability arrests or evolves into a catastrophic debris avalanche remain poorly understood. This study proposes a hydro-mechanical framework for impact-induced debris avalanche inception, integrating an energy-based interpretation of the interaction between a moving saturated mass and a downslope unsaturated deposit. To achieve this, an advanced Material Point Method (MPM) [3] model is developed to simulate the coupled evolution of stresses, pore water pressures, and deformations during and after the impact (Figure 1a). The simulations reproduce the loading exerted by the incoming mass and capture the progressive response of the impacted slope. Results indicate that the abrupt deceleration of the impacting mass leads to rapid pore pressure buildup in the impact zone and stress redistribution in subsequent downslope volumes (Figure 1c). The evolution of kinetic energy reveals progressive energy transfer from the moving mass to the impacted soil, which ultimately governs whether the instability is arrested or propagates downslope (Figure 1b). The parametric analysis demonstrates that initial soil suction (s_0) in the impacted slope is the critical parameter controlling debris avalanche inception (Figure 1d). Cases with low initial suction ($s_0 = 5$ kPa) exhibit sustained energy transfer, progressive volume mobilization, and debris avalanche development with large volume amplification factors. In contrast, cases with higher suction rapidly dissipate kinetic energy after impact, arresting the cascading process with limited volume growth. Variations in basal friction angle of the flow material, soil deposit thickness, and initial flow mass size have secondary effects. These findings provide an interpretation of impact-induced debris avalanche inception in unsaturated pyroclastic slopes, offering significant implications for hazard assessment in similar geomorphological contexts.

Acknowledgements: The authors are grateful to Deltares (Delft, The Netherlands) for the collaboration and for hosting Raffaele Orazzo during his PhD research visit. All the MPM simulations were performed using a specific version of Anura3D, developed in-house by Deltares.



a) Slope model; b) kinetic energy-time curves; c) pore water pressure distribution at time=15s; d) mobilised volume in different scenarios.

References

[1] O. Hungr, S. Leroueil, L. Picarelli, (2014), The Varnes classification of landslide types, an update, Landslides, vol. 11, no. 2, pp. 167-194, doi: 10.1007/s10346-013-0436-y.

[2] L. Cascini, S. Cuomo and M. Pastor, (2013), Inception of debris avalanches: remarks on geomechanical modelling, Landslides, vol. 10, no. 6, pp. 701-711, doi: 10.1007/s10346-012-0366-0

[3] M. Martinelli and V. Galavi, (2022), An explicit coupled MPM formulation to simulate penetration problems in soils using quadrilateral elements, Computers and Geotechnics, vol. 145, 104697, doi: 10.1016/j.compgeo.2022.104697

Numerical modelling of centrifuge tests on flow-like landslides using MPM

Rita Ciagla[1], Sabatino Cuomo[1], Angela Di Perna[1], Mariagiovanna Moscariello[1], Mario Martinelli[2]

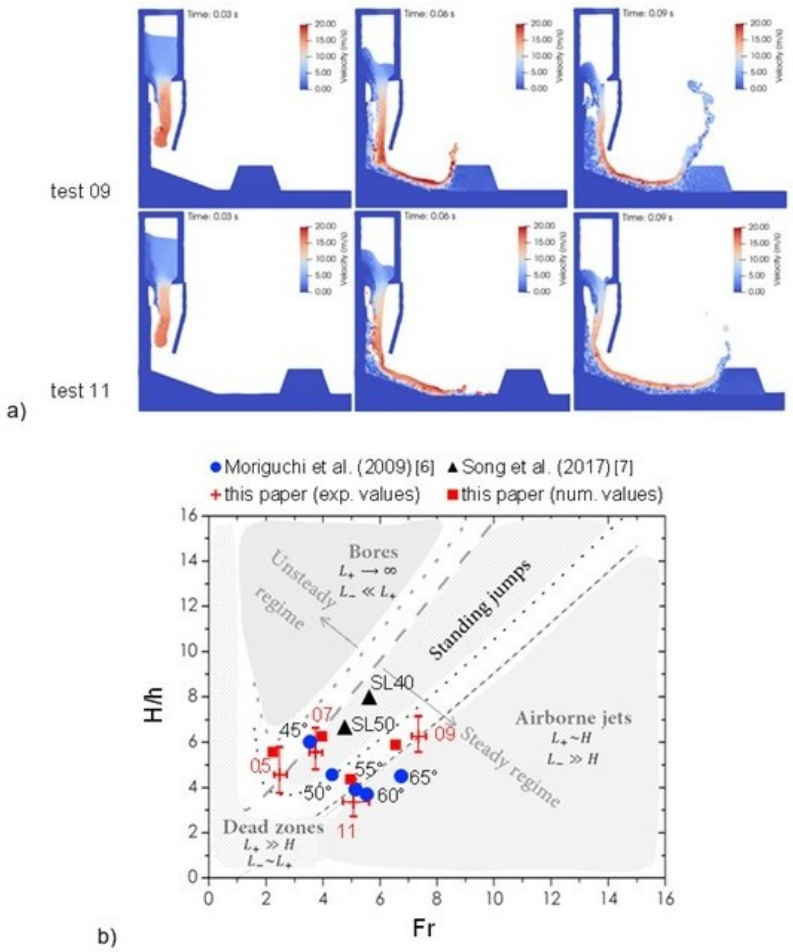
[1] University of Salerno
[2] SPERI Spa

rciaglia@unisa.it

Keywords: Material Point Method, Modelling, Debris Flow, Centrifuge, Barrier, Impact

Flow-like landslides impacting barriers involve complex hydro-mechanical processes, large deformations and rapidly evolving interaction mechanisms that remain challenging to model. This contribution presents the numerical investigation of a series of centrifuge tests performed at the Deltares Geotechnical Centrifuge (Delft, Netherlands) within the EU-funded GEOLAB project, using the Material Point Method (MPM) as the modelling framework. The experimental campaign reproduces the propagation of a saturated natural volcanic silty-sand down a 20° slope and the subsequent impact against a rigid trapezoidal barrier free to slide along its base, for four configurations varying barrier position and released mass. All simulations are performed using a customised version of Anura3D [1], employing a two-phase single-point formulation with explicit time integration and a non-associative Mohr–Coulomb elasto-plastic model for the soil skeleton. This approach naturally handles large deformations and the coupled solid–fluid response of saturated materials, making it particularly suited for flow–barrier interaction problems [2]. The barrier is modelled as a rigid-frictional body free to move along its base. Model calibration follows a two-step back-analysis: first, the saturated hydraulic conductivity (ksat) is identified by minimising the error on barrier final displacement; then, the Young's modulus (E) is refined against the peak kinetic energy of the barrier. The back-analysed ksat spans one order of magnitude across the four tests ($9.81e^{-4}$ to $98.1e^{-4}$ m/s) and is up to three orders of magnitude higher than laboratory values, consistent with porosity increase during rapid shearing [3]. The back-analysed ksat directly governs the energy transfer to the barrier: lower values yield greater barrier displacement and kinetic energy (Fig. 1a). Notably, only a limited portion of the flowing mass effectively contributes to the impact, while the remainder overtops or bypasses the structure. The direct link between ksat and impact intensity is reflected in the flow–barrier interaction mechanisms: for the tested conditions (flow velocities 7–19 m/s, Froude numbers 2.5–7.4), as ksat decreases the dominant regime transitions from bore to standing jump and airborne jet, in agreement with the Faug [4] framework as interpreted by Cuomo et al. (2026) [5] (Fig. 1b). Model validation against flow kinematics and load-cell stress time series confirms satisfactory agreement, demonstrating that MPM provides a physically consistent framework for the design of protective barriers against debris flows.

Acknowledgments: This work was supported by the GEOLAB project, funded by European Union's Horizon 2020 research and innovation programme under Grant Agreement No. 101006512. GEOLAB aims to advance research on critical infrastructure resilience by providing coordinated access to a network of leading European geotechnical research facilities. All the MPM simulations were performed using a specific version of Anura3D, developed in-house by Deltares, Netherlands.



a) MPM-simulated velocity fields for Tests 09 and 11; b) flow–barrier interaction regimes in Fr–H/h space

References

[1] M. Martinelli and V. Galavi, "An explicit coupled MPM formulation to simulate penetration problems in soils using quadrilateral elements," Computers and Geotechnics, vol. 145, p. 104697, 2022, doi: 10.1016/j.compgeo.2022.104697.

[2] S. Cuomo, A. Di Perna, and M. Martinelli, "Material point method (MPM) hydro-mechanical modelling of flows impacting rigid walls," Canadian Geotechnical Journal, vol. 58, no. 11, pp. 1730–1743, 2021, doi: 10.1139/cgj-2020-0344.

[3] R. M. Iverson and D. L. George, "A depth-averaged debris-flow model that includes the effects of evolving dilatancy. I. Physical basis," Proceedings of the Royal Society A, vol. 470, no. 2170, p. 20130819, 2014, doi: 10.1098/rspa.2013.0819.

[4] T. Faug, "Depth-averaged analytic solutions for free-surface granular flows impacting rigid walls down inclines," Physical Review E, vol. 92, no. 6, p. 062310, 2015, doi: 10.1103/PhysRevE.92.062310.

[5] S. Cuomo, A. Di Perna, R. Ciaglia, M. Moscariello, and M. Martinelli, "Impact of flow-like landslide on protection barrier: Centrifuge tests and MPM modelling," Engineering Geology, vol. 366, p. 108681, 2026, doi: 10.1016/j.enggeo.2026.108681.

[6] S. Moriguchi, R. I. Borja, A. Yashima, and K. Sawada, "Estimating the impact force generated by granular flow on a rigid obstruction," Acta Geotechnica, vol. 4, no. 1, pp. 57–71, 2009, doi: 10.1007/s11440-009-0084-5.

[7] D. Song, C. W. W. Ng, C. E. Choi, G. G. D. Zhou, J. S. H. Kwan, and R. C. H. Koo, "Influence of debris flow solid fraction on rigid barrier impact," Canadian Geotechnical Journal, vol. 54, no. 10, pp. 1421–1434, 2017, doi: 10.1139/cgj-2016-0502.

Interaction of flowslides with fixed and movable barriers: centrifuge tests on Baskarp and Vesuvian soils

Mariagiovanna Moscariello[1], Sabatino Cuomo[1], Angela Di Perna[1], Rita Ciaglia[1], Mario Martinelli[2]

[1] Geotechnical Engineering Group (GEG), University of Salerno, Italy
[2] SPERI spa, Roma, Italy

mamoscariello@unisa.it

Keywords: centrifuge testing; flow-barrier interaction; flowslide

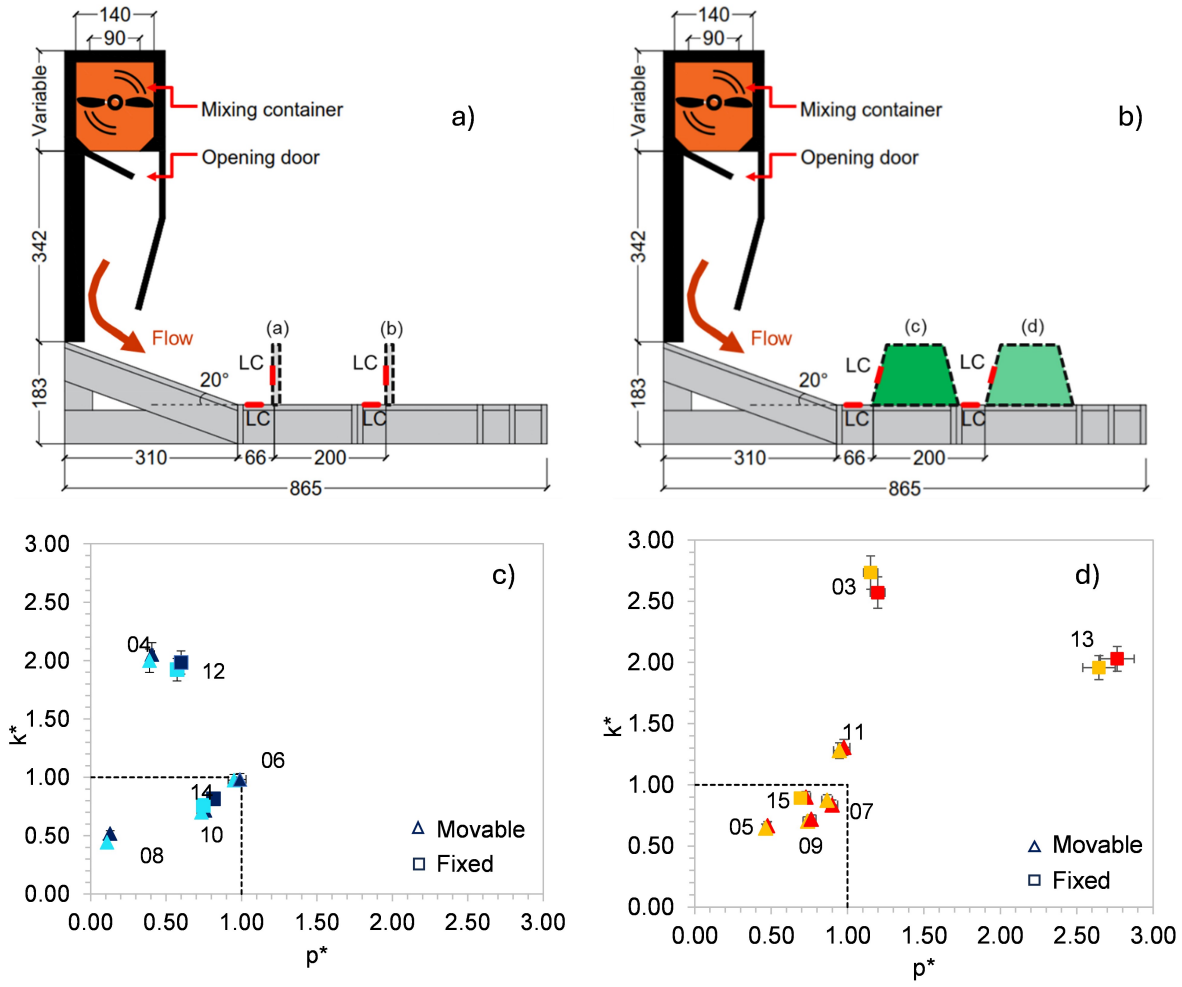
Rainfall-induced landslides have become increasingly widespread in recent decades because of climate change [1,2]. Their impact on buildings and infrastructure can result in severe damage or complete structural failure and may also lead to additional indirect consequences, such as the interruption of essential services. A correct understanding of landslide impact mechanisms is therefore essential to improve the design and performance of protective barriers. In this context, an experimental campaign was specifically designed to reproduce prototype stress conditions and to isolate the effects of barrier mobility, soil characteristics, released mass, and barrier position on flow–barrier interaction mechanisms and impact loading. Sixteen centrifuge tests were performed using the Geocentrifuge facilities (Fig. 1c) at Deltares (Delft, the Netherlands), combining high-speed imaging with high-frequency load cell measurements in order to capture both the kinematic and stress-based aspects of the impact process [3,4].

Two saturated soils with similar median grain size but contrasting granulometric size distribution were tested: a monogranular medium sand (Baskarp B25) and a natural volcanic silty sand from the Vesuvian area, characterized by a wide grain-size distribution and a significant fine fraction. For each soil, two released masses (7.5 kg and 10.5 kg at model scale), two barrier positions (near and far from the slope toe, Fig. 1a and b), and two barrier types were considered. The barriers consisted of a rigid fixed wall (Fig. 1a) and a movable free-sliding block designed to dissipate energy through displacement (Fig. 1b). High-speed cameras operating at up to 2500 frames per second were used to determine flow thickness, front velocity, interaction timing, and, for movable barriers, displacement histories. Impact pressures were measured using total-stress load cells installed both at the barrier face and at the base ground immediately upstream of the barrier, enabling simultaneous monitoring of lateral and vertical stresses during impact.

The experimental results highlight pronounced differences in flow–barrier interaction behavior associated with soil type and barrier configuration. Tests involving the fine-rich volcanic soil consistently exhibited longer interaction durations and more sustained lateral pressures compared to the uniform sand, indicating that fine content strongly influences stress dissipation mechanisms during impact. Movable barriers showed a systematic reduction in transferred load and in the lateral-to-vertical stress ratio compared to fixed barriers, particularly for larger released masses and far barrier positions. Although peak impact pressures were strongly influenced by flow velocity, significant variability was observed, demonstrating that kinematic parameters (i.e. Froude number and height of the undisturbed flow) alone cannot fully describe impact loading.

To support experimental interpretation, dimensionless stress-based parameters were introduced to characterize peak lateral pressure and lateral-to-vertical stress partitioning during impact (Fig. 1 c and d). The experimental dataset provides statistically robust evidence of how barrier mobility and soil granulometry govern impact stress evolution under prototype stress conditions.

Acknowledgements: This work was supported by the GEOLAB project, funded by the European Union's Horizon 2020 research and innovation programme (Grant Agreement No. 101006512). GEOLAB advances research on critical infrastructure resilience through coordinated access to leading European geotechnical research facilities.



a), and b) Experimental setups, c), and d) diagrams dimensionless peak lateral pressure and dimensionless lateral pressure.

References

[1] Jakob, M. (2022). Landslides in a changing climate. In Landslide hazards, risks, and disasters (pp. 892 505-579). Elsevier.

[2] Alcántara-Ayala, I. (2025). Landslides in a changing world. Landslides, 22, 2851–2865.

[3] Cuomo, S., Di Perna, A., Ciaglia, R., Moscariello, M., Martinelli, M. (2026). Interaction of flowslides with fixed and movable barriers: centrifuge tests on Baskarp and Vesuvian soils. Canadian Geotechnical Journal.

[4] Cuomo, S., Di Perna, A., Ciaglia, R., Moscariello, M., Martinelli, M. (2026). Impact of flow-like landslide on protection barrier: Centrifuge Tests and MPM modelling. Engineering Geology, 108681.

Interplay between Pore and Solid Tortuosities of Synthetic Rocks

Alexandre Sac-Morane[1], Maria Olarte-Garzon[1], Jean-Michel Pereira[1], Philipp Braun[1]

[1] Navier

alexandre.sac-morane@enpc.fr

To face the climate change, underground reservoirs are promising candidates to sequester greenhouse gas such as CO2 or balance the intermittency of renewable energy sources by storing H2. The estimation of the hydraulic properties of the host rock appears as pivotal, to predict the migration of injected fluids and associated multiphysical solicitations at the reservoir scale. Thanks to the advancement of imaging techniques, the estimation of hydraulic properties based on microscale simulations has become common practice. However, the correlation of hydraulic properties with geometric measures of the microstructure remains mostly elusive. A widely used set of morphometers are the Minkowski functionals, which are able to predict permeability to some degree [1], but struggle on complex microstructures containing microporosity and surface roughness [2]. In particular, Minkowski functionals fail to capture transport-relevant topology and connectivity. Interestingly, these morphometers appear sufficient to predict the mechanical performances of common porous materials [3, 4]. In this work, we investigate the interplay of additional descriptors, namely pore tortuosity and solid tortuosity, and their impact on hydraulic and mechanical properties. Various studies have highlighted the significance of pore tortuosity for more precise permeability estimation [5], conventionally inferred from electrical resistivity measurements. Similarly, the connectivity of the solid matrix can be interpreted by the thermal conductivity of the dry material. This interplay is first investigated through numerical analysis of digital synthetic rocks. To do so, various microstructures are generated controlling the porosity and exploring different generation algorithms. Subsequently, the pore and the solid tortuosities are determined with geometrical and physical analysis. In particular, a Fast Fourier Method is employed to estimate the thermal, hydraulic and mechanical properties of the synthetic microstructures [6]. This numerical approach is then complemented by an experimental campaign conducted on synthetic rocks. These samples are obtained by thermal sintering of glass beads, allowing a relative control on the microstructure. Once the samples are produced, electrical resistivity, hydraulic permeability, mechanical stiffness, and thermal conductivity are measured with low-cost experiments to estimate the pore and solid tortuosities.

References

[1] S. Zwarts and W. Lindqwister and M. Lesueur, (2026), "Database of Generated Rock Microstructures and their computed Geometrical and Hydraulic properties". *Scientific Data*, doi: 10.1038/s41597-026-07321-0.

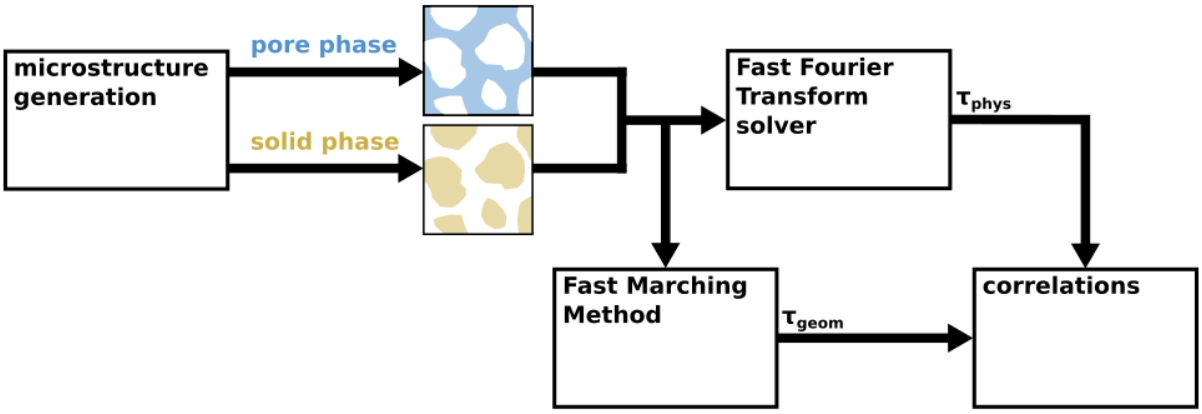
[2] P. A. Slotte and C.F. Berg and H. H. Khanamiri, (2020), "Predicting Resistivity and Permeability of Porous Media Using Minkowski Functionals", *Transport Porous Media*, vol. 131, pp. 705-722, doi: 10.1007/s11242-019-01363-2.

[3] A. Guével and H. Rattez and E. Veveakis, (2022), "Morphometric description of strength and degradation in porous media", *Int. J. Solids Struct.*, vol. 241, pp. 111454, doi: 10.1016/j.ijsolstr.2022.111454.

[4] W. Lindqwister and J. Peloquin and L.E. Dalton and K. Gall and M. Veveakis, (2025), "Predicting compressive stress-strain behavior of elasto-plastic porous media via morphology-informed neural networks", *Com. Eng.*, vol. 4, pp. 73, doi: 10.1038/s44172-025-00410-9.

[5] J. Fu and H. R. Thomas and C. Li, (2021), "Tortuosity of porous media: Image analysis and physical simulation", *Earth-Sci. Rev.*, vol. 212, pp. 103439, doi: 10.1016/j.earscirev.2020.103439.

[6] A. Alavoine and P. Dangla and J.M. Pereira, (2020), "Fast Fourier transform-based homogenisation of gas hydrate bearing sediments", *Géotechn. Lett.*, vol. 10, pp. 367-376, doi: 10.1680/jgele.19.00252.



Porous microstructures are generated and characterized with a FMM and a FFT approachs.

Shifted interface approach for nonsmooth frictional and hydraulically conductive interfaces in porodynamic media

David Riley[1], Guglielmo Scovazzi[2], Ioannis Stefanou[1]

[1] IMSIA (UMR 9219), CNRS, EDF, ENSTA Paris, Institut Polytechnique de Paris, Palaiseau, 91120, France

[2] Department of Civil and Environmental Engineering, Duke University, Durham, 27708, North Carolina, USA

david.riley@ensta.fr

Fluid-saturated geomaterials often contain internal discontinuities such as faults, fractures, joints, and slip surfaces. Because these interfaces are rarely geometrically simple, may be hydraulically conductive or impermeable, and obey nonsmooth mechanical laws that switch among opening, sticking, and sliding, their numerical simulation remains challenging. Body-fitted meshes require costly geometry-conforming discretizations, while unfitted approaches such as XFEM/CutFEM often require enrichment, cut-cell quadrature, and stabilization. In addition, frictional contact is frequently treated through regularization, introducing artificial compliance in the interface response.

We propose a shifted-interface framework for nonsmooth frictional and hydraulically conductive interfaces in two-dimensional dynamic Biot poromechanics [1]. In the shifted interface method, introduced for embedded diffusion problems [2] and extended to quasistatic poroelasticity with linear interface laws [3], the true crack is replaced by a mesh-aligned surrogate interface. Expansions of the interface conditions correct for the geometric offset between the true and surrogate interfaces. This allows non-planar cracks to be represented within standard finite element data structures, without enrichment or cut-cell integration.

The mechanical interface conditions, including Signorini contact, Coulomb friction, and slip-weakening friction, are formulated as normal-cone inclusions and solved via projection, following the nonsmooth contact dynamics framework [4]. This avoids penalty regularization and augmented Lagrangian stabilization, while directly enforcing opening, sticking, and sliding transitions. A representative two-crack simulation, shown in Figure 1, illustrates the proposed shifted-interface framework. (a) True non-mesh aligned cracks, Γ_{c0} and Γ_{c1}, and their mesh-aligned surrogate interfaces, $\tilde{\Gamma}_{c0}$ and $\tilde{\Gamma}_{c1}$. (b) Bulk velocity magnitude, $||v||$, at the time indicated by the horizontal cyan line in panels (c,d). Filled cyan markers denote sliding contact points, while open yellow markers denote sticking points (zero slip velocity). (c,d) Slip-rate magnitude histories, $|v_t|$, along Γ_{c0} and Γ_{c1}, respectively.The resulting framework provides a computational setting for coupled hydromechanical problems involving fault reactivation and frictional slip in fluid-saturated porous media.

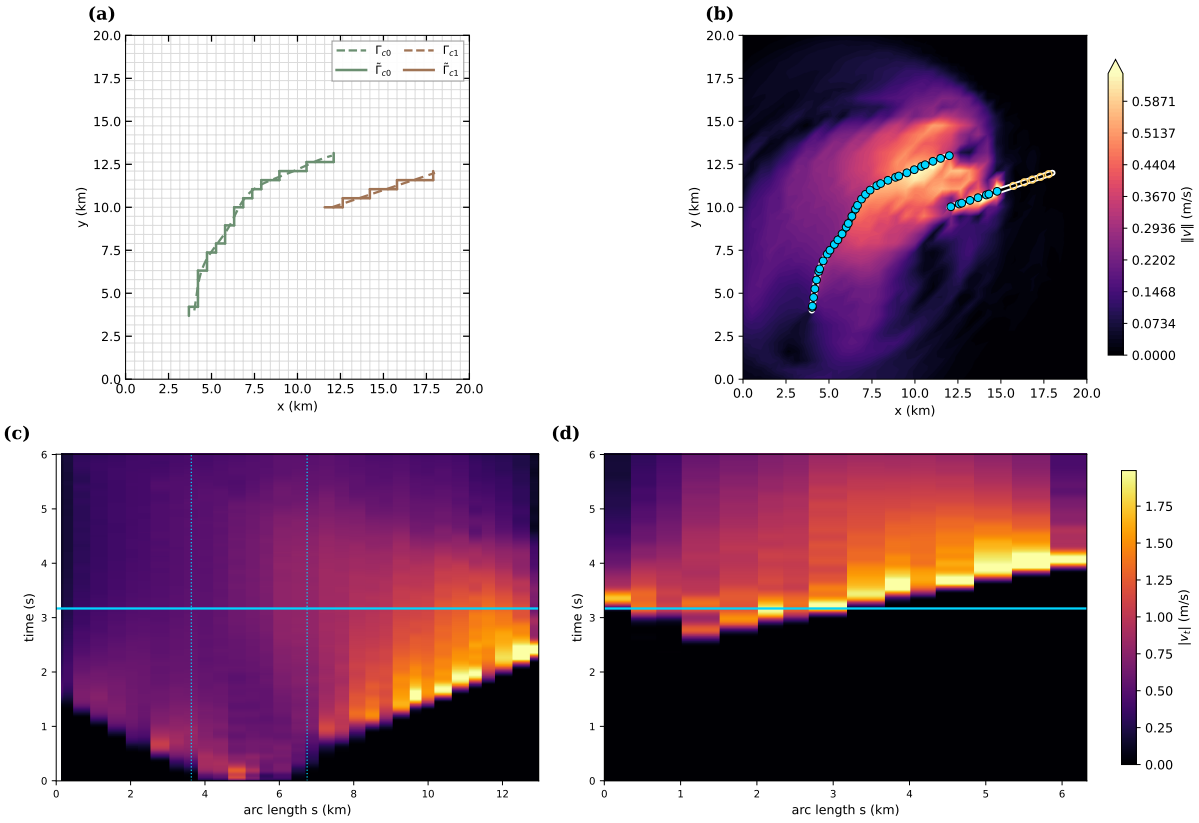
References

[1] M. A. Biot, "Theory of propagation of elastic waves in a fluid saturated porous solid. I. Low frequency range," Journal of the Acoustical Society of America, vol. 28, no. 2, pp. 168–178, doi: 10.1121/1.1908239.

[2] K. Li, N. M. Atallah, G. A. Main and G. Scovazzi, "The Shifted Interface Method: A flexible approach to embedded interface computations," International Journal for Numerical Methods in Engineering, vol. 121, no. 3, pp. 492–518, doi: 10.1002/nme.6231.

[3] D. M. Riley, G. Scovazzi and I. Stefanou, "A shifted interface approach for internal discontinuities in poroelastic media," arXiv preprint, arXiv:2604.15450, doi: 10.48550/arXiv.2604.15450.

[4] M. Jean, "The non-smooth contact dynamics method," Computer Methods in Applied Mechanics and Engineering, vol. 177, no. 3–4, pp. 235–257, doi: 10.1016/S0045-7825(98)00383-1.



Two-crack dynamic simulation showing true and surrogate interfaces, bulk velocity, sliding/sticking states, and slip-rate histories along each crack.

Modeling the Morphological Evolution of Railway Ballast Using a Core–Shell Bonded-Cell Approach

Jitinun Prommarin[1], Peerapong Jitsangiam[2], Mathieu Renouf[1], Emilien Azéma[1]

[1] LMGC, Université de Montpellier, CNRS, Montpellier, France

[2] Chiang Mai University-Advanced Railway Civil and Foundation Engineering Center (CMU-RailCFC), Department of Civil Engineering, Faculty of Engineering, Chiang Mai University, 239 Huay Kaew Road, Muang, Chiang Mai, 50200, Thailand.

jitinun.prommarin@etu.umontpellier.fr

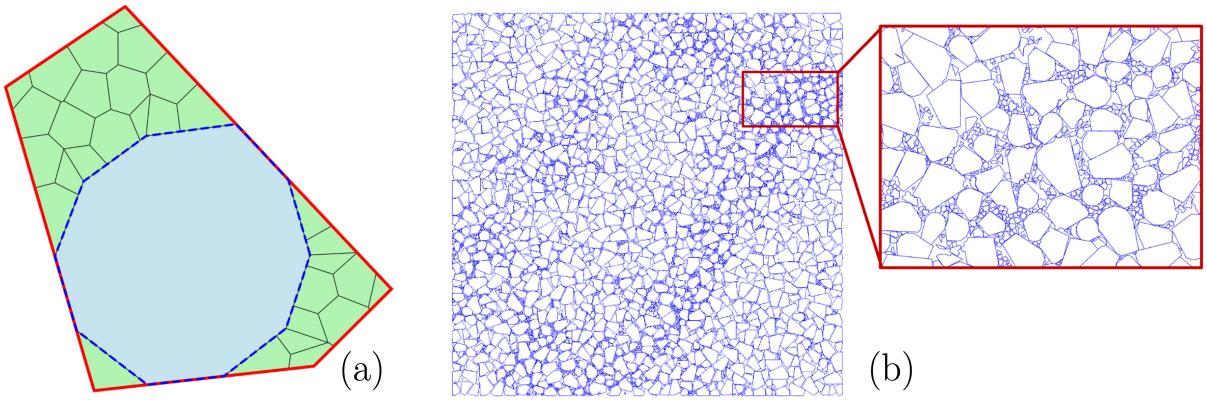
Understanding the micromechanical behavior of ballast degradation is crucial for the design and maintenance of resilient ballasted tracks. In this work, a 2D degradable grain model based on the Bonded-Cell Method (BCM) [1] is implemented within the LMGC90 framework using the Contact Dynamics (CD) approach. The model relies on realistic convex particle geometries in order to better capture the interlocking mechanisms governing ballast behavior. To reproduce the morphological evolution of ballast grains during degradation, a "Core–Shell" strategy is adopted (Fig.1a). A rigid decagonal core represents the ultimate degraded state of the particle, while the outer region corresponding to the initial fresh pentagonal [2] shape is discretized into fragmentable Voronoi cells. This structure enables the progressive generation of fine fragments through edge chipping and asperity abrasion, two major mechanisms involved in ballast fouling. Interactions between neighboring cells are governed by a simplified cohesive law based on normal and tangential failure stresses of Tresca type [3], taken equal in the present study. Biaxial compression simulations were performed using a library of three representative degradable particle shapes with an optimal discretization of 32 cells per grain. This resolution leads to an average fragment size of approximately 3 mm and a minimum size close to 2 mm (Fig.1b), allowing the explicit representation of fine particle production during degradation. To investigate the susceptibility of the granular assembly to breakage, we introduce the Relative Cohesion, η, defined as the ratio between the internal cohesive strength and the confining pressure. By varying η over seven levels ranging from 0.5 to 16, we characterize the transition from highly fragmentable to quasi-rigid regimes. The simulations successfully reproduce a broad range of fragmentation behaviors, together with the associated macroscopic strain-hardening and softening responses. Beyond the macroscopic response, the proposed framework provides detailed micromechanical insights into the coupling between contact network evolution, particle morphology degradation, and fouling generation.

References

[1] D. H. Nguyen, E. Azéma, P. Sornay, and F. Radjai, "Bonded-cell model for particle fracture," *Physical Review E*, vol. 91, no. 2, p. 022203, 2015.

[2] T. Binaree, S. Kwunjai, P. Jitsangiam, E. Azéma, and G. Jing, "Assessment of macro and micro mechanical properties of fresh and deteriorated ballast combining laboratory tests and 2D-discrete element methods," *Construction and Building Materials*, vol. 420, p. 135525, 2024.

[3] D. Cantor, C. Ovalle, and E. Azéma, "Microstructural origins of crushing strength for inherently anisotropic brittle materials," *International Journal of Solids and Structures*, vol. 238, p. 111399, 2022.



2D degradable grain model (a) "Core–Shell" single grain, (b) snapshot of fragmentation within a developed shear band at $\varepsilon_1 = 0.3$

A shifted interface approach for fully coupled 3D poroelastodynamics with non-smooth frictional discontinuities

Clément Rey[1], David Riley[1], Ioannis Stefanou[1]

[1] IMSIA (UMR 9219), CNRS, EDF, ENSTA Paris, Institut Polytechnique de Paris, Palaiseau, 91120, France.

clement.rey@ensta.fr

Simulations of fractured subsurface reservoirs, such as geothermal systems or CO_2 sequestration sites, remain a major challenge for computational geomechanics due to the presence of complex discontinuity networks spanning multiple length scales. Many industrial applications involve strongly coupled hydro-mechanical or thermo-hydro-mechanical phenomena, requiring a continuum description and therefore the use of the finite element method (FEM).

However, classical FEM approaches struggle with complex discontinuities, especially in three dimensions. Body-fitted methods require increasingly fine discretizations as discontinuity geometries become more complex, while unfitted methods such as XFEM and CutFEM require enrichment functions and additional stabilization, making their integration into FEM workflows more complicated [1].

The Shifted Interface Method (SIM), introduced in 2020 [2], avoids both remeshing and enrichment functions by projecting the physical discontinuity onto a nearby set of mesh faces called the surrogate interface. Recently extended to 3D crack propagation [3] and 2D coupled poroelastostatics [4], SIM demonstrated strong robustness, ease of implementation, and the ability to handle geometrically complex and non-planar discontinuities on non-conformal meshes.

In addition, many material interfaces exhibit Coulomb-like stick-slip behaviour, characterized by abrupt transitions between sticking and slipping states. Such non-smooth processes are commonly regularized, replacing a sharp switching condition by a smooth and stiff evolution problem that must be resolved at every time step, increasing both computational cost and implementation complexity.

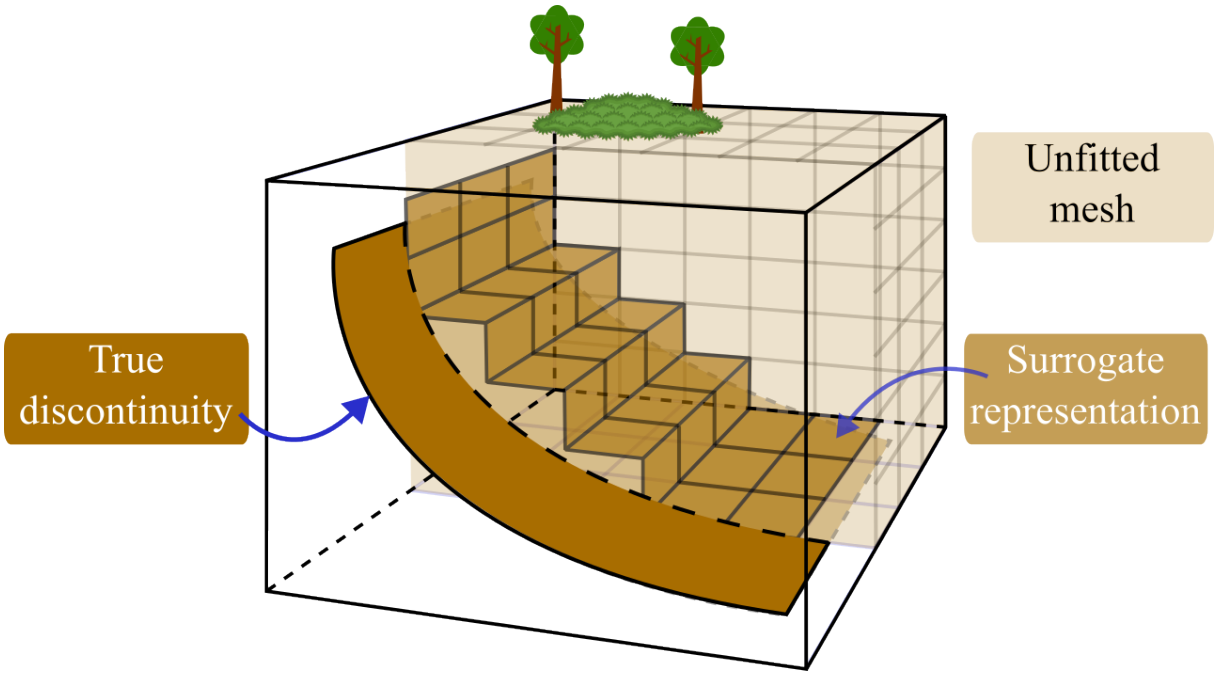
This work presents, to the authors' knowledge, the first extension of SIM to fully coupled 3D poroelastodynamics with non-smooth frictional laws at interfaces. The method directly models Coulomb-type stick-slip transitions without friction regularization with the non-smooth solver 'solve_nivp' [5], making it possible to simulate transients, e.g., frictional instabilities. Combined with the shifted interface method 'PoroSIM' [4], which uses 'Scikit-FEM' [6] for the underlying FEM data structures, it allows the treatment of highly complex and non-planar interfaces (i.e. (n-1)D discontinuities) without conformal meshing or enrichment procedures, while remaining compatible with a broad range of hydro-mechanical interface behaviours such as normal, tangential and mixed interface conditions for fluid flow. The framework therefore remains simple to implement and computationally affordable for large-scale fractured reservoir and induced seismicity simulations.

References

[1] Sinha, Agnivesh Kumar, and Gulab Pamnani. "Applications of XFEM in fracture analysis: a review." Iranian Journal of Science and Technology, Transactions of Civil Engineering (2025): 1-23.

[2] Li, Kangan, et al. "The shifted interface method: a flexible approach to embedded interface computations." International Journal for Numerical Methods in Engineering 121.3 (2020): 492-518.

[3] Li, Kangan, et al. "The shifted fracture method." International Journal for Numerical Methods in Engineering 122.22 (2021): 6641-6679.



3D illustration of the Shifted Interface Method

[4] Riley, David Michael, Guglielmo Scovazzi, and Ioannis Stefanou. "A shifted interface approach for internal discontinuities in poroelastic media." arXiv preprint arXiv:2604.15450 (2026).
[5] Riley, D. M. Stefanou, I. (2025). solve_nivp: A Python toolkit for integrating nonsmooth dynamical systems. Journal of Open Source Software. doi:10.21105/joss.09775
[6] Gustafsson et al., (2020). scikit-fem: A Python package for finite element assembly. Journal of Open Source Software, 5(52), 2369, doi:10.21105/joss.02369

Discrete Compliant-Element Method

Mukesh Singh Bisht[1], Vincent Richefeu[1]
[1] University Grenoble Alpes
mukesh.bisht@3sr-grenoble.fr

In the classical discrete element method (DEM), particles are typically assumed to be rigid (non-deformable), and their small overlaps are used to model local deflections. However, this assumption becomes inadequate for deformable materials or bonded particles forming breakable fragments, since the fracture patterns depend on each particle's ability to store elastic energy temporarily or undergo permanent deformation. To address this limitation, we introduce a novel approach, the discrete compliant-element method (DCEM), which incorporates uniform particle deformation within the DEM framework as implemented in the software Rockable. While in the classical DEM, the macroscopic deformation arises from the collective gaps and overlaps between particles, the DCEM extends this by enabling individual particles themselves to deform. The present framework accounts for elastic deformation of linear isotropic materials. Uniform particle deformation is demonstrated through single-particle simulations under different loading conditions and varying elastic parameters. The approach is further validated through bending simulations of a simply supported beam composed of bonded deformable cubic elements, whose effective flexural stiffness is predicted in closed form from the cell kinematics and the bond geometry alone, with no adjustable parameters. Furthermore, the influence of cell deformability on damage of an impacted bonded-cell tessellation is investigated. At low fracture energy, a mildly deformable tessellation sustains slightly less damage than its rigid counterpart.

References

[1] V. Richefeu, G. Combe, P. Villard, J.-Y. De-lenne, L. Amarsid, S. Nezamabadi, F. Radjai, J.-M. Vanson, R. Prat, P. Mutabaruka, Rockable, Software, HAL hal-04933604, richefeu/rockable (2025).
[2] V. Richefeu, G. Combe, L. Amarsid, R. Prat, J.-M. Vanson, S. Nezamabadi, P. Mutabaruka, J.-Y.Delenne, F. Radjai, Advanced strategies for discrete simulations with three-dimensional r-shapes in rockable framework, Computer Physics Communications (2025) 109997.
[3] L. F. Orozco, J.-Y. Delenne, P. Sornay, F. Radjai, Discrete-element model for dynamic fracture of a single particle, International Journal of Solids and Structures 166 (2019) 47–56.
[4] D.-H. Nguyen, É. Azéma, P. Sornay, F. Radjai, Rheology of granular materials composed of crushable particles, The European Physical Journal E 41 (4) (2018) 50.

Influence of particle gradation on the surface erosion resistance of MICP-treated soils

Angelo Giuseppe Tarullo[1], Michele Calvello[1], Tae-Hyuk Kwon[2], Marcopolo Alcantara Fuentes[2], Juyeon Jeong[2]

[1] University of Salerno

[2] Korea Advanced Institute of Science and Technology (KAIST)

atarullo@unisa.it

Microbially induced carbonate precipitation (MICP) has emerged as a promising bio-mediated geotechnical improvement technique for enhancing the mechanical and hydraulic properties of soils. However, the correlation between particle size distribution, carbonate content, and erosion resistance requires further systematic characterization. This study presents an experimental investigation of the surface erosion behavior of MICP-treated soils with varying soil gradation characteristics. Four distinct granular materials were investigated, representing different particle size distributions: (i) a reference 100% silica sand, (ii) a sand–gravel mixture with 10% gravel, (iii) a sand–gravel mixture with 20% gravel, and (iv) a sand–silt mixture containing 10% silt derived from crushed silica sand. All materials were treated with MICP to achieve two target calcium carbonate contents (CC $\simeq 3.5\%$ and $\simeq 6\%$). Treatment strategies were tailored to the hydraulic characteristics of each material: a percolation approach was adopted for the low-permeability sand–silt mixture, whereas bottom-up grouting injection was employed for sand and sand–gravel mixtures. Erosion resistance was quantified via Erosion Function Apparatus (EFA) testing, enabling determination of critical shear stress and erosion rates. The results demonstrate that MICP effectiveness is governed by a coupled interaction between calcium carbonate content and soil physical properties. Moderate cementation enhances the erosion resistance of finer and more uniform soils. In contrast, materials characterized by larger particles exhibit substantial improvements only at higher calcium carbonate levels, where sufficient bonding density is established. A threshold behavior is identified, beyond which interparticle bonding becomes mechanically effective, leading to a non-linear increase in erosion resistance. The findings highlight that erosion resistance can be effectively enhanced through MICP treatment; however, the optimal treatment strategy is strongly dependent on the intrinsic properties of the soil. In particular, the influence of calcium carbonate content on erosion resistance is not uniform but varies systematically with the particle size distribution of the treated material.

References

[1] Briaud, J.-L., Govindasamy, A.V., Shafii, I., 2017. Erosion Charts for Selected Geomaterials. J. Geotech. Geoenviron. Eng. 143, 04017072. https://doi.org/10.1061/(ASCE)GT.1943-5606.0001771

[2] Dejong, J.T., Soga, K., Kavazanjian, E., Burns, S., Van Paassen, L.A., Al Qabany, A., Aydilek, A., Bang, S.S., Burbank, M., Caslake, L.F., Chen, C.Y., Cheng, X., Chu, J., Ciurli, S., Esnault-Filet, A., Fauriel, S., Hamdan, N., Hata, T., Inagaki, Y., Jefferis, S., Kuo, M., Laloui, L., Larrahondo, J., Manning, D.A.C., Martinez, B., Montoya, B.M., Nelson, D.C., Palomino, A., Renforth, P., Santamarina, J.C., Seagren, E.A., Tanyu, B., Tsesarsky, M., Weaver, T., 2013. Biogeochemical processes and geotechnical applications: progress, opportunities and challenges. Géotechnique 63, 287–301. https://doi.org/10.1680/geot.sip13.p.017

[3] Ham, S.-M., Jeon, M.-K., Kwon, T.-H., 2023. Surface erosion of MICP-treated sands: Erosion function apparatus tests and CFD-DEM bonding model. Geomechanics and Engineering 33, 133–140. https://doi.org/10.12989/GAE.2023.33.2.133

Reservoir-Induced Hydromechanical Response in a Homogeneous Earth Dam from Coupled MASW-ERT In-situ Measurements.

Yogarish Narasinga Raja[1], Sourav Sarkar[1], P Anbazhagan[2]

[1] International Center of Excellence for Dams, Department of Civil Engineering, Indian Institute of Science Bengaluru

[2] Department of Civil Engineering, Indian Institute of Science Bengaluru

yogarishnraja@gmail.com

Reservoir level fluctuations significantly impact the hydro-mechanical behaviour of earth dams by changing internal moisture distribution and embankment stiffness. Therefore, understanding the relationship between saturation levels and mechanical response is essential for assessing the internal state of earth structures under different hydraulic conditions. This research examines the reservoir-induced hydromechanical response of a homogeneous earth dam using coupled in-situ Multichannel Analysis of Surface Waves (MASW) and Electrical Resistivity Tomography (ERT) measurements [1,2]. ERT surveys were conducted to characterise the spatial distribution of resistivity within the embankment under different reservoir conditions. To ensure data consistency and validate measurement reliability, three resistivity datasets (S1, S2, and S3) were acquired at the same location at 24-hour intervals under constant water-level conditions for both Full Reservoir Level (FRL) and Half Reservoir Level (HRL). The degree of saturation (S_r) was estimated using the Waxman-Smits petrophysical relationship [3], calibrated with laboratory ERT measurements under saturated conditions. Concurrently, MASW investigations were conducted to derive shear-wave velocity (V_s) profiles depicting the small-strain stiffness distribution of the dam body [4]. The integration of S_r from ERT and V_s from MASW enabled an assessment of the coupled saturation-stiffness response to reservoir fluctuations.

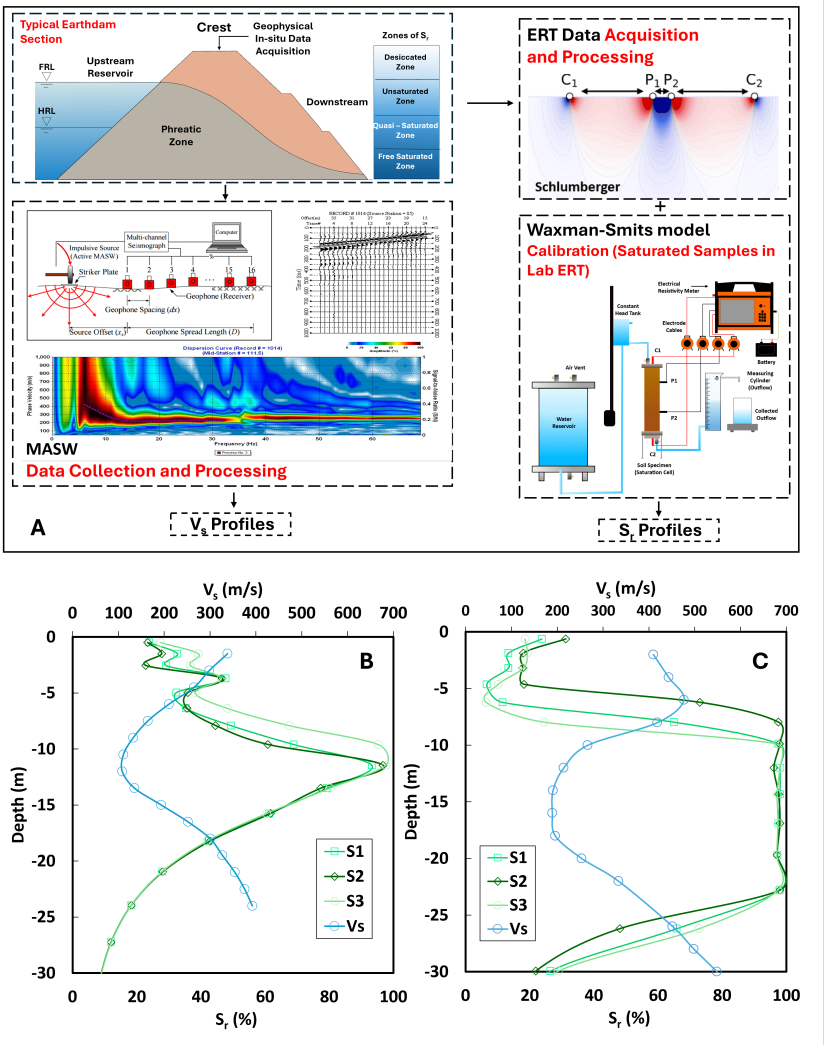
Field measurements using ERT and MASW, shown in Figure 1(A), were used to evaluate the relationship between S_r and V_s at FRL and HRL (Figure 1(B-C)). Under FRL conditions, the S_r curves show a relatively localised saturation zone centred approximately between -14 m and -10 m depth within the embankment. In this region, S_r values increase sharply towards near-saturated conditions (95-98%) and decrease rapidly away from the seepage zone. The corresponding V_s profile shows a localised reduction in velocity within the same region, with values decreasing from approximately 350-400 m/s near the outer portions of the embankment to nearly 100-150 m/s near the high S_r zone. This indicates that the stiffness reduction under FRL conditions remains spatially confined to the central seepage-influenced region.

The HRL condition exhibits a distinct response: S_r remains approximately 98% across a broad region (-24 m to -10 m), indicating extensive moisture redistribution compared with the localised saturation peak observed under FRL. Additionally, the V_s profile indicates a broad low-velocity zone (180-220 m/s) coinciding with high S_r levels, suggesting a significant reduction in stiffness during HRL.

This behaviour can be interpreted as a transient hydromechanical response associated with reservoir-level fluctuations. During FRL conditions, the higher hydraulic gradient promotes relatively concentrated seepage flow, resulting in a narrower saturation zone. As reservoir levels decrease toward HRL, the hydraulic gradient decreases, and moisture redistribution within the partially saturated zone becomes increasingly extensive over time.

This allows capillary-controlled saturation to spread laterally and vertically, producing the broader high S_r plateau observed in the HRL profiles.

The inverse relationship observed between V_s and S_r indicates that zones of higher saturation are generally associated with lower shear wave velocities. This behaviour is qualitatively consistent with hydromechanical coupling in partially saturated soils, where increased saturation may influence matric suction and effective stress conditions governing small-strain stiffness [5].



(A) Coupled ERT-MASW workflow; (B) V_s and S_r variations at FRL; and (C) corresponding variations at HRL within the dam.

References

[1] M.H. Loke, D.F. Rucker, J.E. Chambers, P.B. Wilkinson, O. Kuras, Electrical Resistivity Surveys and Data Interpretation, in: Encyclopedia of Solid Earth Geophysics, Springer, Cham, 2021: pp. 344-350. https://doi.org/10.1007/978-3-030-58631-7_46.

[2] C.B. Park, R.D. Miller, J. Xia, Multichannel analysis of surface waves, Geophysics 64 (1999) 800-808. https://doi.org/10.1190/1.1444590.

[3] M.H. Waxman, L.J.M. Smits, Electrical Conductivities in Oil-Bearing Shaly Sands, SPE J. 8 (1968) 107-122. https://doi.org/10.2118/1863-A.

[4] B.O. Hardin, W.L. Black, Vibration Modulus of Normally Consolidated Clay, Journal of the Soil Mechanics and Foundations Division 94 (1968) 353-369. https://doi.org/10.1061/JSFEAQ.0001100.

[5] D.G. Fredlund, H. Rahardjo, Soil Mechanics for Unsaturated Soils, John Wiley & Sons, 1993.

An integrated analytical framework for the thermo-mechanical response of groups of energy piles subjected to multi-axial

Rosario Mattia Moniaci[1], Tomáš Mladý[1], Gianvito Scaringi[1]
[1] Charles University
moniacir@natur.cuni.cz

The use of thermoactive foundations, or energy piles, is growing rapidly due to their ability to combine structural support with sustainable heat exchange.

Despite these advantages, the interaction between piles within a group under cyclic thermo-mechanical loads remains a complex area of study, especially with regard to horizontal displacements. This work presents the development of an analytical framework implemented in MATLAB, designed to predict the behavior of pile groups in granular soils. The aim is to integrate three established models:

the analytical solution by Abdelaziz & Ozudogru (2016) for estimating thermal variations induced by heating and cooling cycles (20 °C – 50 °C); the Costanzo-Lancellotta method (1998) for evaluating interactions between piles subjected to vertical loads; the Randolph model (1981) for analyzing group response under horizontal loads.

By superimposing the effects and using interaction matrices, the code allows for an analysis of how the thermal gradient influences the interaction coefficients of the pile group as the center-to-center distance-to-diameter ratio (s/d between 3 and 10) varies. Preliminary results obtained through numerical simulation highlight the impact of thermal deformations on the redistribution of loads at the pile heads and on the overall stability of the system. This analytical tool constitutes an essential preliminary step for calibrating subsequent small-scale tests at the Soil Mechanics Laboratory, providing the theoretical predictions necessary to optimize the experimental setup and interpret the phenomena of "thermal short-circuiting" in pile groups.

References

Abdelaziz, S. L., Ozudogru, T. Y. (2016). Selection of the design temperature change for energy piles. Applied Thermal Engineering, 107:1036-1045.

Costanzo, D., Lancellotta, R. (1998). A note on pile interaction factors. Soil And Foundations, 29(4):251:253.

De Gennaro, V., Frank, R., Pande, G. N., Canou, J. (1999). Finite element modelling of model piles in calibration chamber. Proc. 7th Int. Symp. on Numer. Models Geomech. (eds G. N. Pande, S. Pietruszczak and H. F. Schweiger), 419–424.

Kalantidou, A., Tang, A.M., Pereira, J.M., Hassen, G. (2012). Studio preliminare sul comportamento meccanico del palo dello scambiatore di calore nel modello fisico. Géotechnique, 62(11):1047-1051.

Lupatelli, A. (2021). Analisi numerica di fondazioni su pali termicamente attivi. In: Ceccato, F., Rosone, M., Stacul, S. (eds.), Proceedings of the 10th Annual Meeting of the Italian Young Geotechnical Engineers (IAGIG 2021), Italian Geotechnical Association, Rome, Italy:115-118, in Italian.

Randolph, M.F. (1981). The response of flexible piles to lateral loading. Géotechnique, 31(2):247:259.

Russo, G., Maiorano, R.M.S., Marone, G. (2017). Simulazione numerica ed analisi del comportamento di pali geotermici. Proceedings of the Italian Annual Meeting of Geotechnical Researchers (IARG 2017), in Italian.

Yavari, N., Tang, AM, Pereira, JM. et al. (2014). Experimental study on the mechanical behaviour of a heat exchanger pile using physical modelling. Acta Geotech, 9:385–398.

Robotic Automated Specimen Preparation (RASP): Specimen Homogeneity and Reproducibility in Centrifuge Physical Modelling

Faith Abimaje[1], Luis Mugele[1], Tristan Quinten[2], Miguel Cabrera[2], Hans Stutz[1]
[1] Institute of Soil Mechanics and Rock Mechanics (IBF), Karlsruhe Institute of Technology, Germany
[2] Faculty of Civil Engineering and Geosciences, TU Delft, Netherlands
faith.abimaje@kit.edu

In centrifuge modelling, prepared sand specimens are often characterised using a global density value, although this may not fully describe vertical and radial density variations within the model. Local density variations can influence in-flight measurements such as cone tip resistance (q_c) and affect the reproducibility and interpretation of test results. Manual air pluviation is inherently operator-dependent, introducing inconsistencies in fall height, flow rate and deposition pattern that compromise specimen homogeneity and reproducibility [1,2]. Existing automated alternatives reduce operator dependency but can result in considerable material waste, dust generation and provide no traceable documentation of the preparation process for quality assurance purposes. This study uses the recently proposed Robotic Automated Specimen Preparation (RASP) system as an alternative air pluviation technique for centrifuge model preparation [3,4]. RASP uses a six-degree-of-freedom collaborative robot to control the nozzle trajectory, fall height, deposition pattern and layer sequence during pluviation. The performance of RASP was evaluated using centrifuge tests conducted at 50g, with specimens prepared at two target relative densities ($I_D = 0.404$ and $I_D = 0.841$). In-flight miniature cone penetration tests (CPTs) were performed at the centre and radial positions within the model container to evaluate the consistency of cone resistance with depth and position, as an indicator of specimen uniformity and reproducibility. The results were partially compared against specimens prepared manually following the standard laboratory protocol. It was observed that manually prepared specimens exhibited greater variability in q_c between positions and poorer agreement between repeated preparations. In contrast, RASP-prepared specimens produced generally consistent q_c profiles with close agreement across positions and between repeated tests. In the loose specimen comparison, RASP specimen showed higher average q_c values, approximately 35% higher than manually prepared counterparts analysed over a depth range of 20-100 mm at comparable relative densities. This indicates that the preparation method influences the measured penetration response. This sensitivity has direct implications for CPT-derived parameters, including back-calculated relative density, friction angle, stiffness and bearing capacity. It is particularly important when centrifuge tests are performed to model a specific prototype problem, where the model specimen should closely represent the intended density distribution and soil state of the prototype system. These findings show that specimen preparation is not merely a procedural detail, but a key factor affecting the quality and interpretation of centrifuge CPT data. RASP therefore provides a reproducible preparation approach for high-quality centrifuge modelling, with potential relevance for inter-laboratory benchmarking [5].

References

[1] Y. P. Vaid and D. Negussey, "Relative density of pluviated sand samples," Soils and Foundations, vol. 24, no. 2, pp. 101–105, 1984, doi: 10.3208/sandf1972.24.2_101.
[2] R. Lagioia, A. Sanzeni, and F. Colleselli, "Air, water and vacuum pluviation of sand specimens for the triaxial apparatus," Soils and Foundations, vol. 46, no. 1, pp. 61–67, 2006, doi: 10.3208/sandf.46.61.

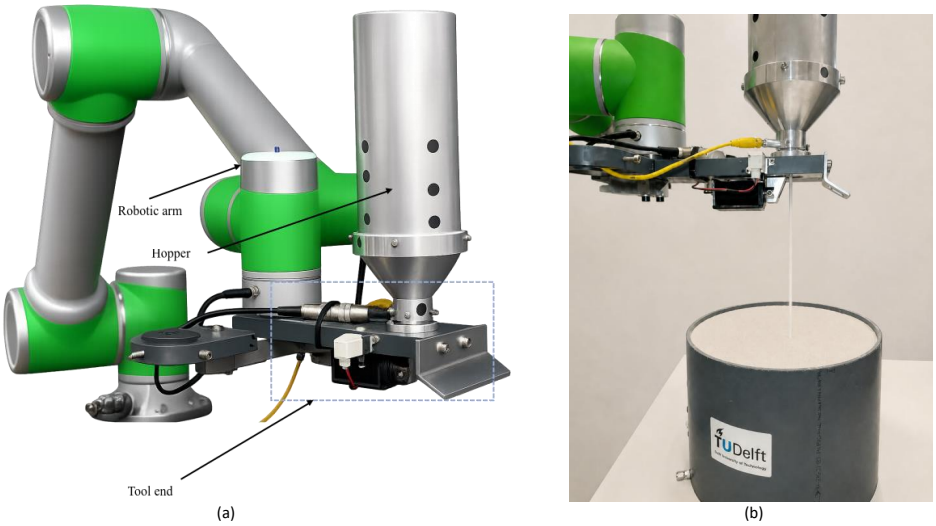


Figure 1. RASP system: (a) robotic arm fitted with the hopper and pluviation tool; (b) sand deposition into the centrifuge model container.

RASP system: (a) robotic arm fitted with the hopper and pluviation tool; (b) sand deposition into container

[3] L. Mugele, J. D. Arroyo López, J. Zürn, and H. H. Stutz, "Robotic Automated Specimen Preparation (RASP): Applied to air pluviation," Acta Geotechnica, 2026, in press.
[4] H. H. Stutz, L. Mugele, J. Zürn, and J. D. Arroyo López, "Robotic-aided specimen preparation (RASP) technique for soil mechanics," in Proceedings of the 21st International Conference on Soil Mechanics and Geotechnical Engineering, Vienna, Austria, 2026.
[5] B. L. Kutter et al., "LEAP-UCD-2017 comparison of centrifuge test results," in Model Tests and Numerical Simulations of Liquefaction and Lateral Spreading: LEAP-UCD-2017, Springer, pp. 69–103, 2019, doi: 10.1007/978-3-030-22818-7_4.

Terrain Interaction Mechanics of Off-road Heavy-duty Vehicles

Alejandro Secades[1,2], Wolfgang Fellin[1], Manuel Ferdik[2]
[1] University of Innsbruck / Department of Geotechnical Engineering
[2] Management Center Innsbruck / Department of Industrial Engineering
alejandro.secades-rodriguez@student.uibk.ac.at

The development of simulation models which provide reliable representations of vehicles' performance in different environments has been an increasing important factor for multitude of areas, specially within the off-road heavy-duty vehicles manufacturers. The improvement of these digital twins directly influences the quality of the industry knowledge on their products performance, as well as resulting in shorter and more cost-effective product development processes, which in turn increases their competitiveness [1].

These computer models shall not only cover the internal mechanisms of the powertrains, as well as the kinematics and dynamics of the vehicles, but also focus on the interaction of their different terrain-engaging elements - running gear, blade, winch, tiller, etc. - with their surroundings [2]. The field of study that focusses on describing this interaction is called Terramechanics.

There are essentially three types of state-of-the-art methods to represent the terrain-vehicle interaction: empirical, semi-empirical and numerical approaches. The empirical methods are based solely on experimental relationships to define the material-vehicle interaction, whereas semi-empirical approaches make use of well-known physical properties and phenomena to develop the interaction models, which are then in turn calibrated with the aid of experimental data. Finally, the numerical approaches, such as finite element, discrete element or hybrid methods, would potentially offer higher quality and precision however becoming computationally far more expensive. [3]

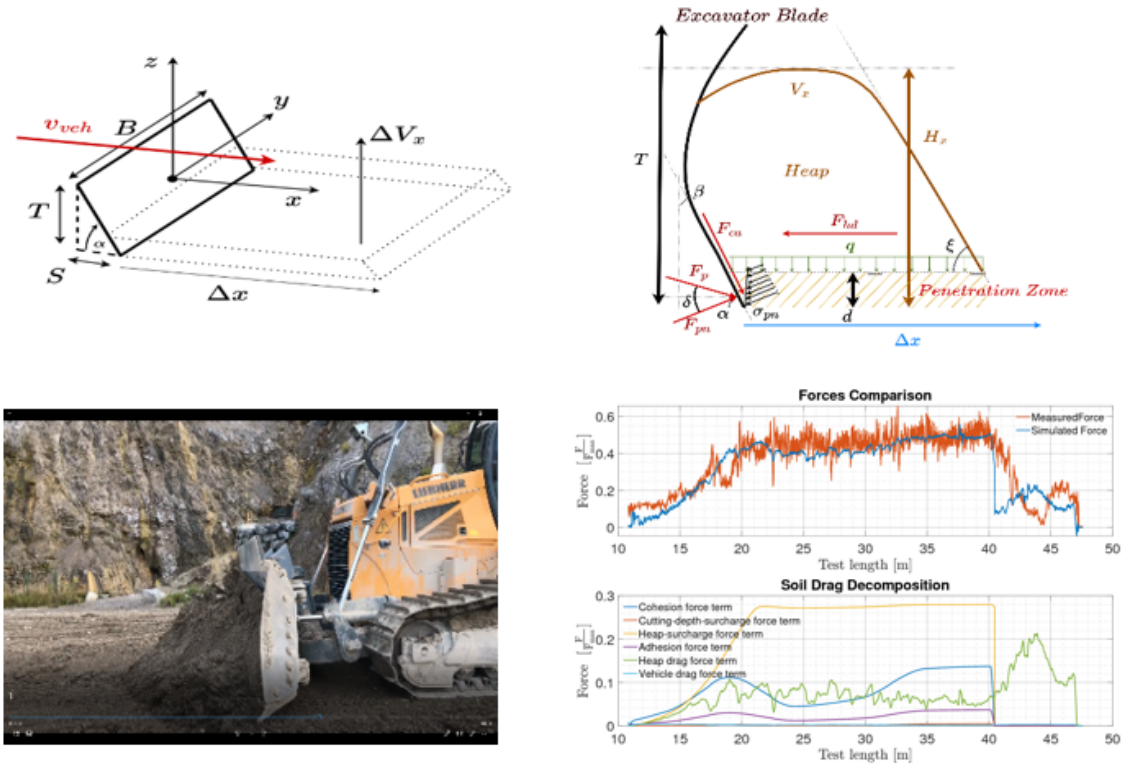
In the presentation, a generic semi-empirical approach for off-road heavy-duty tracked-vehicles is shown, where the different terrain-vehicle interaction mechanisms are defined through geotechnical and empirical relationships. For instance, the track traction is being represented as a combination of passive earth pressure and different shear-stress slip-dependent displacement models [2, 4] – depending on the ground material type. The static sinkage of the vehicle is modeled as a combined function of an empirical relationship, the Bekker pressure-settlement ratio, and geotechnical relationships regarding lateral earth pressure. [5]. In a similar manner, the track terrain resistances to the motion, and other vehicle-equipment-to-ground drag (in the present solely focusing on the vehicle blades), are also derived from the passive earth pressure [6], among other effects.

Combining these interaction models within a dynamic vehicle representation, introducing the system's inertia, slip, slip-related sinkage, vehicle kinematics and dynamics, etc.; yields a complete dynamic interaction model [7]. Different ground material characteristics and vehicle configurations are taken into account in the form of different parametric arrays, as well as different performance' relationships (interaction formulas).

Field measurements have been performed in order to calibrate the model and to validate its reliability. Thus, a generic tracked vehicle-ground material interaction tool is hereby presented, in which different terrain and vehicle configurations can be represented in a dynamic phasion, with the ability to be integrated with other simulation environments – such as, to name a few, vehicle powertrains, working hydraulics and control systems.

References

[1] J. Y. Wong. "Theory of Ground Vehicles" (2001). Ottawa. John Wiley & Sons



Blade-terrain interaction model overview for a real case scenario, showing the forces comparison between measurement and simulation.

[2] J. Y. Wong. "Terramechanics and Off-Road Vehicle Engineering" (2024). Butterworth-Heinemann
[3] E. Karpman, J. Kövecses, D. Holz, K. Skonieczny. „Discrete element modelling for wheel-soil interaction and the analysis of the effect of gravity" (2020), Journal of Terramechanics, vol. 91, pp. 139-153, doi: https://doi.org/10.1016/j.jterra.2020.06.002
[4] Z. Xu, Y. Liu, G. Yan, J. Xia, Z. Dou, Q. Meng, X. Xu, "Research on contact model of track-soft sediment and traction performance of four-tracked seabed mining vehicle" (2022), Ocean Engineering, doi: https://doi.org/10.1016/j.oceaneng.2022.111902
[5] Z. Guan, D. Jiang, M. Zhang, M. Jin, H. Li, T. Jiang, "Effect of vertical load on track traction under different soil moisture content" (2025), Journal of Terramechanics, vol. 11, doi: https://doi.org/10.1016/j.jterra.2024.101044
[6] A. R. Reece, "The Fundamental Equation of Earth-Moving Mechanics", *Institution of Mechanical Engineering*, vol. 179, issue 6, doi: https://doi.org/10.1243/PIME_CONF_1964_179_134_02
[7] S. Tang, S. Yuan, J. Hu, X. Li, J. Zhou, J. Guo, "Modeling of steady-state performance of skid steering for high-speed tracked vehicles", Journal of Terramechanics, vol. 79, pp. 25-35, doi: http://dx.doi.org/10.1016/j.jterra.2017.06.003

Influence of potassium sulfate on the mineralogical and physicochemical properties of an expansive clay

Alan Ribeiro-Santos[1], Benjamin Dardé[1], Anh-minh Tang[2]

[1] Institut de Recherche de la Construction (IRC), ESTP, Grande école d'ingénieurs de la construction, Cachan, France

[2] Navier, ENPC, Institut Polytechnique de Paris, Univ Gustave Eiffel, CNRS, Marne-la-Vallée, France

aribeirosantos@estp.fr

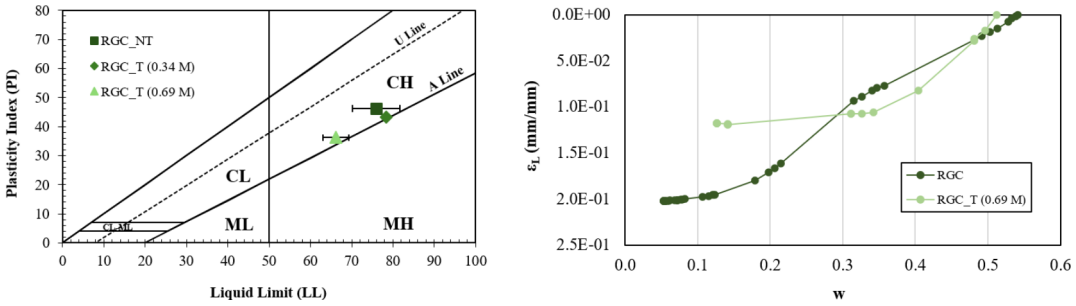
Clay shrink–swell (CSS) cycles may compromise the durability and integrity of structures interacting with clayey soils by imposing significant additional loads [2, 4, 15]. Climate change may intensify this phenomenon and increase damage to buildings and infrastructure [2, 4]. Clayey-soil deformation is partly governed by physicochemical processes, including the expansion of swelling clay minerals, particularly smectites and interstratified minerals containing smectitic layers [5, 8]. Among the strategies proposed to reduce clay swelling, potassium salts represent a promising approach. K^+ ions may limit swelling because of their low hydration energy and ability to fit into the hexagonal cavities of tetrahedral sheets and remain near the negatively charged surfaces of 2:1 clay minerals[3, 7]. K^+ may also produce a thinner electrical double layer (EDL) than more strongly hydrated cations, reducing interparticle repulsion and aggregate volume [6, 12]. In this context, this study investigates the effects of potassium sulfate (K_2SO_4) on the mineralogical and physicochemical properties of Romainville Green Clay (RGC), a highly expansive clay from the Paris region, France. X-ray diffraction (XRD), methylene blue value (VBS), and consistency limit tests were performed on untreated and treated samples to assess changes in clay mineral behavior and soil activity.

RGC was sampled in Champs-sur-Marne, in the eastern Paris region. It is classified as moderately to highly active [1] and highly susceptible to shrink–swell behavior based on its lithology, mineralogy, and geotechnical behavior according to BRGM reports. XRD and VBS tests and liquid limit (LL), plastic limit (PL), and shrinkage limit (SL) determinations were performed on untreated and treated samples. For XRD analysis, oriented samples were prepared by depositing suspensions of the $< 2\ \mu m$ RGC fraction, obtained by decantation, onto glass slides. After air-drying, the slides were analyzed with a Bruker D2 Phaser diffractometer. Treated slides were prepared by pipetting K_2SO_4 solutions of different concentrations directly onto the air-dried untreated oriented samples. Additional mounts were exposed to ethylene glycol (EG) vapor to study swelling clay minerals. They were placed in a desiccator containing EG and heated at 65°C for 16 h following [11]. For the VBS and consistency limit tests, the ¡400 µm RGC fraction was obtained by wet sieving, drying, and mechanical crushing. SL, Atterberg limits and VBS tests were conducted according to XP P 94-060-1 [13], NF EN ISO 17892-12 [10] and NF EN 17542-3 [9], respectively. Treated samples were prepared by soaking RGC in K_2SO_4 solutions with K^+ concentrations of 0.34 and 0.69 M, corresponding to 25% and 50% of the K_2SO_4 saturation concentration at 25°C (120 g/L). Dry soil and solution were mixed at a 1:5 mass ratio, agitated for 10 min, rested for 48 h, oven-dried, and crushed. For the VBS test, an additional rinsing procedure was adopted, treated samples were repeatedly washed with pure water until the supernatant EC fell below 1 mS/cm, following a procedure adapted from [14].

The Atterberg and shrinkage limit results are presented in the figure, with the former plotted on the Casagrande plasticity chart. Both tests indicated reduced soil activity after

K_2SO_4 treatment. The 0.69 M treatment reduced LL, despite variations related to the natural heterogeneity of RGC. Only minor changes were observed at 0.34 M, although soil heterogeneity must also be considered. In turn, shrinkage limit test revealed an altered water retention behavior and an increase in the SL from 14% to 35.5% following treatment. XRD results showed weakening and alteration of reflections associated with swelling clay minerals. In contrast, VBS values changed only slightly after treatment, possibly because of the treatment procedure and/or interactions between K_2SO_4 and methylene blue.

Although sample preparation and nonchemical salt effects must be carefully considered, the results support potassium salts as a potential treatment for expansive clays and encourage further investigation under more representative field conditions.



Consistency limits: Atterberg limits plotted on the Casagrande plasticity chart (left) and Shrinkage limit tests results (right). Horizontal bars indicate test variability with two tests performed on each treated RGC and three on the untreated RGC.

References

[1] Audiguier, M., Geremew, Z., Laribi, S., Cojean, R., 2007. Caractérisation au laboratoire de la sensibilité au retrait-gonflement des sols argileux. Rev. Fr. Geotech. 67–82.

[2] Barthelemy, S., Bonan, B., Calvet, J.-C., Grandjean, G., Moncoulon, D., Kapsambelis, D., Bernardie, S., 2024. A new approach for drought index adjustment to clay-shrinkage-induced subsidence over France: advantages of the interactive leaf area index. Nat. Hazards Earth Syst. Sci. 24, 999–1016.

[3] Behnsen, J., Faulkner, D.R., 2013. Permeability and frictional strength of cation-exchanged montmorillonite. JGR Solid Earth 118, 2788–2798.

[4] Charpentier, A., James, M., Ali, H., 2022. Predicting drought and subsidence risks in France. Nat. Hazards Earth Syst. Sci. 22, 2401–2418.

[5] Christidis, G.E., 2011. The concept of layer charge of smectites and its implications for important smectite-water properties, in: Brigatti, M.F., Mottana, A. (Eds.), Layered Mineral Structures and Their Application in Advanced Technologies. Mineralogical Society of Great Britain and Ireland, pp. 237–258.

[6] Di Maio, C., 1996. Exposure of bentonite to salt solution: osmotic and mechanical effects. Géotechnique 46, 695–707.

[7] Liu, X., Lu, X., 2006. A Thermodynamic Understanding of Clay-Swelling Inhibition by Potassium Ions. Angew Chem Int Ed 45, 6300–6303.

[8] Madsen, F.T., Müller-Vonmoos, M., 1989. The swelling behaviour of clays. Applied Clay Science 4, 143–156.

[9] NF EN 17542-3, 2022. Earthworks - Geotechnical laboratory tests - Part 3: Methylene blue value VBS on soils and rocks.

[10] NF EN ISO 17892-12, 2018. Geotechnical investigation and testing - Laboratory testing of soil - Part 12: determination of liquid and plastic limits.

[11] Poppe, L., Paskevich, V., Hathaway, J., Blackwood, D., 2001. U.S. Geological Survey Open-File Report 01-041 https://pubs.usgs.gov/of/2001/of01-041/ (accessed 11.20.25).

[12] Sridharan, A., 1991. Engineering behaviour of fine grained soils: A fundamental approach. Indian geotechnical journal 21, 1–136.

[13] XP P 94-060-1, 1997. Soils: Investigation and testing - Shrinkage test - Part 1: Determination of shrinkage characteristic on remoulded soil passing a 400 µm test sieve.

[14] Yukselen, Y., Kaya, A., 2008. Suitability of the methylene blue test for surface area, cation exchange capacity and swell potential determination of clayey soils. Engineering Geology 102, 38–45.

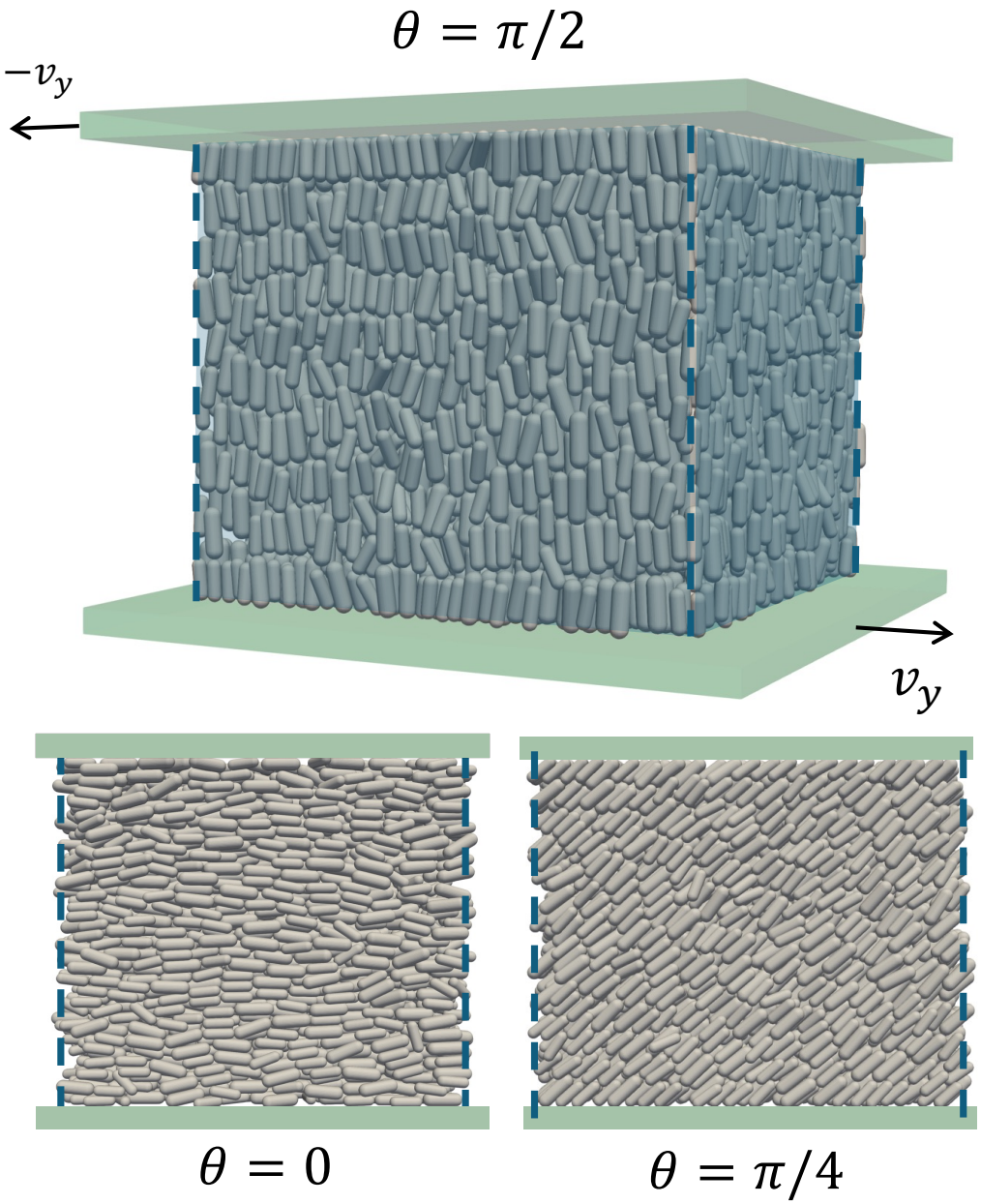
[15] Zemenu, G., Martine, A., Roger, C., 2009. Analyse du comportement d'un sol argileux sous sollicitations hydriques cycliques. Bull Eng Geol Environ 68, 421–436.

Fabric Orientation and Liquefaction Susceptibility of Granular Materials

Carolina Castro-Malaver[1,2], Manuel Cárdenas-Barrantes[1], Mathieu Renouf[2], Emilien Azéma[1,2], Carlos Ovalle[1]

[1] Department of Civil, Geological and Mining Engineering, Polytechnique Montréal, Canada
[2] Laboratoire de Mécanique et Génie Civil, Université de Montpellier, CNRS, France
lady-carolina.castro-malaver@polymtl.ca

The mechanical behavior of granular materials is linked to their structure, which comprises both the fabric—the spatial arrangement of particles and voids—and the inter-particle force network. While heterogeneity is a common feature in most soils, in mine tailings it is specifically driven by industrial comminution and deposition methods. These processes influence the initial fabric, often resulting in a preferred particle orientation and inherent anisotropy. The state of this arrangement during undrained loading is a relevant factor, as its evolution throughout the shearing process directly influences the mechanical response of the assembly. However, capturing the link between internal configurations and bulk behavior remains challenging, particularly because obtaining undisturbed in-situ samples is often unfeasible. To bridge the gap between the micro- and macro-mechanical response under these constraints, this study analyzes multiscale descriptors of virtual samples with different initial preferred particle orientations under constant-volume shearing conditions. Using the Discrete Element Method, spherocylindrical particles were uniaxially consolidated to create loose and dense specimens with five initial preferential grain orientations (0, $\pi/6$, $\pi/4$, $\pi/3$ and $\pi/2$ radians), as shown in the Figure. Additionally, a control sample with random particle orientation was generated for comparison. The specimens were subsequently subjected to constant volume monotonic shearing. Preliminary results indicate that the initial fabric orientation influences the onset of instabilities, sometimes overriding the effect of density. In the loose specimens, orientations of $\pi/3$, $\pi/2$ and $\pi/4$ exhibit static liquefaction; characterized by a pronounced drop in the stress tensor invariants and a sudden decrease in the coordination number. Conversely, within the dense cases, liquefaction is only observed for the $\pi/2$ grain orientation. At the microscale, while random-fabric samples exhibit negligible initial force anisotropy that evolves rapidly during constant-volume shearing, samples with predefined particle orientations display an initial force anisotropy signature that appears to trigger instabilities under shear. The observed instability in dense specimens at high orientation angles demonstrates that the initial fabric imposes a structural constraint that requires a reorganization of the contact network before the inter-particle force system can develop a mechanical shear resistance. Consequently, higher density does not guarantee resistance to shear-induced liquefaction. The multiscale analysis suggests that liquefaction triggering is fundamentally coupled with the initial particle arrangement and its subsequent force distribution evolution, rather than solely dictated by initial density.



Snapshots of initial DEM specimen configurations for three different particle orientations.

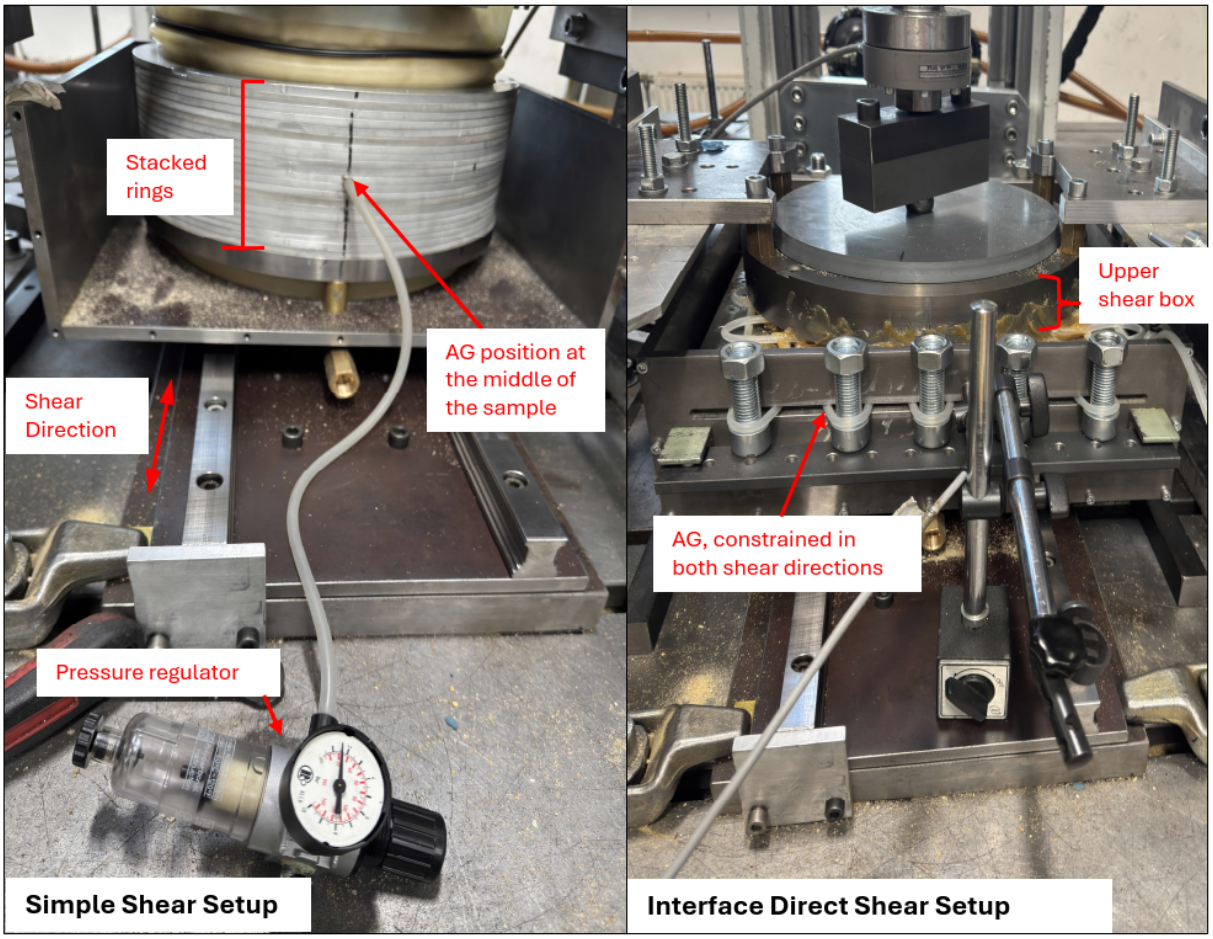
Active geogrids – a new approach to controlling earthquake wave propagation

Lutf Al-Subari[1], Ali Akbar[1], Raul Fuentes[1]

[1] Institute of Geomechanics and Underground Technology, RWTH Aachen University, 52074 Aachen, Germany.

al-subari@gut.rwth-aachen.de

Geogrids are widely used as passive reinforcement elements in geotechnical engineering, yet their mechanical contribution is fixed once installed and cannot be adjusted to changing loading conditions. This limitation is particularly relevant under dynamic and seismic loading, where the required balance between stiffness, damping, and energy dissipation may vary during an event. While the monotonic behaviour of geogrid-reinforced soils has been extensively studied, the dynamic response of integrated soil–geogrid systems remains less well understood. This study addresses this gap by combining experimental characterisation and constitutive modelling of both passive and active geogrid–soil interaction. The active concept investigated in this work is inspired by a patented reinforcement system in which embedded actuators can modify the mechanical state of a reinforcement grid and its interaction with the surrounding ground. A novel active geogrid prototype was therefore developed using pneumatically tunable tubular silicone-elastomer elements. Unlike conventional geogrids, the proposed system allows the soil–reinforcement interaction to be adjusted through internal pressure, providing a potential means of actively controlling shear stiffness, damping, and seismic wave transmission in reinforced soil layers. The experimental programme examined bare soil, passive geogrid-reinforced soil, and active geogrid-reinforced soil under different activation levels. The active geogrid was tested at internal pressures equal to 0, 1.0, and 1.5 times the applied normal confining pressure. Small-strain stiffness was measured using bender element tests under confining pressures from 25 to 500 kPa. Monotonic simple shear and direct interface shear tests were performed at normal stresses of 50, 100, and 200 kPa. Cyclic simple shear and cyclic interface shear tests were conducted at 100 kPa normal stress and shear strain amplitudes of 0.01, 0.1, 1.0, and 3.0%. The results show that cyclic loading produces a characteristic evolution of the reinforced soil response: stiffness increases and damping decreases during the initial cycles, followed by stabilisation. Passive geogrid inclusion reduces the apparent shear stiffness and increases damping, indicating a softer and more dissipative interface response. In contrast, pressurisation of the active geogrid increases the overall stiffness of the reinforced soil, probably due to enhanced local confinement and densification around the pressurised elements. The active system therefore enables the reinforced soil response to shift between more compliant, energy-dissipative states and stiffer, confinement-enhanced states. A constitutive model was developed to reproduce the observed nonlinear response using a hyperbolic interface law implemented through a virtual-thickness layer for finite element analysis. Calibration against monotonic and cyclic tests enables prediction of stiffness degradation and damping across different strain amplitudes and confining pressures. These findings demonstrate the potential of active geogrids as adaptive geotechnical seismic isolation devices, transforming soil reinforcement from a passive inclusion into a controllable ground–structure interaction system.



Geogrid placement and confinement in simple shear (left) and interface direct shear (right) apparatus.

Numerical Simulation of CPT in sands using Finite Element Analysis

Ana Karine Santos Dantas[1], Arash Alimardani Lavasan[1]
[1] University of Luxembourg
ana.santos.002@student.uni.lu

The global effort to reduce greenhouse gas emissions, limit global warming, and mitigate climate change is accelerating the transition from fossil fuels towards cleaner and more sustainable energy sources. Within this transition, wind energy—particularly offshore wind—has emerged as a promising alternative because of its high energy potential, consistency, and efficiency. However, offshore wind development presents considerable geotechnical challenges related to site characterization, foundation design, and installation.

The Cone Penetration Test (CPT) is widely used in offshore geotechnical investigations because it provides continuous profiles of cone-tip resistance and sleeve friction during penetration [2]. Nevertheless, CPT measurements obtained in calibration chambers can be significantly affected by the boundary conditions and dimensions of the soil specimen [1, 3]. Understanding these effects is therefore essential for interpreting calibration-chamber measurements and relating them to soil behaviour.

This study will evaluate the CPT response under different boundary conditions using numerical simulations performed in PLAXIS 2D. Particular attention will be given to the influence of the imposed boundaries on cone-tip resistance, sleeve friction, soil displacements, and stress redistribution around the advancing cone. The progressive insertion of the cone will be modelled to account for the soil disturbance and accumulation of plastic strains generated during penetration.

The primary numerical challenges are associated with the large deformations developing near the cone tip and shaft, which may cause severe mesh distortion, numerical instability, and convergence difficulties [4, 5]. Another critical aspect is the selection and calibration of a constitutive model capable of representing the complex and highly nonlinear soil response at different strain levels. Addressing these challenges requires appropriate constitutive formulations, mesh refinement, soil–cone interface conditions, and robust numerical strategies. The results are expected to improve understanding of boundary effects on CPT measurements and support the interpretation of calibration-chamber tests.

References

[1] Baldi, Giuseppe, Roberto Bellotti, Vincenzo Ghionna, Michele Jamiolkowski, and Ernesto Pasqualini. 1986. "Interpretation of CPTs and CPTUs, Part 2: Drained Penetration of Sands." In Proceedings of the 4th International Geotechnical Seminar on Field Instrumentation and In Situ Measurements, 143–156. Singapore: Nanyang Technological Institute.

[2] Lunne, Tom, Peter K. Robertson, and John J. M. Powell. 1997. Cone Penetration Testing in Geotechnical Practice. London: Blackie Academic & Professional. Publisher information.

[3] Parkin, Alan K., and Tom Lunne. 1982. "Boundary Effects in the Laboratory Calibration of a Cone Penetrometer for Sand." In Proceedings of the Second European Symposium on Penetration Testing, vol. 2, 761–768. Rotterdam: A. A. Balkema. Bibliographic record.

[4] Van den Berg, Peter, René De Borst, and Han Huétink. 1996. "An Eulerian Finite Element Model for Penetration in Layered Soil." International Journal for Numerical and Analytical Methods in Geomechanics 20 (12): 865–886. https://doi.org/10.1002/(SICI)1096-9853(199612)20:12%3C865::AID-NAG854%3E3.0.CO;2-A.

[5] Wei, Lei, Murad Y. Abu-Farsakh, and Mehmet T. Tumay. 2005. "Finite-Element Analysis of Inclined Piezocone Penetration Test in Clays." International Journal of Geomechanics 5 (3): 167–178. https://doi.org/10.1061/(ASCE)1532-3641(2005)5:3(167).

Permeability Assessment of Weathered and Poorly Graded Rockfill: Experimental Testing and Numerical Validation

Carlos Laina Gómez[1], Diego Escudero-Merino[2], Mario Caballero-Ezquerro[1], Enrique Asanza-Izquierdo[1]

[1] Laboratorio de Geotecnia - CEDEX
[2] Universidad Politécnica de Madrid

carlos.laina@cedex.es

The upstream rockfill of earth dams plays a key role in protecting the impervious core and ensuring adequate drainage conditions. However, long-term exposure to environmental actions such as wetting–drying cycles, thermal oscillations, freeze–thaw processes, and changes in rainfall patterns may accelerate the weathering and degradation of rockfill particles, leading to significant changes in permeability and mechanical performance. Over the last decade, investigations conducted by CEDEX have identified clear signs of particle alteration and crumbling in several aged rockfill structures.

This study presents the experimental and numerical analysis of an in-situ percolation test carried out on the upstream slope of the Alcorlo Dam, a large earth dam constructed between 1976 and 1978. After more than forty years of service, the rockfill exhibited advanced weathering, with particles breaking down into sandy material and generating localized bulging and dusty patches. Preliminary inspections suggested that the bulk permeability of the rockfill had significantly decreased, potentially compromising slope stability during rapid drawdown conditions due to the development of excess pore pressures.

To evaluate the hydraulic behavior of the degraded rockfill under real field conditions, the Geotechnical Laboratory of CEDEX designed and performed a full-scale in-situ percolation test. Unlike laboratory permeability tests, large-scale field tests preserve the natural porosity, compaction, particle-size distribution, and boundary conditions of the material, providing more representative permeability values. The interpretation of these tests is traditionally based on the analytical solution proposed by Vedernikov (1934), which assumes steady unconfined seepage flow but neglects the influence of unsaturated soil properties.

To assess the validity of this theoretical framework, a numerical model reproducing the percolation test was developed and calibrated. The simulations incorporated unsaturated flow conditions and were used to validate Vedernikov's analytical equations under the specific conditions of the Alcorlo Dam rockfill. The numerical results showed good agreement with the analytical interpretation and confirmed the suitability of the in-situ test methodology for estimating the permeability of weathered and poorly graded rockfills. The combined experimental and numerical approach provides a robust framework for assessing the hydraulic performance and long-term safety of aging rockfill structures.

References

[1] C. Laina-Gómez, D. Escudero-Merino, and E. Asanza-Izquierdo, "Brief insights: In-situ permeability test in weathered and poorly-graded rockfill," in Proceedings of the XVIII European Conference on Soil Mechanics and Geotechnical Engineering (ECSMGE 2024): Geotechnical Engineering Challenges to Meet Current and Emerging Needs of Society, Lisbon, Portugal, 2024.

[2] M. Caballero-Ezquerro and C. Laina-Gómez, "Validación del marco teórico del ensayo de percolación mediante modelización numérica," in 12 Simposio Nacional de Ingeniería Geotécnica, Santander, Spain, Sep. 2026.

[3] P. C. Carman, "Fluid flow through granular beds," Transactions of the Institution of Chemical Engineers, vol. 15, pp. 150–166, 1937.

[4] P. C. Carman, Flow of Gases through Porous Media. London, United Kingdom: Butterworths, 1956.
[5] B. R. Chahar, "Extension of Vedernikov's graph for seepage from canals," Journal of Irrigation and Drainage Engineering, vol. 127, no. 5, pp. 319–322, 2001.
[6] W. R. Gardner, "Some steady-state solutions of the unsaturated moisture flow equation with application to evaporation from a water table," Soil Science, vol. 85, no. 4, pp. 228–232, 1958.
[7] M. E. Harr, Groundwater and Seepage. New York, NY, USA: Dover Publications, 1990, pp. 231–248.
[8] W. A. Jury and W. R. Gardner, Soil Physics, 5th ed. Hoboken, NJ, USA: John Wiley & Sons, 1991.
[9] J. Kozeny, "Über Grundwasserbewegung," Wasserkraft und Wasserwirtschaft, vol. 22, pp. 67–70, 1927.
[10] D. W. Taylor, Fundamentals of Soil Mechanics. New York, NY, USA: John Wiley & Sons, 1948.
[11] V. V. Vedernikov, Seepage from Channels. Moscow, Russia: Gosstroizdat, 1934.

Assessment of inclined dry soil cover systems for reactive mine waste in boreal climatic conditions

Abdalla Saafan[1], Jasmina Toromanovic[1], Jan Laue[1], Christian Maurice[1]

[1] Department of Civil, Environmental and Natural Resources Engineering, Luleå University of Technology, Luleå, Sweden.

abdalla.saafan@ltu.se

In Sweden, 13 metal mines are currently in production, and the large volume of mining waste generated annually, estimated at 127 million tons in 2022, together with long-term mine closure requirements, emphasizes the need for engineered cover systems capable of limiting water and oxygen transport into reactive mine waste. Dry soil cover systems are engineered barriers placed over reactive mine waste to reduce water infiltration and oxygen ingress, thereby limiting sulfide oxidation and the generation of acid mine drainage (AMD). Their performance depends on the interaction between soil hydraulic properties, cover geometry, climatic condition, and material stability.

This study assesses the performance of inclined dry soil cover systems, where slope geometry affects water movement. Compared with horizontal covers, inclined systems develop non-uniform moisture conditions, with lower moisture near the upper slope and greater moisture accumulation downslope. This affects infiltration, run off, and moisture redistribution within the cover profile. Therefore, the cover layer configuration should be adapted to the site geometry to improve maintaining acceptable moisture content. In this context, different designs of sealing layers are used to enhance water retention capacity and reduce infiltration under both saturated and unsaturated conditions.

Acceptable cover performance requires maintaining a high degree of saturation $> 85\%$ and soil hydraulic conductivity $< 10^{-8}$ m/s in the sealing layer. High saturation reduces air-filled porosity and limits oxygen diffusion through the cover. Soil hydraulic properties are commonly described using retention and conductivity models such as those proposed by van Genuchten [6] and Mualem [3]. Special attention is required for problematic soils, particularly swelling soils e.g. bentonite-amended soils. Although such materials initially show low saturated hydraulic conductivity, wetting-induced swelling, which modify the pore structure. which increase effective porosity and reduce cover hydraulic performance. Also, boreal climates add further complexity, which have long winters with snow cover and a short, intense snowmelt period. Infiltration is limited during frozen winter conditions, while summer rainfall and evaporation control the cover water balance.

The proposed assessment is based on data from two field pilot cover systems: one horizontal and one inclined configuration, combined with SEEP/W numerical modelling. The horizontal pilot provides reference information on vertical infiltration and moisture redistribution, while the inclined pilot allows evaluation of slope-related processes such as runoff, and lateral flow. SEEP/W modelling is calibrated and validated by measured field monitoring data, then used to assess how cover geometry and deferent weather condition affect overall cover performance. This approach supports the design of dry soil cover systems for reactive mine waste under cold and boreal climatic conditions by allowing additional design scenarios to be evaluated numerically.

References

[1] Corey, A. T. (1957). Measurement of water and air permeability in unsaturated soil. Soil Science Society of America Journal, 21(1), 7–10. https://doi.org/10.2136/sssaj1957.03615995002100010003x

[2] Geological Survey of Sweden. (2026). Mines in Sweden. SGU — Geological Survey of Sweden. https://www.sgu.se/en/mining-inspectorate/mines/mines-in-sweden/

[3] Mualem, Y. (1976). A new model for predicting the hydraulic conductivity of unsaturated porous media. Water Resources Research, 12(3), 513–522. https://doi.org/10.1029/WR012i003p00513
[4] Nason, P., Alakangas, L., Öhlander, B. (2013). Using sewage sludge as a sealing layer to remediate sulphidic mine tailings: A pilot-scale experiment, northern Sweden. Environmental Earth Sciences, 70, 3093–3105. https://doi.org/10.1007/s12665-013-2369-0
[5] Swedish Environmental Protection Agency. (2025). Waste quantities in Sweden. Swedish Environmental Protection Agency. https://www.naturvardsverket.se/data-och-statistik/avfall/avfallsmangder/
[6] van Genuchten, M. T. (1980). A closed-form equation for predicting the hydraulic conductivity of unsaturated soils. Soil Science Society of America Journal, 44(5), 892–898.
https://doi.org/10.2136/sssaj1980.03615995004400050002x
[7] Yanful, E. K. (1993). Oxygen diffusion through soil covers on sulphidic mine tailings. Journal of Geotechnical Engineering, 119(8), 1207–1228. https://doi.org/10.1061/(ASCE)0733-9410(1993)119:8(1207)

Grain morphology effects on liquefaction-driven submarine landslide

Govind Mishra[1], Vanessa Magnanimo[1], Stefan Luding[1], Hongyang Cheng[1]
[1] University of Twente
g.k.mishra@utwente.nl

Submarine landslides are among the most destructive geohazards in offshore environments, posing serious risks to offshore infrastructure such as subsea cables, pipelines, and foundation systems. Understanding the mechanisms governing their initiation and runout is essential for effective risk mitigation. Although significant research has been devoted to this field, the influence of grain morphology on these processes remains poorly understood. Unlike onshore landslides, submarine landslides initiate on remarkably gentle inclines, making them difficult to anticipate. Liquefaction is widely recognised as the primary triggering mechanism, and under submarine conditions, this process can be further amplified by gas hydrate dissociation. From these aspects, this study develops an experimental framework to investigate how the grain morphology influences the initiation and runout of liquefaction-driven submarine flows through physical modelling.

This framework consists of a rectangular flume in which the granular sample rests under an impermeable layer in a submerged condition. The flume is then tilted to a prescribed angle, progressively driving excess pore pressure build-up within the sample until liquefaction is triggered. The liquefied mass flows over the impermeable base, which also imparts basal friction to the moving material, and eventually comes to rest before reaching the far end of the flume. Throughout this process, pore pressure sensors track the evolution of excess pore pressure, while PIV (Particle Image Velocimetry) captures the kinematics of the flow front. Together, these measurements provide a detailed picture of the initiation, development, and deposition phases of the flow.

A key challenge in laboratory-scale modelling of submarine landslides is reproducing liquefiable behaviour under static conditions. Natural sand requires very high confining pressures to enter the liquefiable state, which is far beyond what a modest water column can provide. To overcome this, LECA (Lightweight Expanded Clay Aggregate) is selected as the model material. Its low bulk density allows it to liquefy under the small stress levels generated by the water column height alone, making it well-suited to the physical modelling. One of the most attractive features of LECA for this study is how particle shape can be controlled within its natural size distribution. The smaller particles within the available grading are used directly as spherical specimens, while the larger ones are simply crushed to produce angular fragments of the same target size. This gives direct control over particle shape without changing the grain size.

Triaxial tests have been carried out on LECA to characterise its mechanical behaviour. These results establish the liquefaction susceptibility envelope and identify the stress and density conditions needed to trigger the flow in the flume. Alongside the physical experiments, numerical investigation has also been conducted using a coupled CFD-DEM framework modelling the interaction between individual particles and the surrounding pore fluid. This provides particle-scale insight into the undrained response of LECA during shearing by capturing the evolution of contact forces and pore pressure. Together, this integrated framework provides a physically controlled platform for systematically isolating the role of grain morphology in submarine, contributing grain-scale insight towards improved geohazard assessment for offshore infrastructure.

Modeling of the poro-viscoplastic behavior of the Callovo-Oxfordian claystone

Corentin Donius[1], Philipp Braun[1], Maxime Pierre[1], Carlos Plúa[2], Siavash Ghabezloo[1]

[1] Navier, ENPC, Institut Polytechnique de Paris, Champs-sur-Marne, France
[2] Andra, Meuse/Haute-Marne Underground Research Laboratory, Bure, France

corentin.donius@enpc.fr

In the context of feasibility studies of the deep underground nuclear waste storage conducted by Andra (Agence nationale pour la gestion des déchets radioactifs), in-depth studies are made on the source rock of the project: the Callovo-Oxfordian claystone (COx). These studies, that aim to assess the rock behavior over the lifespan of the structures, revealed that it may be required to undergo mechanical unloading during the tunnel excavations, as well as heating induced by radioactive waste storage, causing a decrease of effective stress. In addition, the long-term behavior of the rock raises questions. Significant convergence of the test galleries of the underground laboratory (URL) is observed.

To investigate these behaviors of the COx, triaxial tests highlighted significant time-dependent strain, whose rate varies with the deviatoric stress. Moreover, isotropic loading and unloading tests showed the occurrence of plasticity during unloading. A thermo-poro-mechanical model is proposed in this work to account for these phenomena. Based on thermodynamics, the modified Cam-Clay model is extended by incorporating a viscoplastic formulation and a nonlinear kinematic hardening law, following the the Perzyna and Armstrong-Frederick approaches, respectively. Peculiarly, the kinematic hardening combined with the Cam-Clay model allows to generate plastic strain under isotropic loading and unloading conditions. Besides, the nonlinear hardening leads to an increasing viscoplastic strain rate during the loading.

The model is used to simulate thermo-hydro-mechanical couplings occurring in the triaxial and isotropic tests, using MFRONT for the constitutive modeling and FEniCSx for the finite element analysis.

A coordinate-free elliptic general interface model for geomaterial interphases

Alexandros Stathas[1], Matthias Neuner[1]
[1] BOKU University
alexandros.stathas@boku.ac.at

Thin interphase layers play a central role in many geomaterial systems, including gouge-filled faults. In fault mechanics, such localized zones may also host strongly coupled processes, such as thermal pressurization, which control friction during seismic slip [1,2]. Resolving these thin layers with full three-dimensional finite element models is often computationally expensive. Reduced interface formulations, which replace the interphase layer by an effective interface while retaining its dominant effective properties, are therefore useful.

In this contribution, we present a coordinate-free elliptic general interface model for thin geomaterial interphases, based on the variational framework developed in [3]. A key feature of the formulation is that the ellipticity of the proposed interface model is preserved whenever the underlying interphase material is elliptic. Moreover, the model is formulated in a general Cartesian setting, allowing the treatment of arbitrarily oriented interfaces. The proposed framework provides a rigorous basis for the dimension reduction of geomaterial interphases and can be extended to incorporate multiphysics fault-zone processes and nonlinear frictional behaviour.

References

[1] Kanamori, H., Brodsky, E. E. (2004). The physics of earthquakes. Reports on Progress in Physics, 67(8), 1429–1496.
[2] Stathas, A., Stefanou, I. (2023). Fault friction under thermal pressurization during large seismic-slip: Numerical analyses and extension of the model of frictional slip. International Journal of Mechanical Sciences, 248, 108184.
[3] Stathas, A., Neuner, M. (2026). A coordinate-free variational continuum interface model for thin interphases: Ellipticity and convergence analysis. International Journal of Engineering Science, 225, 104553.

Investigation of Air Fluidization during Intruder Penetration in Sand

Bowen WANG[1]

[1] Chair of Geotechnical Engineering and Institute of Geomechanics and Underground Technology

b.wang@gut.rwth-aachen.de

Airflow-assisted penetration offers a promising strategy for reducing resistance in granular media, with direct relevance to geotechnical applications and bio-inspired burrowing robots. However, the mechanisms governing airflow-granular interactions remain poorly understood. To address this knowledge gap, we employ a coupled computational fluid dynamics and discrete element method (CFD-DEM) approach as the primary investigative tool, validated and supplemented by experimental cone penetration tests (CPT) under varying airflow conditions. This integrated approach enables a systematic investigation of the effects of aeration on penetration resistant force. Our results reveal a nonlinear relationship between penetration resistance reduction and depth, wherein resistance approaches near-zero values up to a critical depth, beyond which well fluidization stops. Simulations demonstrate that higher airflow rates enhance the mobilization of overlying particles, thereby increasing the critical depth. A detailed meso- and micro-scale analysis of grain motion, contact forces, and pore air pressure fields further reveals four distinct penetration stages: grain ejection and channel formation, channel sealing, channel refill, and final compaction. Throughout these stages, when pore air pressure is nearly 2 times of lithostatic pressure, the penetration resistant force could drop to zero. This explicit grain-scale linkage between pore air pressure evolution and stress transfer elucidates the fundamental mechanisms behind fluidization-induced reduction in penetration resistant force, providing a quantitative framework for optimizing aeration strategies in geotechnical engineering, excavation technologies, and the design of self-burrowing robots.

References

[1] D. Geldart, “Types of gas fluidization,” Powder Technology, vol. 7, no. 5, pp. 285–292, 1973.
[2] S. Ergun, “Fluid flow through packed columns,” Chemical Engineering Progress, vol. 48, no. 2, pp. 89–94, 1952.Wang, B., Peng, Y., Vergara, Á., Boyle, J. H., and Fuentes, R. ”Investigation of Air Fluidization during Intruder Penetration in Sand”,2026

Paths to critical state under partial drainage

Jochen Zürn[1], Luis Mugele[1], Hans Henning Stutz[1]
[1] Karlsruhe Institute of Technology - Institute of Soil Mechanics and Rock Mechanics
jochen.zuern@kit.edu

The concept of the critical state is fundamental for describing soil behaviour [1]. The path by which this attractor ($\dot{e} = 0$ and $\dot{\boldsymbol{\sigma}} = \mathbf{0}$ for a monotonic loading with $\dot{\boldsymbol{\varepsilon}} \neq \mathbf{0}$) is reached depends on the type of loading. Soil behaviour under fully drained and undrained conditions has been extensively investigated. In contrast, the behaviour under unconventional so-called partially drained conditions has been studied only to a limited extent due to the lack of suitable methods for testing controlled partially drained loading paths. However, many geotechnical problems in practice lead to partially drained soil behaviour and consequently to loading paths deviating from the classical drained and undrained cases. The objective of this study is to investigate how the critical state line (CSL) is approached under partially drained loading paths compared to conventional drained and undrained conditions.

A novel experimental method for triaxial testing under partially drained conditions has recently been proposed [2]. In this approach the degree of drainage can be controlled by adjusting the pore fluid compressibility using a defined enclosed gas volume. This method enables rate-independent partially drained conditions while preserving the assumptions of an element test. Details of the test setup are provided in [2].

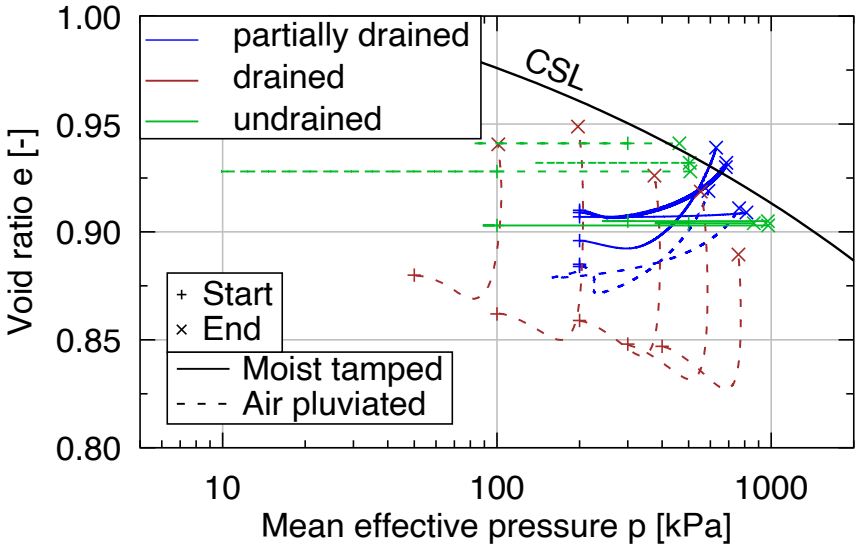
In the present study, partially drained monotonic triaxial tests on Karlsruhe fine sand from [2] are re-analysed. All tests considered started from the same initial mean effective pressure $p = 200\,\mathrm{kPa}$ using initially medium-dense specimens with initial void ratios in the range $0.884 \leq e_0 \leq 0.910$. The selected tests include specimens prepared by both moist tamping and air pluviation. The degree of drainage was varied across the tests. For comparison, drained and undrained triaxial tests on medium-dense specimens of Karlsruhe fine sand from [3] were also considered. All experiments reached an axial strain of $\varepsilon_1 \geq 20\ \%$ and the corresponding end states are therefore considered to be close to the critical state line.

Figure 1 shows the loading paths of the specimens in the $e - \log p -$ plane. The critical state line $e_\mathrm{c}(p)$ can be described by the Bauer compression law [4] $e_\mathrm{c}(p) = e_{\mathrm{c}0}\exp\left(-\left(3p/h_\mathrm{s}\right)^n\right)$ with $e_{\mathrm{c}0} = 1.054$, $h_\mathrm{s} = 4000\,\mathrm{MPa}$ and $n = 0.27$. The corresponding material parameters for the compression relationship were adopted from [3].

The results show that all specimens in the partially drained, drained, and undrained tests converge towards the critical state line. However, the loading path differs significantly depending on the drainage condition. In particular, in the partially drained tests, the loading paths vary depending on the imposed degree of drainage and lie between the conventional drained and undrained test results. These findings highlight the influence of the degree of drainage on the path towards the critical state line.

References

[1] A. N. Schofield and C. P. Wroth, "Critical State Soil Mechanics," McGraw-Hill, 1968.
[2] J. Zürn, L. Mugele, and H. H. Stutz, "Novel experimental method for rate-independent triaxial tests under partial drainage condition," Geotechnique Letters, vol. 14, no. 3, pp. 100–105, 2024, doi: 10.1680/jgele.23.00120.
[3] T. Wichtmann, " Soil behaviour under cyclic loading - experimental observations, constitutive description and applications," Habilitation, Karlsruher Institut für Technologie, Institut für Bodenmechanik und Felsmechanik, Heft 181, Karlsruhe, Germany, 2016.



Loading paths in the $e - \log p -$ plane *for initially medium-dense Karlsruhe fine sand under drained, undrained, and partially drained conditions [2,3].*

[4] E. Bauer, "Calibration of a Comprehensive Hypoplastic Model for Granular Materials," Soils and Foundations, vol. 36, no. 1, pp. 13–26, 1996, doi: 10.3208/sandf.36.13.

Hybrid DLVO/CGMD approach for THM modelling of clay particles in COx formation

Alissar Alrifai[1], Alice Di Donna[1], Majdouline Laanaiya[1]
[1] Univ. Grenoble Alpes, CNRS, Grenoble INP, 3SR, 38000, Grenoble (France)
alissar.alrifai@3sr-grenoble.fr

The Callovo-Oxfordian claystone (COx) was selected by ANDRA (Agence nationale pour la gestion des déchets radioactifs) as the host rock formation for the French Industrial Centre for Geological Disposal (Cigéo proejct). Its clay matrix is mainly composed of illite and smectite particles, and these latter are the main responsible for its low permeability, self-sealing capacity and long-term stability, which have driven the choice. A good understanding of these characteristics, and more generally of the thermo-hydro-mechanical (THM) behavior of COx, are fundamental to ensuring the safety of such storage systems.

The macroscopic responses are strongly influenced by mechanisms occurring at smaller scales, especially at the level of clay particles. In particular, processes like water adsorption and electrostatic interactions between clay platelets play a key role, but are still not fully captured by most existing macroscopic models, especially when temperature effects are involved.

In this context, this work aims to develop a mesoscale modeling framework to better describe clay behavior by explicitly accounting for mineralogical characteristics and solid–fluid interactions at the molecular scale. The proposed approach is based on a hybrid model combining an extended version of the DLVO (Derjaguin, Landau, Verview, and Overbeek) theory, which describes electrostatic interactions between charged clay particles separated by a fluid, with coarse-grained molecular dynamics (CGMD). More precisely, the interaction energy (Coulombic + Van der Walls) obtained with the extended DLVO for various configurations will be used as an input to describe the particles interactions in the CGMD model.

The standard DLVO theory is valid for interparticle separation distances greater than approximately 1 nm (Gonçalves et al., 2026), while at shorter distances, which are governing the behavior in swelling clays, additional interactions become significant, and a modified DLVO formulation is needed. The extended formulation proposed by Gonçalves et al. (2026) was selected for this work. This extended formulation includes in the Coulombic component the variation of the relative permittivity of water as a function of the particles distance, the hydration free energy of ions (Born effect) and the steric effects (ions volume). These effects lead to strong nonlinearities in the DLVO equations and require numerical solutions.

The extended DLVO model proposed by Gonçalves et al. (2026) was implemented in a Finite Element solver and first validated against the results provided by the same authors for infinite parallel smectite clay particles. Then, the model was applied to finite particles in 3D configurations, to investigate the influence of particles geometry and size. Three particle geometries—square, elliptical, and hexagonal—were considered (an example for hexagonal particles in face-to-face configuration is provided in Figure 1). Based on the first numerical results (Figure 2a) and some experimental observations (Cadène et al. (2005), Tong et al. 2024) the elliptical geometry was found to be reasonably representative of COx clay particles. Considering the size, the first results show a significant effect of particles size on the interaction energy (Figure 2b). Further studies are ongoing to develop a full database of interaction energy for various configurations (face-to-face, edge-to-face, edge-to-edge, ..) and various temperature, to be introduced the CGMD model.

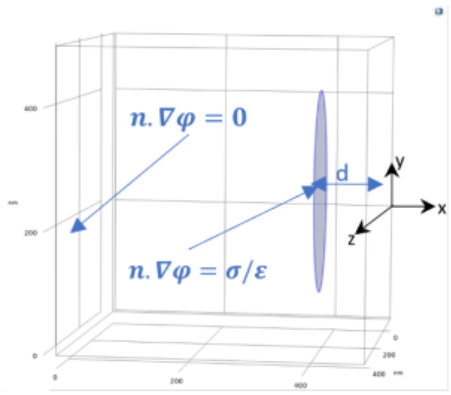


Figure 1 FEM model of elliptical particles in a face-to-face configuration using a half-model based on geometric symmetry. Here, d denotes half the separation distance between the particles, ϕ the electrical potential, n the surface normal vector, σ the surface charge density, and ε the dielectric permittivity. The computational domain has dimensions 500 × 500 × 500 nm³.

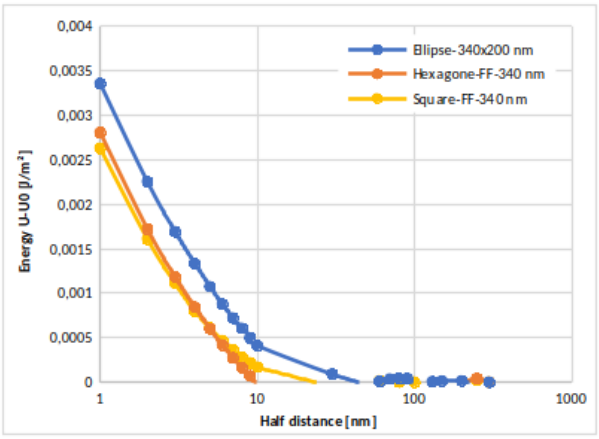


Figure 2a Coulombic energy vs interparticle distances for different particle shapes

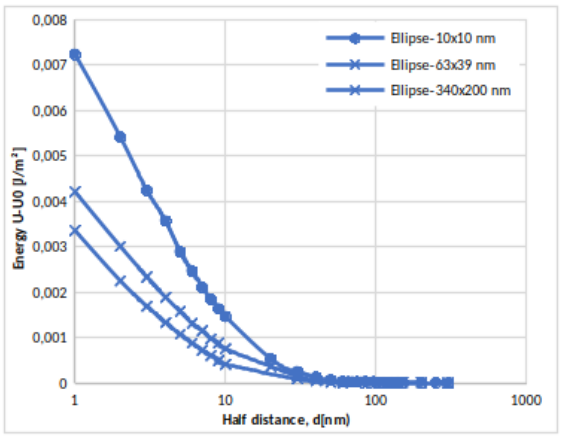


Figure 2b Coulombic energy vs interparticle distances for different elliptical particle sizes

References

[1] Gonçalvès, J., Rouil, L., Gaboreau, S., Robinet, J.-C., & Talandier, J. (2026). Reassessment of DLVO theory at sub-nanometric scale: Application to Na-smectite. Applied Clay Science, 279, 108049. https://doi.org/10.1016/j.clay.2025.108049

[2] Cadène, A., Durand-Vidal, S., Turq, P., & Brendle, J. (2005). Study of individual Na-montmorillonite particles size, morphology, and apparent charge. Journal of Colloid and Interface Science, 285(2), 719–730. https://doi.org/10.1016/j.jcis.2004.12.016

[3] Tong, K.-W., Yu, F., Dai, Z.-J., Wang, H., Huang, K., Chen, S.-X., & Guo, J.-H. (2024). Micro-level unloading behaviors of clay aggregates: A coarse-grained molecular dynamics study. Powder Technology, 443, 119922. https://doi.org/10.1016/j.powtec.2024.119922

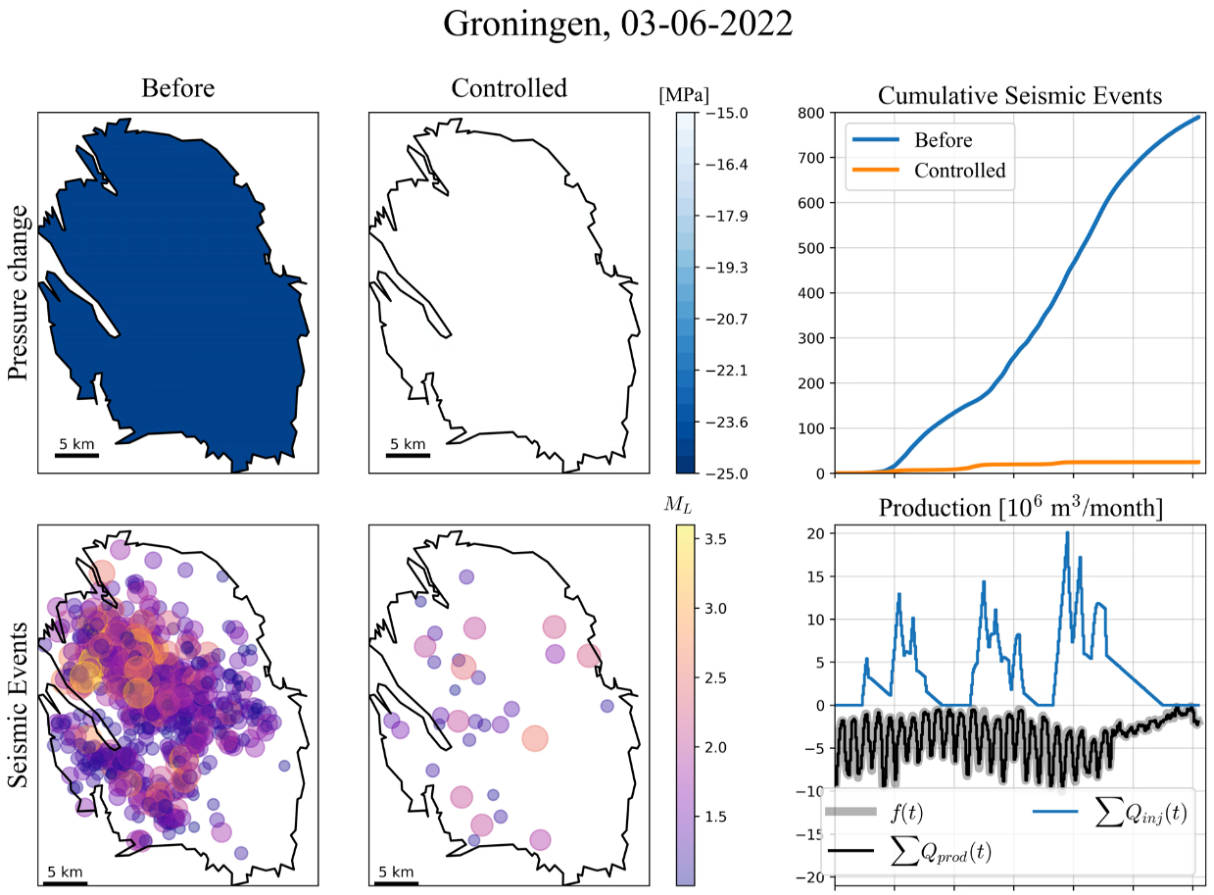
On the control of Groningen's induced seismicity: stochastic and discrete-time extensions

Diego Gutiérrez-Oribio[1], Ioannis Stefanou[1]
[1] ENSTA Paris, Institut Polytechnique de Paris
diego.gutierrez@ensta.fr

The Groningen gas field represents a well-documented benchmark for studying and mitigating induced seismicity generated by long-term gas extraction. This work presents stochastic and discrete-time extensions of a control-oriented framework for reducing seismic activity in such an underground reservoir. The physical model combines pressure diffusion with Dieterich's seismicity-rate formulation. To account for the discrete and random nature of earthquakes, induced events are interpreted as a non-homogeneous Poisson process, with temporal event generation, spatial sampling by thinning, and magnitudes drawn from a Gutenberg–Richter distribution fitted to the observed catalog. A robust feedback controller, based on a MIMO generalized super-twisting algorithm, updates well fluxes at discrete sampling times using seismic measurements. Two scenarios are considered: extraction-only operation, where seismicity can only be limited through production reduction, and combined extraction–injection operation, where the controller actively redistributes fluxes to reduce seismic activity. The results show that discrete-time sampling, saturation constraints, and stochastic event generation provide more realistic simulation conditions, while robust feedback control can reduce induced seismicity and adapt production strategies. The study also highlights the limitations of smeared seismicity-rate models and motivates future developments involving control direction uncertainty, porodynamics, and robust control of discrete faults.

References

[1] M. Acosta, J.-P. Avouac, J. D. Smith, K. Sirorattanakul, H. Kaveh, and S. J. Bourne, "Earthquake nucleation characteristics revealed by seismicity response to seasonal stress variations induced by gas production at Groningen," Geophysical Research Letters, vol. 50, no. 19, Art. no. e2023GL105455, 2023, doi: 10.1029/2023GL105455.
[2] E. R. Heimisson, J. D. Smith, J.-P. Avouac, and S. J. Bourne, "Coulomb threshold rate-and-state model for fault reactivation: Application to induced seismicity at Groningen," Geophysical Journal International, vol. 228, no. 3, pp. 2061–2072, 2022, doi: 10.1093/gji/ggab467.
[3] D. Gutiérrez-Oribio and I. Stefanou, "Control of human-induced seismicity in underground reservoirs governed by a nonlinear 3D PDE-ODE system," arXiv preprint, arXiv:2412.06327, 2024, doi: 10.48550/arXiv.2412.06327.
[4] D. Gutiérrez-Oribio and I. Stefanou, "A control framework for induced seismicity mitigation in Groningen gas reservoir," arXiv preprint, arXiv:2604.26802, 2026, doi: 10.48550/arXiv.2604.26802.
[5] T. Kim, D. Gutiérrez-Oribio, I. Stefanou, M. Acosta, and J.-P. Avouac, "Single-well based control and optimization of hydraulic stimulation and induced seismicity: Application to the Otaniemi geothermal project," Geothermics, vol. 132, Art. no. 103396, pp. 1–19, 2025, doi: 10.1016/j.geothermics.2025.103396.



Feedback control limits Groningen induced seismicity by adjusting production and activating injection under discrete-time updates.

Extending the H-model to Mechanics of Permafrost

Vincent Guigonnet[1], Jérôme Aubry[1], François Nicot[1]
[1] ISTerre, Université Savoie Mont Blanc, Le Bourget-du-Lac, France
vincent.guigonnet@univ-smb.fr

Permafrost, ground remaining at or below 0°C for at least two consecutive years, underlies about 25% of the Northern Hemisphere land surface and 10–20% of the area above 2000 m a.s.l. in the French Alps [1]. Its degradation under climate warming drives slope instability and threatens mountain infrastructure [2]. Its mechanical strength is governed by four coupled parameters: temperature, ice content, strain rate, and confining pressure.

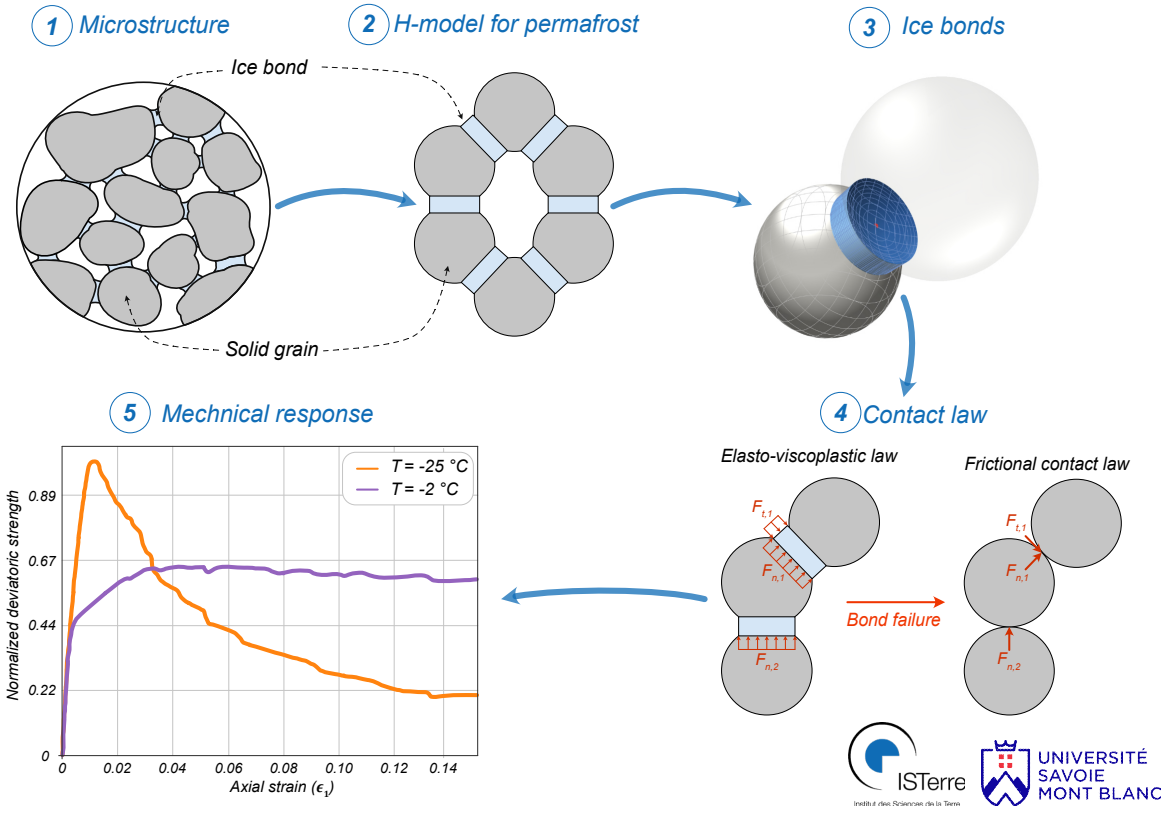
Experimental data show a near-exponential strength increase with decreasing temperature, a non-monotonic trend with ice content, power-law strengthening with strain rate following Glen's flow law [3], and a confining-pressure dependence restricted to low ice contents.

Existing models often treat temperature and ice content as scalar modifiers rather than resolving grain-scale mechanisms. This work adapts the H-model [4], a multi-scale, mesodirectional constitutive framework, to permafrost. Following an approach developed for dense snow [5], ice bonds cylinders capped by hollow hemispherical surfaces are added in parallel with grain-grain contacts, linking microstructural geometry to ice content. These bonds contribute stiffness and cohesion until failure in tension, compression, or shear, governed by temperature-dependent criteria calibrated from pure ice data [6].

Biaxial simulations qualitatively reproduce the expected cohesion-to-friction transition, the ductile-to-brittle transition, and the strength minimum at intermediate ice fractions, confirming the model's ability to capture permafrost's multi-parametric physics. Next steps include quantitative calibration, cold-chamber UCS testing, and finely FEM/FDM implementation for slope-scale simulations.

References

[1] J. Obu et al., "Northern Hemisphere permafrost map based on TTOP modelling for 2000–2016 at 1 km2 scale," Earth-Science Reviews, vol. 193, pp. 299–316, 2019, doi: 10.1016/j.earscirev.2019.04.023.
[2] P.-A. Duvillard, L. Ravanel, M. Marcer, and P. Schoeneich, "Recent evolution of damage to infrastructure on permafrost in the French Alps," Regional Environmental Change, vol. 19, pp. 1281–1293, 2019, doi: 10.1007/s10113-019-01465-z.
[3] J. W. Glen, "Experiments on the deformation of ice," Journal of Glaciology, vol. 2, no. 12, pp. 111–114, 1952, doi: 10.3189/S0022143000034067.
[4] F. Nicot and F. Darve, "The H-microdirectional model: Accounting for a mesoscopic scale," Mechanics of Materials, vol. 43, no. 12, pp. 918–929, 2011, doi: 10.1016/j.mechmat.2011.07.006.
[5] M. Miot, A. Wautier, P. Polfer, P. Philippe, T. Fülöp, and F. Nicot, "Mechanics of densely packed snow across scales: A constitutive modelling strategy based on the 3-D H-model," Journal of Glaciology, vol. 71, p. e62, 2025, doi: 10.1017/jog.2024.112.
[6] A. M. Fish and Y. K. Zaretsky, "Ice strength as a function of hydrostatic pressure and temperature," Defense Technical Information Center, Fort Belvoir, VA, 1997, doi: 10.21236/ADA333030.



From soil microstructure to H-model cells with ice bonds, contact-scale failure law, and simulated stress-strain response under varying temperature.

Increase in granular drag forces near boundaries

Mahsa Azizi[1], Pierre Rognon[1], François Guillard[1]
[1] The University of Sydney
mahsa.azizi@sydney.edu.au

Predicting and understanding granular drag force is important in several geotechnical and industrial applications, including excavation, mixing, and underground locomotion. Earlier studies have established models supported by experiments that capture this force when the moving object is far from boundaries. However, several applications as well as experimental setups involve objects moving near boundaries. Whether and how the presence of boundaries affects granular drag force remains to be established.

To investigate this, we experimentally study the drag force experienced by a rod moving horizontally in a packing of glass beads under quasi-static conditions. Results show that the drag force increases substantially as the rod approaches a rigid front boundary. In contrast, the increase in drag force is much weaker when the rod moves closer to a lateral boundary. Based on these findings, we propose a phenomenological granular-lubrication model that describes the evolution of drag force near the boundary. It includes an exponential increase of the drag force when approaching the boundary, with a characteristic length scale determined by the rod diameter and the glass beads size. This model is found to be valid for various rod sizes, glass bead sizes, and rod embedment depths. This model, somewhat reminiscent of lubrication forces in viscous fluids, complements the established models capturing granular drag forces far from boundaries.

Testing the validity of a nonlinear kinematic hardening model with data-driven identification

Ludovic Druette[1,2], Jérémy Bleyer[1], Siavash Ghabezloo[1], Goustan Bacquaert[2]
[1] Laboratoire Navier, École nationale des ponts et chaussées, Univ. Gustave Eiffel, CNRS, Champs-sur-Marne, France
[2] Électricité de France, R&D Division, Palaiseau, France
ludovic.druette@enpc.fr

The assessment of the seismic safety of earth-fill dams requires numerically robust constitutive laws for geomaterials that are suitable for finite element simulation at the structural scale. These simulations require the constitutive model to reproduce the cyclic behavior of undrained sand. As a first step, the focus is placed on the cyclic behavior of drained sand.

The cyclic behavior of drained sand exhibits a Bauschinger effect that is classically modeled using kinematic hardening in elastoplastic constitutive laws. The Armstrong-Frederick kinematic hardening model is a nonlinear kinematic hardening widely used to model the cyclic behavior of metals [2] [3]. Despite its simplicity and popularity, this model remains underexploited in the geomaterials community.

This study evaluates the suitability of the Armstrong-Frederick kinematic hardening to model the deviatoric behavior of drained sands under cyclic loading. The focus is restricted to the deviatoric behavior; volumetric behavior and consolidation will be addressed in future work. Specifically, we assess the model's ability to reproduce variations in the secant shear modulus and the damping ratio for strain amplitudes ranging from 10^{-6} to 10^{-2}.

A single Armstrong-Frederick mechanism produces exponential stress-strain curves that saturate at large plastic strains [3], leading to overestimated damping ratios. To overcome this limitation and reproduce non-saturating behavior across the full strain range of interest, multiple kinematic hardening mechanisms are combined. However, each additional mechanism introduces two parameters, significantly increasing the complexity of the calibration.

To expedite parameter identification and validate the model for drained sand, we adopt a data-driven approach implemented through the Python library Jaxmat [4]. This library is specifically designed for the integration of solids constitutive laws and uniquely leverages machine learning tools, particularly automatic differentiation. This functionality enables us to compute gradients of cost functions that incorporate the integration of nonlinear constitutive behavior, and perform gradient descent optimization of model parameters.

The approach is validated against synthetic data generated using Hujeux's model [1], calibrated for dense Hostun sand. This dataset consists of 29 simple shear tests with distinct amplitudes ranging from 10^{-6} to 10^{-2}. The multi-mechanism model has then been optimized to reproduce the 29 stress-strain curves of these tests.

Results demonstrate that the stress-strain curves generated by the optimized model are in good agreement with the reference data, both qualitatively and quantitatively. Consequently, the damping ratio and secant shear modulus are also accurately reproduced.

Future work will focus on modeling the volumetric behavior and evaluating the model on several stress paths. Efforts will also be made to test the data-driven identification with experimental data instead of synthetic data.

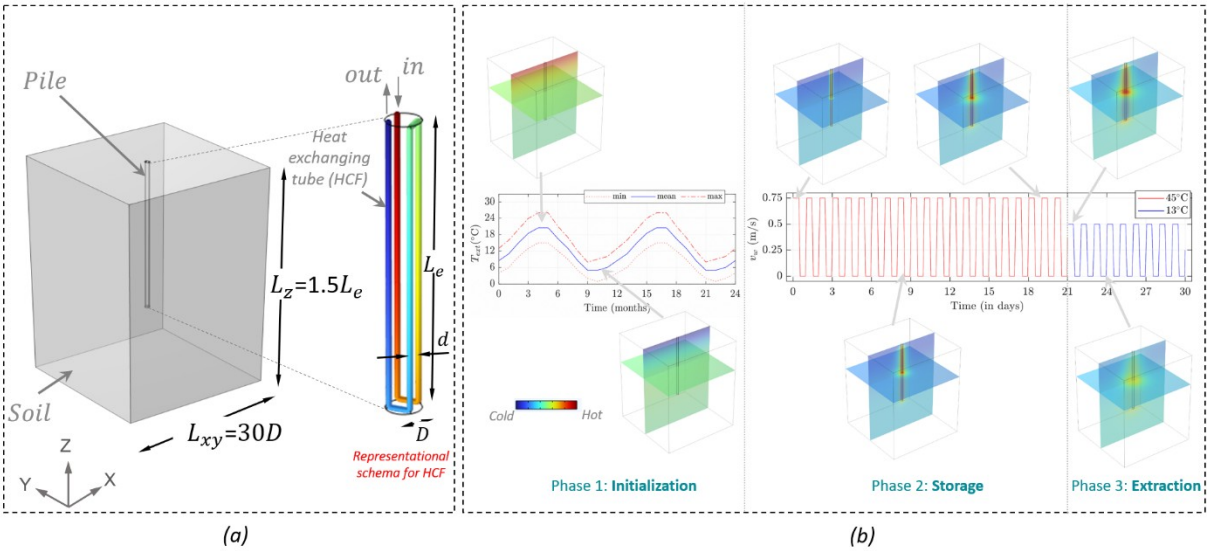
References

[1] J.-C. Hujeux, "Une loi de comportement pour le chargement cyclique des sols," Génie Parasismique, pp. 287–302, 1985.
[2] C. O. Frederick and P. J. Armstrong, "A mathematical representation of the multiaxial Bauschinger effect," Mat. at High Temp., vol. 24, no. 1, pp. 1–26, Apr. 2007, doi: 10.3184/096034007X207589.
[3] J. Besson, G. Cailletaud, J.-L. Chaboche, and S. Forest, Non-Linear Mechanics of Materials, vol. 167. in Solid Mechanics and Its Applications, vol. 167. Dordrecht: Springer Netherlands, 2010. doi: 10.1007/978-90-481-3356-7.
[4] J. Bleyer, P. Bouteiller, and J. S. Hale, jaxmat. (Apr. 12, 2026). Zenodo. doi: 10.5281/ZENODO.17611833.

Numerical exploration for feasibility of heat storage in the ground via energy piles

Mattia Garza[1], Ritesh Gupta[1], Alice Di Donna[1]
[1] UGA - Laboratoire 3sr
mattia.garza@3sr-grenoble.fr

In conventional applications of energy geostructures (such as piles, diaphragm walls, or tunnels), heat is transferred into the ground and then extracted using a heat transfer fluid to meet heating and cooling needs for buildings. The use of alternative heat sources, such as solar technologies, can lead to an imbalance between available heat and energy demand due to seasonal temperature variations. In many cases, this results in surplus heat production in the summer and reliance on the electrical grid in the winter. Storing this surplus heat in the ground using energy geostructures is a promising area of research [1, 2]. While this represents a major advancement in the use of energy geostructures, a key question remains: is this approach viable while considering: (1) the influence of soil conditions, (2) the impact of surface temperature performance, and (3) the optimization of the heating/unloading thermal profile? These elements are essential for assessing the feasibility and profitability of the process [3]. In this work, these three aspects are studied using numerical modeling with COMSOL Multiphysics software, applied to an energy pile. The efficiency of heat storage and release is numerically evaluated (equivalent experimental full-scale energy is also constructed, awaiting exploitation). A dynamic controller schema is implemented for mode (storage/extraction) switches based on thermal performance indicators. A parametric study is carried out to express the relative influence of the constituent parameters. This study contributes to improving the understanding and efficiency of heat storage in the ground by coupling energy geostructures with other renewable heat sources.



Numerical model of the energy pile: (a) pile–soil system, including a schematic representation of the heat exchange tube, and (b) evolution of heat transfer in the soil over the three phases of the investigation.

References

[1] Rotta Loria, A. F. (2021). The thermal energy storage potential of underground tunnels used as heat exchangers. Renewable Energy, Vol. 176, pp. 214–227. https://doi.org/10.1016/j.renene.2021.05.076
[2] Dupray F., Laloui L., Kazangba A. (2014). Numerical analysis of seasonal heat storage in an energy pile foundation, Computers and Geotechnics, Vol. 55, pp.67–77. https://doi.org/10.1016/j.compgeo.2013.08.004
[3] Gupta R., and Di Donna A. (2026). Modélisation numérique pour l'étude de la rentabilité du stockage de chaleur dans le sol grâce aux géostructures énergétiques. 13èmes Journées Nationales de Géotechnique et de Géologie de l'Ingénieur (JNGG), Grenoble, France, avril 2026.
https://jngg2026.sciencesconf.org/668120/document

Neural constitutive models under hard thermodynamic constraints and differentiable finite-element solvers

Edoardo Fabbrini[1], Vincent Acary[1], Filippo Masi[1]

[1] Univ. Grenoble Alpes, Inria, CNRS, Grenoble INP, Institute of Engineering, LJK, 38000 Grenoble, France

edoardo.fabbrini@inria.fr

Machine learning has offered new routes to discovering constitutive models directly from measurement data. However, existing physics-informed and data-driven approaches often lack a rigorous thermodynamic structure or achieve consistency only within specific constitutive classes, leaving open the question of their applicability across a broad range of material behaviours.

This work presents a framework for learning inelastic constitutive models under hard thermodynamic constraints [1], extends it to equivariant formulations, and integrates the learned models into a computationally efficient, fully differentiable finite-element (FE) solver.

The learning framework builds on non-equilibrium thermodynamics, enforces objectivity through a reduced set of invariant representations, and imposes energy balance and non-negative dissipation as hard, scalable constraints. At the material-point level, analytical benchmarks, including rate dependence, hardening, and non-associative flow, show that the learned models remain thermodynamically admissible and generalise to unseen loading paths. The framework is also applied to granular media using discrete-element simulations as virtual experiments [2]. From macroscopic stress–strain histories, the approach identifies admissible constitutive representations and predicts cyclic responses, including the emergence of hysteresis absent from the training set.

Building on these results, the learned neural constitutive models are embedded within an FE framework coupling FEniCS [3] and PyTorch to assess their predictive performance in the solution of boundary-value problems. The focus lies on the time integration of the evolution equations induced by the transport operator and on the consistent tangent operator required by implicit FE schemes. The tangent is computed via automatic differentiation combined with the implicit function theorem, avoiding differentiation through the individual integration steps and thereby improving the computational efficiency of the FE solver. Numerical experiments under various multiaxial loading paths are compared against analytical constitutive laws to validate both the framework and its implementation. Finally, an equivariant formulation is introduced to extend the objectivity guarantees from controlled material-point loading paths to the arbitrary loading orientations encountered in boundary-value problems.

The resulting framework provides a bridge from thermodynamically constrained constitutive identification to robust, objective, and fully differentiable finite-element simulations of history-dependent materials.

References

[1] F. Masi, "Learning inelastic constitutive models from stress–strain data under hard thermodynamic constraints," arXiv, 2026, doi: 10.48550/arXiv.2605.16837.

[2] F. Masi and I. Stefanou, "Physics-Informed and Thermodynamics-Based Neural Networks", Machine Learning in Geomechanics 2 (eds I. Stefanou and F. Darve), 2024, doi: 10.1002/9781394325665.ch3.

[3] I. A. Baratta, J. P. Dean, J. S. Dokken, M. Habera, J. S. Hale, C. N. Richardson, M. E. Rognes, M. W. Scroggs, N. Sime, and G. N. Wells. DOLFINx: The next generation FEniCS problem solving environment (2023).

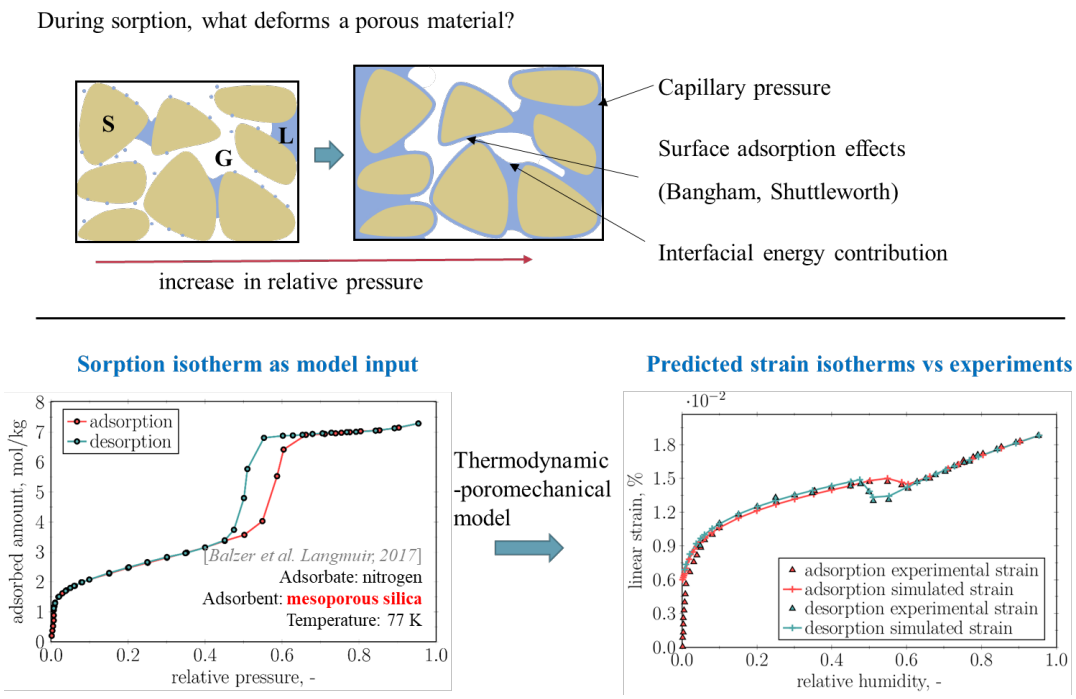
Modeling of sorption-induced deformations of porous materials

Jingyi LENG[1], Patrick DANGLA[1], Laurent BROCHARD[1], Matthieu VANDAMME[1]

[1] Navier, ENPC, Institut Polytechnique de Paris, Univ Gustave Eiffel, CNRS, Marne-la-Vallée, France

jingyi.leng@enpc.fr

A clear understanding of the physical mechanisms underlying sorption-induced deformation in porous materials is essential for predicting the mechanical response of solid matrices encountered in civil engineering and energy geotechnics. To describe the drying shrinkage of partially saturated porous materials with broad pore size distributions, we extend the poromechanical model proposed by El Tabbal et al. (2020) within a thermodynamic framework accounting for capillary forces, the Bangham effect, and the Shuttleworth effect. We demonstrate that several sources of uncertainty—namely the choice of cavitation pressure, the experimentally defined dry state, and the estimation of BET-specific surface area—have negligible influence on the resulting shapes of strain isotherms. The model is validated using sorption experiments reported by various authors for a wide range of adsorbent–adsorbate systems. Without introducing any fitting parameters, the proposed approach successfully reproduces the characteristic shapes of sorption-induced deformation isotherms in silicates, cementitious materials, coals, clays, and wood.



References

[1] El Tabbal, G., Dangla, P., Vandamme, M., Bottoni, M., & Granet, S. (2020). Modelling the drying shrinkage of porous materials by considering both capillary and adsorption effects. Journal of the Mechanics and Physics of Solids, 142, 104016. https://doi.org/10.1016/j.jmps.2020.104016 [2] Leng, J., Dangla, P., & Vandamme, M. (2026). Modeling of sorption-induced deformations of porous materials due to surface adsorption, capillary effects, and cavitation. International Journal of Solids and Structures, 327, 113808. https://doi.org/10.1016/j.ijsolstr.2025.113808

Implementation of rough contact models in modelling the direct shear behaviour of Crushed Waste Glass

Xinran Zhang[1], Yi Pik Helen Cheng[1]

[1] Civil, Environmental and Geomatic Engineering, University College London, London

xinran.zhang.20@ucl.ac.uk

Crushed waste glass (CWG) has been considered a potential alternative to natural sand because of its recyclability and geomechanical properties that are comparable to those of natural aggregates [1]. CWG particles generally exhibit irregular shapes, this study first captures the three-dimensional geometries using X-ray micro-computed tomography (μCT) . A representative particle whose morphological parameters corresponded to the 50% cumulative distribution values was then selected as the chosen geometry.

Based on the chosen particle geometry, direct shear tests on the CWG sample were simulated using the discrete element method (DEM) with clump. By introducing different contact constitutive models, the influence of particle surface roughness on the direct shear response was investigated. The contact models include the simplified Hertz–Mindlin model built into PFC, as well as the Otsubo et al. (2015) [2] rough contact model and its modified form implemented through a C++ user-defined constitutive model. The parameters n1 and n2 in the modified Otsubo model were automatically calibrated based on normal contact tests of glass ballotini [3].

The simulation results indicate that , due to the contact responses under medium and strong contact-force states are relatively similar, their influence of roughness on the shear strength at larger shear strains is limited. Meanwhile, (n_1) and (n_2) have a significant effect on the volumetric strain response. Higher values of n_1 and n_2 gives higher the rough contact area, leads to a higher probability in the weak-force , and more contacts will appear in the asperity-dominated and transitional stages by the end of shearing.

References

[1] A.Mohajerani, J. Vajna, T. H. H. Cheung, H. Kurmus, A. Arulrajah and S. Horpibulsuk, “Practical recycling applications of crushed waste glass in construction materials: A review”. Construction and Building Materials, 156, 443-467, Year 2017, doi:10.1016/j.conbuildmat.2017.09.005

[2] M. Otsubo, C. O’sullivan, W.W.Sim and E. Ibraim, ”Quantitative assessment of the influence of surface roughness on soil stiffness”. Géotechnique, 65(8), 694-700, Year 2015, doi: 10.1680/geot.14.T.028

[3] Cavarretta, I., Coop, M. and O’SULLIVAN, C., ”The influence of particle characteristics on the behaviour of coarse grained soils”. Géotechnique, 60(6), pp.413-423. Year 2010, doi: 10.1680/geot.2010.60.6.413

Crushing behavior of sand grains with Voronoi-based heterogeneous initial damage: a peridynamics investigation

Guangzhi Li[1], Takashi Matsushima[1]

[1] Department of Engineering Mechanics and Energy, University of Tsukuba, Tsukuba, Japan

s2530209@u.tsukuba.ac.jp

This study develops a lightweight peridynamics (PD) solver for simulating the crushing of individual sand grains. The solver implements the ordinary state-based linear peridynamics solid (LPS) formulation proposed by Silling et al. [1], irreversible critical-stretch bond failure (damage model), and grain-platen contact (contact model). Its performance is evaluated against the benchmark study of Zhu and Zhao [2], using uniaxial compression of a 1.5 mm spherical grain between two opposing platens. The comparison considers the load-displacement response, loading-rate dependence of the maximum contact force, characteristic crushing strength, contact-initiated damage evolution, and the resulting orange-slice splitting pattern. The solver reproduces the reported response trends, force and strength magnitudes, and principal fracture morphology with satisfactory agreement.

Conventional PD simulations of grain crushing frequently rely on homogeneous grains or pre-defined weak planes, which may constrain crack initiation and propagation. To generate more natural and stochastic fracture networks, a Voronoi-based heterogeneous initial-damage framework is therefore introduced. Voronoi tessellation partitions the grain into internal domains and controls the scale and density of heterogeneous regions, whereas a decay power factor governs the radial localization of initially broken bonds relative to Voronoi-cell boundaries: larger exponents concentrate damage near the boundaries, while smaller exponents distribute it farther into cell interiors. Five Voronoi-cell levels (2, 8, 32, 128, and 512) and five decay-factor levels (0.25, 1, 4, 16, and 64) are investigated. Combined with three Voronoi seeds and three repeated simulations for every parameter combination, the balanced orthogonal factorial design comprised 225 cases. The results show that the proposed initial damage scheme effectively promotes spontaneous child grain formation. Cracks preferentially nucleated from and propagated through initially damaged regions, producing between two and ten child grains. Compared with the homogeneous control, the scheme caused only modest changes in peak stress, although the overall mean peak stress is slightly higher. Even when the Voronoi cell number and decay factor are identical, changing the tessellation seed substantially altered the number and morphology of child grains. Nevertheless, the simulated fragmentation patterns remained consistent with the irregular crushing behavior of natural grains. The proposed framework therefore provides a physically interpretable and computationally practical route for representing grain-to-grain variability and natural initial defects in large-scale studies of granular crushing.

References

[1] S. A. Silling, M. Epton, O. Weckner, J. Xu, and E. Askari, "Peridynamic states and constitutive modeling," Journal of Elasticity, vol. 88, no. 2, pp. 151–184, 2007, doi: 10.1007/s10659-007-9125-1.

[2] F. Zhu and J. Zhao, "A peridynamic investigation on crushing of sand particles," Géotechnique, vol. 69, no. 6, pp. 526–540, 2019, doi: 10.1680/jgeot.17.P.274.

Deterioration and Damage Features of Rock Masses within the Fluctuating Zone of Three Gorges Reservoir Area under Complex Dynamic Water Conditions

Zhiqiang YI[1,2,3], Yueping YIN[3], Gonghui WANG[4], Shouding LI[5], Tianqiao MAO[5], Xuebing WANG[6]

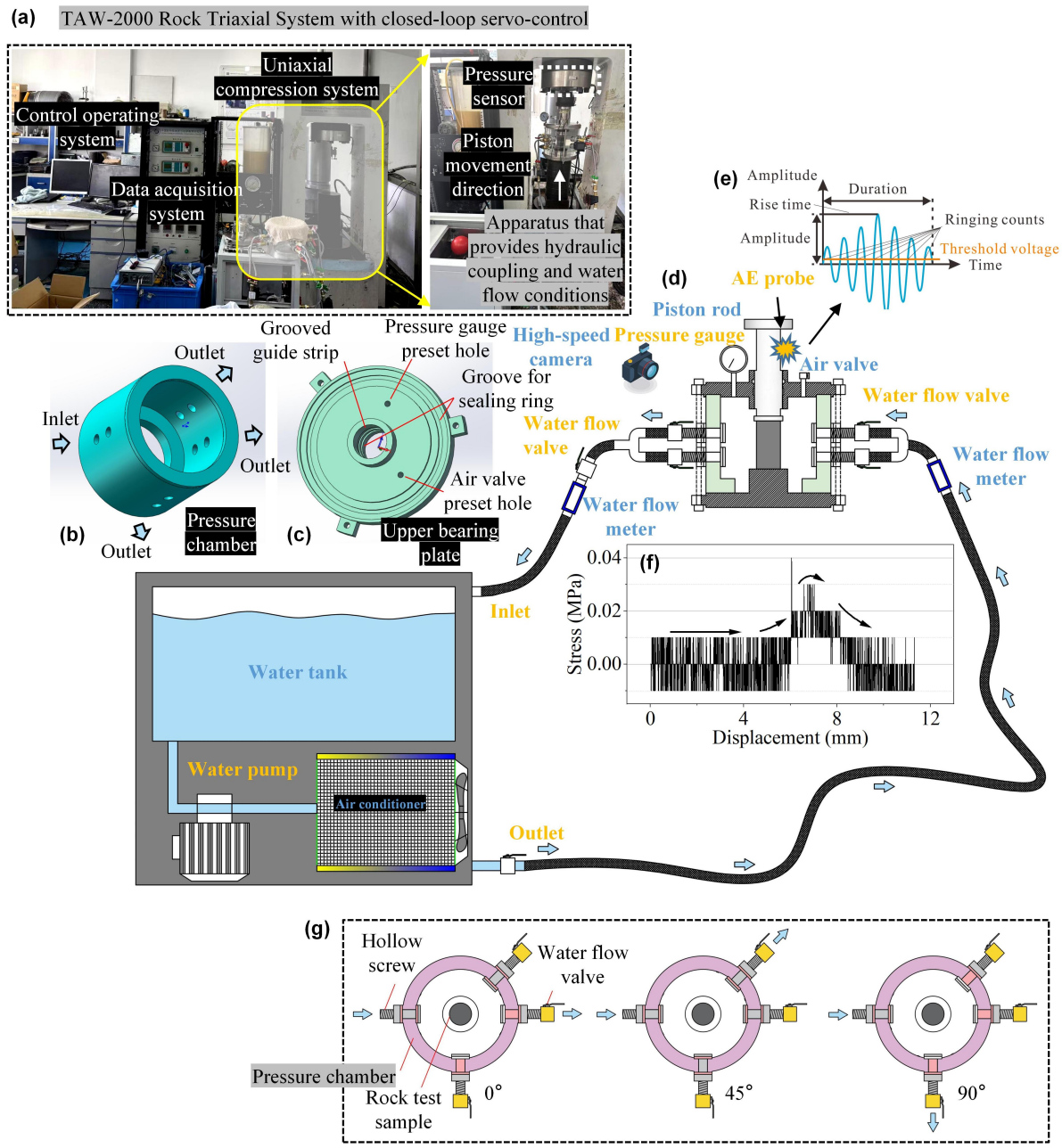
[1] Chinese Academy of Geological Sciences, Beijing 100037, China
[2] China University of Geosciences (Beijing), Beijing 100083, China
[3] China Institute of Geo-Environment Monitoring, Beijing 100081, China
[4] Disaster Prevention Research Institute, Kyoto University, Kyoto 6110011, Japan
[5] Institute of Geology and Geophysics, Chinese Academy of Sciences, Beijing 100029, China
[6] Nanjing Hydraulic Research Institute, Nanjing 210029, China

zhiqiang_yi@outlook.com

Keywords: High and steep dangerous submerged rocks, rock mechanics test, complex dynamic water conditions, deterioration and damage features.

A series of rock mechanics tests have been conducted on the rock masses within the fluctuating zone of Three Gorges Reservoir Area in China. This study designed and fabricated an apparatus that provides hydraulic coupling and water flow conditions. Under complex dynamic water conditions, the stress-time curves demonstrate instantaneous failure characteristics and progressive failure characteristics under varying numbers of Dry-Wet Cycles (DWC). When the number of DWC is relatively low (DWCs=1, 2, 8), an increase in water flow velocity results in higher elastic modulus and peak stress. Specifically, the elastic modulus and peak stress increase in the order of 2, 6, and 10 L/min, while for different water flow impact angles (DWCs=1 and 2), they increase in the order of 0°, 90°, and 45°. Consequently, the trends in the elastic modulus and peak stress are reversed when the number of DWC is relatively high. Under all testing conditions, the fracture modes of the argillaceous limestone are classified as "mixed mode I and II fracturing". In both the drying and hydraulic coupling conditions, tensile fractures dominate. However, in the saturated and water flow conditions, there is a transition in crack types towards a predominance of shear fractures.

Acknowledgments: This work was supported by National Natural Science Foundation of China (Grant U2244227).



Rock mechanics strength testing system: (a) Photograph of the testing system; (b) Pressure chamber; (c) Upper bearing plate; (d) Apparatus that provides hydraulic coupling and water flow conditions; (e) AE characteristic curve; (f) Stress-displacement curve of the piston rod sidewall; and (g) Schematic diagram of testing conditions for different water flow impact angle.

Geobattery: a dimensionless criterion for seasonal heat storage in flooded mine workings

Ali Ahmadi[1]

[1] Geomechanics and Multiphysical Systems (GEMS), Institute of Geotechnology and Mineral Resources, TU Clausthal

ali.ahmadi@tu-clausthal.de

Flooded mine workings are being reconsidered as underground heat stores [1]. The need is seasonal: in Germany's 50 Hz zone, 89 % of the 2023 photovoltaic surplus arrived between May and July, while heat demand peaks in November to February and vanishes from June to August. Bridging that gap means holding heat for months; we ask whether a real mine drift's bare geometry suffices.

Our test case is a surveyed drift at the Reiche Zeche research mine, Freiberg, under a hypothetical ten-year duty cycle: charging at 80 C for 61 d, sealing for 123 d, discharging at 10 C for 61 d, recovering for 120 d. The geometry is real; the cycle is invented. We solve conjugate heat transfer, one temperature field over water, rock, concrete and air on a Taylor-Hood Stokes flow [2] computed once and frozen, plus a one-way thermoelastic response $\sigma_{ij,j} = 0$.

As built, the drift fails this test. Within one storage phase the conduction front penetrates $\sqrt{\alpha_r t} \approx 3.87$ m into the gneiss, well past the effective radius $L_c = 2V/A$ of 1.05 m, so the wall settles near 37 C and the year returns only 7.3 %. This generalises: retention depends only on the Fourier number and the conductivity and capacity ratios, so absolute size drops out and surface-to-volume is the criterion. Seasonal retention needs 0.59 m^{-1}; this drift offers 1.91 m^{-1}, a gap closed only by a wider chamber ($L_c \geq 3.4$ m) or a drift array.

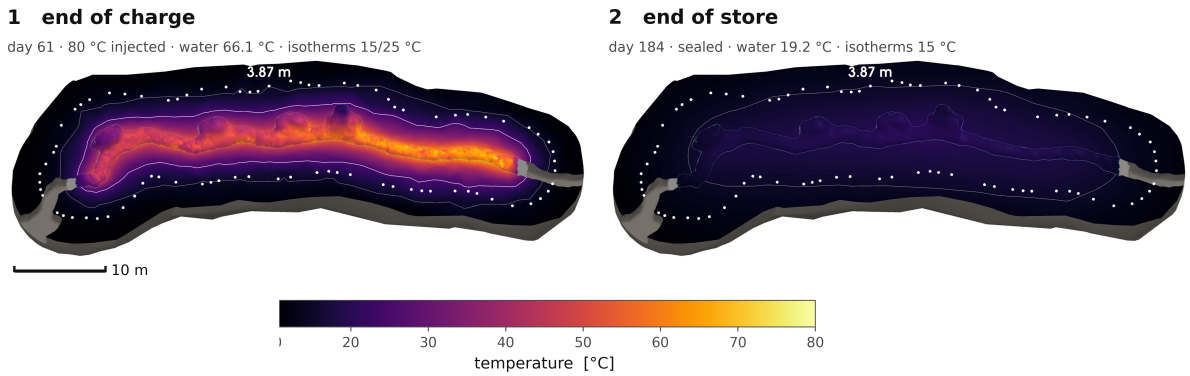
Five decade-long 3-D runs test the remedies. Doubling the radius pre-warms the near rock and lifts the per-cycle return from 16 % to 23 %. Warming the rock from 10 C to 30 C leaves retention unchanged, because conduction is linear, yet raises the delivered water to 46 C; a linear decomposition separates the geothermal share. What works is removing the far-field sink. As the unit cell of a 10 m pitch array with adiabatic symmetry planes, the drift retains nearly all the injected heat once the rock saturates: the annual return climbs from 27 % to 98.5 %, settling after about six cycles. Since a closed cell loses no heat, its balance approaches unity; the informative outputs are the approach time and the grade: 58 C stored, 25 C delivered.

Three numerical issues kept surfacing. Heat crossing a temperature-pinned boundary is not the nodal gradient but the reaction on the constrained degrees of freedom, the consistent boundary flux of Carey and co-workers as given by Gresho et al. [3], closing the balance to 10^{-6} kWh per phase. Dirichlet values on sealed faces over-constrain shared corner nodes, so the no-flux condition enters weakly by penalty [4]. Incompressibility leaves the discrete Stokes operator symmetric indefinite [5], forcing a memory-bound direct factorisation that caps mesh refinement.

A single flooded drift of the size common in old metal mines is thus a monthly buffer, not a seasonal store. Geometry sets how much heat returns and rock temperature sets its grade, both readable from the survey before any simulation.

References

[1] J. Menendez, A. Ordonez, R. Alvarez, and J. Loredo, "Energy from closed mines: underground energy storage and geothermal applications," Renewable and Sustainable Energy Reviews, vol. 108, pp. 498–512, 2019, doi: 10.1016/j.rser.2019.04.007.



Year-1 charge (left) and storage (right): the stored heat spreads into the surrounding rock, not the water.

[2] C. Taylor and P. Hood, "A numerical solution of the Navier-Stokes equations using the finite element technique," Computers & Fluids, vol. 1, pp. 73–100, 1973.
[3] P. M. Gresho, R. L. Lee, R. L. Sani, M. K. Maslanik, and B. E. Eaton, "The consistent Galerkin FEM for computing derived boundary quantities in thermal and/or fluids problems," International Journal for Numerical Methods in Fluids, vol. 7, no. 4, pp. 371–394, 1987, doi: 10.1002/fld.1650070406.
[4] I. Babuska, "The finite element method with penalty," Mathematics of Computation, vol. 27, pp. 221–228, 1973.
[5] M. Benzi, G. H. Golub, and J. Liesen, "Numerical solution of saddle point problems," Acta Numerica, vol. 14, pp. 1–137, 2005.

Grain morphological effects on the pullout response of soil-geogrid interface

Amrisha KHANDELWAL[1], Debayan BHATTACHARYA[1], J.T. SHAHU[1], Manoj DATTA[1]
[1] Civil and Environmental Engineering, Indian Institute of Technology Delhi, New Delhi, India
cez228139@iitd.ac.in

The design of geogrid-reinforced soil structures greatly depends on the interface behaviour of the granular backfill and the geogrid reinforcement. Current design practices, largely overlook the influence of this critical particle shape aspect on the soil–geogrid interaction mechanism, thereby introducing a significant amount of uncertainty in the estimation of pullout resistance and the interface friction parameters [1]. Grain morphological characteristics have been well recognized as fundamental feature governing the mechanical behaviour of frictional materials, i.e., the macro-scale global system response emanates from the underlying micromechanical signatures. Several quantitative shape-based indices including Wadell's sphericity, roundness, aspect ratio, and convexity, etc. are already available in existing literature to characterize the morphology of particulate media [2,3]. A few studies asserting the influence on shear strength, dilatancy of granular assemblies under monotonic loading [4,5] shed some light on particle shape aspects. However, the specific role of particle shape in the context of soil–geogrid interface which is central to the mobilization of pullout resistance remains largely unexplored. To address this gap on the pullout response of soil–geogrid interface we take recourse to 3-Dimensional Discrete Element Method. The discrete granular setting owing to its formulation inherently captures particle-scale kinematics and contact force evolution for the soil–geogrid interaction under pullout loading conditions [6,7,8]. Here we first benchmark the DEM model against existing laboratory geogrid pullout test results. Thereafter, four distinct granular assemblies with varying morphology indices were generated using polyhedra, enabling a controlled investigation of the isolated effect of particle shape on the soil-geogrid interface response.

Our initial results point out to the fact that both pullout resistance and the interface friction coefficient are strongly dependent on particle shape feature e.g., true sphericity in the present study. Notably, both the parameters exhibit a decreasing trend with increasing sphericity. Consequently, it suggests that the relatively angular particles, characterized by lower sphericity measures generate enhanced interlocking with the geogrid apertures and develop greater passive resistance against the transverse ribs. Furthermore, micromechanical analyses of the granular specimen composed of these "avatar paradigms" reveal that shear band thickness and particle rotation are also functions of the shape indices, with lower-sphericity (i.e., predominantly angular) particles exhibiting thicker shear zones and greater rotational restraint This may primarily be attributed to the interlocking mechanism at the soil-geogrid interface. Our findings across multiple "length-scales" highlight the importance of incorporating particle shape characteristics into the pullout design framework for geosynthetic-reinforced soil structures.

References

[1] FHWA, Design and Construction of Mechanically Stabilized Earth Walls and Reinforced Soil Slopes–Volume I, Technical Report, 2009.
[2] G. C. Cho, J. Dodds, and J. C. Santamarina, "Particle shape effects on packing density, stiffness, and strength: Natural and crushed sands," Journal of Geotechnical and Geoenvironmental Engineering, vol. 132, no. 5, pp. 591–602, 2006.
[3] H. Wadell, "Volume, shape, and roundness of rock particles," The Journal of Geology, vol. 40, no. 5, pp. 443–451, 1932.

[4] H. Shin and J. C. Santamarina, "Role of particle angularity on the mechanical behavior of granular mixtures," Journal of Geotechnical and Geoenvironmental Engineering, vol. 139, no. 2, pp. 353–355, 2013.
[5] W. H. Zhou, X. Y. Jing, Z. Y. Yin, and X. Geng, "Effects of particle sphericity and initial fabric on the shearing behavior of soil–rough structural interface," Acta Geotechnica, vol. 14, no. 6, pp. 1699–1716, 2019.
[6] G. Gao and M. A. Meguid, "Effect of particle shape on the response of geogrid-reinforced systems: Insights from 3D discrete element analysis," Geotextiles and Geomembranes, vol. 46, no. 6, pp. 685–698, 2018.
[7] C. Miao, Y. Jia, J. Zhang, and J. Zhao, "DEM simulation of the pullout behavior of geogrid-stabilized ballast with the optimization of the coordination between aperture size and particle diameter," Construction and Building Materials, vol. 255, p. 119359, 2020.
[8] Y. Jia, J. G. Zornberg, J. Zhang, J. J. Zheng, and Y. Zheng, "DEM evaluation of the mobilization of mechanisms governing the geogrid-aggregate interaction," Computers and Geotechnics, vol. 176, p. 106742, 2024.

THCM Feedbacks In Volcanic Edifices: Bridging Transport-Driven Alteration To Mechanical Factor Of Safety

Jens Niclaes[1], Poulet Thomas[2], Delmelle Pierre[1], Rattez Hadrien[1]
[1] UCLouvain
[2] CSIRO
jens.niclaes@uclouvain.be

Hydrothermal circulation in volcanic environments drives complex multiphysics interactions that fundamentally reorganize the physical, hydraulic, and mechanical properties of host rocks. Circulating fluids replace primary minerals with secondary clay- and silica-rich assemblages, inducing strong spatial heterogeneities in matrix porosity, unit weight, and shear strength. Concurrently, these self-organizing alterations restructure internal permeability, promoting localized pore-pressure build-up that can ultimately trigger unheralded volcanic flank collapse. Despite its critical role in geohazard assessment, the feedback loop linking fluid flow, alteration damage, and mechanical stability remains computationally prohibitive to model at the regional scale using fully kinetic reactive transport schemes.

In this work, we present a sequential Thermo-Hydro-Chemo-Mechanical (THCM) modeling framework to evaluate the stability of highly altered volcanic edifices. Thermo-hydraulic fluid circulation is simulated using the finite element framework MOOSE/PorousFlow, dynamically coupled to an evolving permeability field governed by a transport-based Rock Alteration Index (RAI). Serving as a reduced-complexity proxy for cumulative thermodynamic disequilibrium, the RAI transiently updates matrix porosity and Kozeny-Carman permeability throughout the simulation. Our results demonstrate massive spatial self-organization: progressive hydrothermal sealing of the surrounding lowlands focuses fluid flow toward the edifice interior, generating localized fluid overpressures and highly heterogeneous, "jigsaw-like" alteration shells along the volcanic flanks.

To quantify the direct structural consequences of these emergent patterns, the end-state physical distributions resulting from the THC simulations—encompassing spatially varying unit weights, elevated pore pressures, and local mechanical degradation mapped directly to accumulated alteration intensity—are extracted. This highly heterogeneous matrix state is directly embedded into a secondary geomechanical model to perform a localized stability assessment and determine the overall Factor of Safety (FoS) of the volcanic slope. By bridging the gap between transport-driven alteration patterns and macroscopic mechanical strength reduction, this framework offers a rigorous, computationally tractable approach to assess the stability of self-organizing natural geological edifices.

Gravity-driven granular rheology with cloned particles and its impact behaviour with safety measures

Prity Dhanai[1], Debayan Bhattacharya[1]

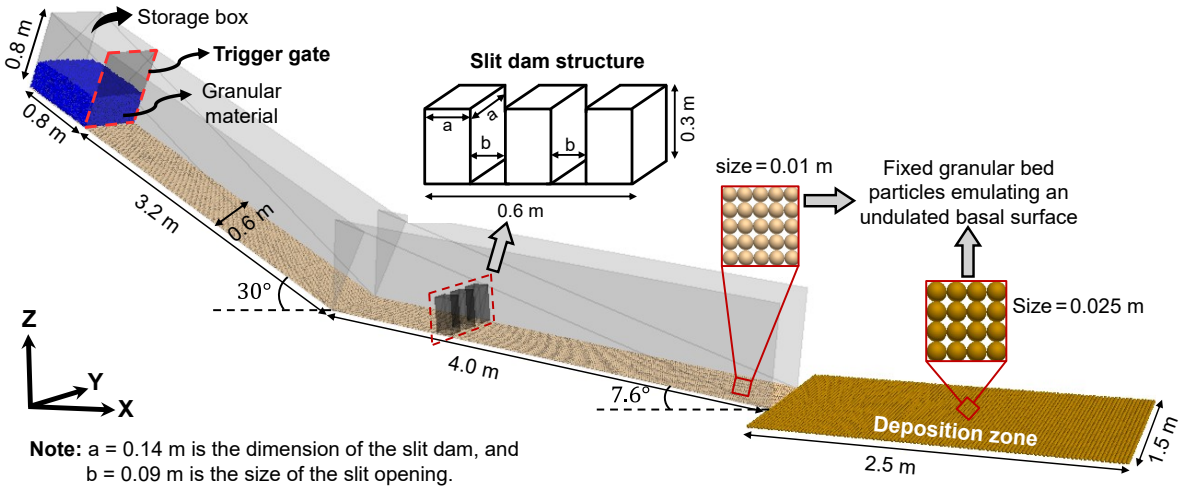
[1] Department of Civil & Environmental Engineering, Indian Institute of Technology Delhi, New Delhi, 110016, India

cez218673@iitd.ac.in

Gravity-driven geophysical mass flow events, e.g., landslides, debris flows, etc., involve rapid downslope movement of geomaterials. To reduce the destructive potential of such catastrophic events, slit dams are widely employed because of their ability to quickly dissipate the flow energy while partially retaining the relatively coarser particles and simultaneously allowing a controlled portion of the granular mass to pass through the slits [1]. Previous studies have shed some light on the interaction between granular flows and mitigation structures. Nevertheless, particle shape effect on granular rheology in conjunction with impact dynamics remains underexplored [2]. Here, we resort to a 3D Discrete Element Method (DEM)-based micromechanical framework to gain a mechanistic understanding of the role of "avatar paradigms" or "cloned" particle morphologies and basal undulations (replicated by a square lattice arrangement of spherical particles to the flume base) in dry granular flows impacting the barrier system. We conduct our numerical experiments in a bi-planar inclined flume setting adopted after Gong et al. (2021) [1], which features a steep upstream section transitioning into a gentler flume downstream. By and large, it closely mimics the natural topographic irregularities with bumpy actions commonly encountered in granular flow pathways in an actual field scenario. Grain morphology characteristics have been evaluated using particle shape-based indices, e.g., Wadell's true sphericity (ψ_T) measure that characterizes the deviation of particles from an ideal spherical shape.

We first benchmark our results against Gong et al.'s study using conventional spherical particles and then extend it to actual "cloned" granular morphologies incorporating non-spherical particle shapes. Our initial findings indicate that decreasing ψ_T significantly enhances geometric interlocking among granular media, thereby increasing internal shear resistance and reducing the overall flow mobility. Consequently, the "cloned avatar paradigm" assemblies exhibit relatively lower flow velocities and reduced kinetic energy than their spherical counterparts. Micromechanical analyses further reveal that particle morphology strongly influences the evolution and distribution of contact force chains during flow propagation and impact. Variations in force-chain intensity measures, along with normal contact orientation, alter the force transmission paths to the slit dam, thereby affecting the impact forces (e.g., peak and residual components) exerted on the slit dam. Moreover, flows composed of particles with lower sphericity exhibit greater retention behind the slit dam due to reduced flow transfer through the slit openings. This increased trapping efficiency results in higher residual forces (in case of actual cloned particles) acting on the barrier compared to flows consisting only of perfectly spherical particles ($\psi_T = 1$). This study offers new insights into the micro–macro relationship between particle morphology, granular rheology on an undulated bumpy base, and impact behaviour against mitigation structures. We emphasize the critical importance of incorporating non-spherical particle shapes or consideration of "surrogate" granular morphology interaction into the design and analysis of protective barriers for geophysical mass flows. Insights obtained from this study envision contributing to the optimized design of slit dam geom-

etry and improving the resilience and effectiveness of mitigation systems in hazard-prone regions that are on the rise in this dynamic and erratic climate-change scenario.



Schematic representation of flume geometry (adopted after Gong et al., 2021)

References

[1] M. Marchelli, A. Leonardi, M. Pirulli, C. Scavia. (2020), "On the efficiency of slit-check dams in retaining granular flows", Géotechnique, 70(3), 226-237, https://doi.org/10.1680/jgeot.18.P.044

[2] S. Gong, T. Zhao, J. Zhao, F. Dai, G. G. Zhou (2021), "Discrete element analysis of dry granular flow impact on slit dams", Landslides, 18(3), 1143-1152. https://doi.org/10.1007/s10346-020-01531-2

Bio-Inspired Cone Pressuremeter propulsion as active soil-structure interface problem in planetary regolith exploration

Harsha Vardhan Kurugodu[1], Debayan Bhattacharya[1], Prashanth Vangla[1], David Frost[2]

[1] Indian Institute of Technology Delhi
[2] Georgia Institute of Technology

cez218277@iitd.ac.in

Planetary subsurface exploration requires energy-efficient penetration mechanisms that can advance reliably under limited payload and reaction force. With the recent renewed interest in planetary explorations, terra-mechanics aimed at community infrastructure settlements in the Lunar and Martain environments, it is no longer restricted to science-fiction stories. Bio-inspired penetration strategies offer a promising alternative by using staged propulsion mechanisms, such as radial expansion, contraction, and controlled probe advancement, rather than relying only on continuous external push. In this study, we investigate the mechanics of a multicycle Bio-Inspired Cone Pressuremeter (BICP) propulsion in dense to loose granular regolith under reduced-, terrestrial-, and hyper-gravity conditions. This problem is interpreted as a soil-structure interface problem, where the probe does not merely penetrate the surrounding material; rather, repeated loading and unloading modify the interface zone around the probe, enabling subsequent advancement into the regolith. The BICP probe combines the functions of a cone penetrometer in conjunction with a pressuremeter module within a single staged system. Each propulsion cycle consists of pressuremeter module expansion, followed by contraction, and subsequent probe advancement. During these stages, the probe-regolith interface experiences complex changes in the normal stress, stress relaxation, local densification or dilation, and unloading-reloading responses [1]. These mechanisms are strongly influenced by probe–granular media interface roughness. Accordingly, smooth and rough probe configurations are examined to evaluate how interface condition modifies the regolith response around the BICP system. To simulate this multistage process [1], we take recourse to the Material Point Method (MPM), a hybrid Eulerian-Lagrangian framework well-suited for large deformation penetration problems with evolving contact conditions. The soil regolith is modelled using a combined isotropic-kinematic hardening plasticity based constitutive relationship within the critical-state-framework [2, 3]. Furthermore, we ensure that the small-strain stiffness has been formulated within an energy-conserved mechanism, and it is nonlinear in nature [4]. While an isotropic hardening reliably takes into account the state-dependent changes in strength and confinement, it cannot fully capture the directional memory, stress reversal, and cyclic translation of the loading surface induced by repeated pressuremeter expansion and contraction. A combined isotropic-kinematic hardening formulation enables the model to account for both evolving material state and loading-direction memory within the probe-regolith interface zone. Our numerical scheme considers loose as well as dense regolith states subjected to varying gravitational acceleration. The initial findings highlight that gravity controls the initial stress field and confinement level, and therefore influences stiffness, strength, dilatancy, stress relaxation, and cyclic recovery around the BICP probe. The numerical experiments examine the coupled action of gravity and interface roughness on the cone resistance, pressuremeter reaction, stress relaxation in the granular media near the cone tip, and accumulated deformation around the module. The results provide insight into the mechanics by which

bio-inspired probes use cyclic interface modification to advance through granular media. More broadly, this work frames multicycle BICP propulsion as an active soil-structure interface mechanics problem, where the evolving transition zone between the probe and the surrounding regolith governs penetration resistance, cyclic mobility, and the feasibility of lightweight subsurface exploration systems for planetary applications.

References

[1] H. V. Kurugodu, D. Bhattacharya, P. Vangla, and J. D. Frost, "Numerical investigation of compound bio-inspired cone pressuremeter probe mechanisms with Material Point Method," Computers and Geotechnics, vol. 179, Art. no. 107013, 2025, doi: 10.1016/j.compgeo.2024.107013.

[2] Z. Mróz and S. Pietruszczak, "A constitutive model for sand with anisotropic hardening rule," International Journal for Numerical and Analytical Methods in Geomechanics, vol. 7, no. 3, pp. 305–320, 1983, doi: 10.1002/nag.1610070304.

[3] S. Pietruszczak and D. F. E. Stolle, "Modelling of sand behaviour under earthquake excitation," International Journal for Numerical and Analytical Methods in Geomechanics, vol. 11, no. 3, pp. 221–240, 1987, doi: 10.1002/nag.1610110302.

[4] P. V. Lade and R. B. Nelson, "Modelling the elastic behaviour of granular materials," International Journal for Numerical and Analytical Methods in Geomechanics, vol. 11, no. 5, pp. 521–542, 1987, doi: 10.1002/nag.1610110507.

A data-driven machine learning approach for decision-making in the context of abandoned underground mines

Fernan Villanueva Zavala[1], Lina Maria Guayacan Carrillo[1], Nathalie Conil[2], Jean Sulem[1], Jean-Michel Pereira[1]

[1] École nationale des ponts et chaussées

[2] Institut national de l'environnement industriel et des risques (INERIS)

fernan.villanueva@enpc.fr

France faces significant public safety and environmental risks from abandoned shallow underground mines, a threat exacerbated by climate change. Traditional prediction methods struggle with the complex, non-linear factors triggering mine collapses, while machine learning (ML) solutions are often hindered by their "black-box" lack of transparency. This PhD project addresses these challenges by developing a transparent decision-support framework to assist Ineris and local communities. The project utilizes an Ineris dataset containing over 4000 documented French mine collapses. The primary objectives are to build a high-quality, ML-ready database utilizing synthetic data generation to overcome data sparsity, and to develop interpretable predictive models using ensemble methods (such as Random Forest and XGBoost) [1] alongside Symbolic Regression [2].

Methodology

Evidence from previous works suggested that mine stability depends heavily on pillar strain-softening [3], structural discontinuities [4], excavation and pillar geometry, and depth [5]. However, relying solely on these established parameters is insufficient for accurate prediction, as collapses are frequently precipitated by hidden variables and triggering factors that this study must unveil. Consequently, to capture these complex geomechanical responses, the project's first approach integrates the Ineris inventory [6] with a historical underground mine database [7]. The robust data processing pipeline includes Standardizing data formats, extracting temporal features, and removing uninformative variables; Mitigating class imbalance through targeted undersampling; Implementing strict feature engineering and StandardScaler normalization to actively prevent data leakage and multicollinearity.

Preliminary results

Benchmarking tests demonstrated that a tuned Random Forest classifier significantly outperformed baseline models. The model yielded highly encouraging results:

- It achieved 87% accuracy, a 0.79 AUC, and 100% recall, identifying all historical collapse cases without producing any false negatives.
- It identified multilevel excavation, geological variables (like karst presence and pillar health), and structural geometry as the most critical collapse predictors.

To operationalize these predictive outputs, the project established a probability-of-failure (PoF) risk stratification matrix (see Figure).

When tested against 74 historical cases, the framework successfully categorized 24 as critical, 28 as high risk, and 22 as low-moderate risk, proving its viability for practical field applications.

Expected results

Ultimately, this thesis will deliver a novel, curated database augmented by hybrid techniques that synergize physics-based synthetic data with statistical oversampling. Its most significant practical contribution is the delivery of an interpretable, equation-based

decision-support tool. By prioritizing transparency through Symbolic Regression, this tool successfully bypasses conventional black-box algorithms, empowering engineers and public authorities to make evidence-based, trusted decisions regarding critical safety investments.

Stable	Low-moderate	High	Critical
<15% PoF	15-60% PoF no surface damage	≥60% PoF no structure affected	≥60% PoF surface structures damaged

Risk stratification matrix.

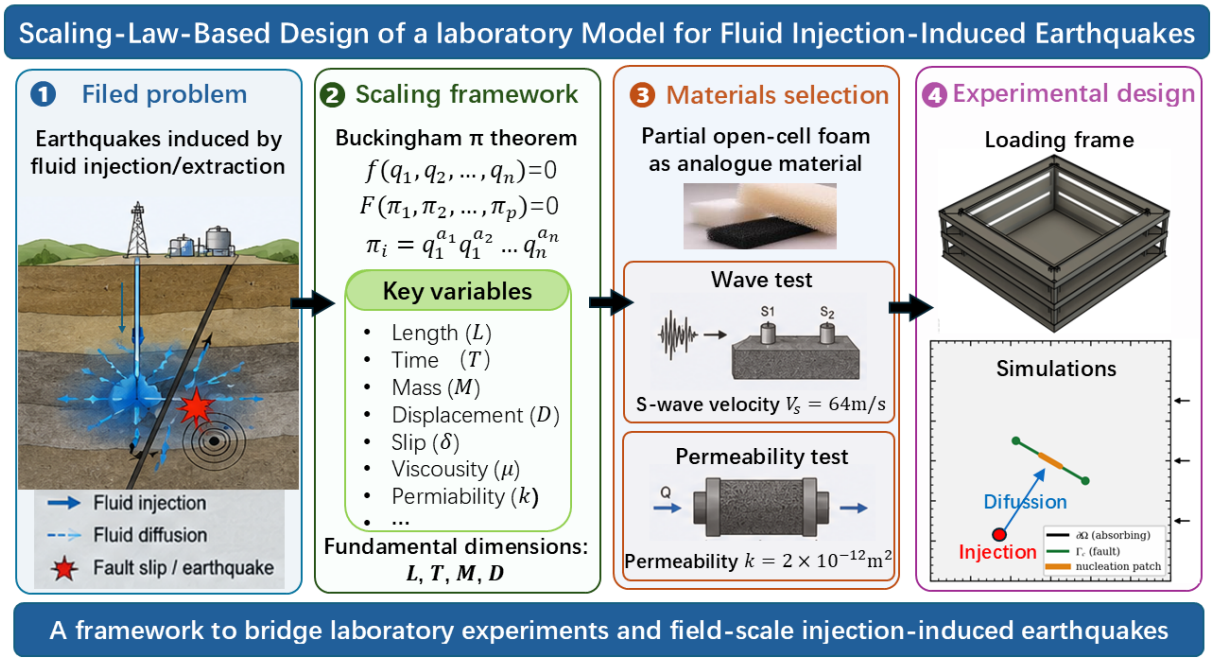
References

[1] Guayacán-Carrillo, LM., Conil, N., Kadri, A. (2025). Using Machine Learning for Predicting Collapse extending in Abandoned Underground Mines. EUROCK 2025. Trondheim, June 2025.
[2] Stephens, T. (2022). Welcome to gplearn's documentation! —gplearn 0.4.2 documentation. URL: https://gplearn. readthedocs. io/en/stable.
[3] Mortazavi, A., Hassani, F., Shabani, M. (2009). A numerical investigation of rock pillar failure mechanism in underground openings. Computers and Geotechnics, 36(5), 691–697.
https://doi.org/10.1016/j.compgeo.2008.11.004
[4] Esterhuizen, G. S., Tyrna, P. L., Murphy, M. M. (2019). A case study of the collapse of slender pillars affected by through-going discontinuities at a limestone mine in Pennsylvania. Rock Mechanics and Rock Engineering, 52(12), 4941 4952. https://doi.org/10.1007/s00603-019-01959-6
[5] Winn, K., Wong, L. N. Y., Alejano, L. R. (2019). Multi-approach stability analyses of large caverns excavated in low-angled bedded sedimentary rock masses in Singapore. Engineering Geology, 259, 105164.
https://doi.org/10.1016/j.enggeo. 2019.105164
[6] Conil, N., Gombert, P. (2024). Amélioration de la connaissance des mécanismes d'instabilité et de l'impact du changement climatique sur les carrières souterraines abandonnées en France: premiers résultats - Ineris.
https://www.ineris.fr/fr/amelioration-connaissance-mecanismes-instabilite-impact-changement-climatique-carrieres.
[7] Kheder, K. (1996). Méthodologie d'études de la stabilité des carrières souterraines complexes exploitées par chambres et piliers abandonnés. Université de Lorraine.
https://docnum.univ-lorraine.fr/public/INPL_T_1996_KHEDER_K.pdf

Scaling-Law-Based Design of a Laboratory Model for Fluid Injection-Induced Earthquakes

Yubao ZHOU[1], Ioannis STEFANOU[1]
[1] ENSTA , Institut Polytechnique de Paris
yubao.zhou@ensta.fr

Fluid injection-induced earthquakes are of increasing concern in subsurface engineering applications such as geothermal energy, CO_2 sequestration and hydrogen storage. Laboratory experiments provide a valuable approach for investigating the coupled hydro-mechanical processes governing fault reactivation and slip, but the design of physically representative scaled models remains challenging. This work presents a scaling-law-based methodology for designing a laboratory model of fluid injection-induced earthquakes. Buckingham's π theorem is employed to establish the governing dimensionless relationships and derive scaling laws linking laboratory models with field-scale seismic events. Based on the proposed scaling framework, the geometry, loading conditions, material properties and fluid injection parameters are systematically determined. Open-cell foam is selected as the analogue material, and its material properties are experimentally characterised to evaluate its suitability for reproducing the target hydro-mechanical behaviour. Numerical simulations are further conducted to verify the feasibility of the proposed experimental design under representative injection scenarios. The developed framework provides a rational basis for constructing scaled laboratory models that capture the essential mechanisms of fault slip and fluid diffusion, offering a promising setup for future experimental investigations of injection-induced seismicity.



A scaling-law-based framework to bridge laboratory experiments and field-scale injection-induced earthquakes

Spontaneous imbibition and pore throat size distribution in volcaniclastic rocks: implications for UGS

Gimena Biene[1], Sandra Orlandi[2], Diego Manzanal[1]
[1] Universidad Politécnica de Madrid
[2] Universidad Nacional de la Patagonia
gimena.biene.heredia@alumnos.upm.es

Pore throat size distribution and connectivity control permeability and fluid retention in natural porous media [2], thereby determining the hydraulic response of both reservoir units and seals. This relationship is particularly critical for underground gas storage (CO2, H2, natural gas), where gas migration, trapping, and seal integrity are directly governed by the hydraulic properties of the porous medium [1]. Microstructural characterization, therefore, provides a means of anticipating potential risks and estimating permeability and mechanical behavior.

This study aims to characterize the relationship between macroscopic hydraulic response and pore throat size distribution in volcaniclastic rocks from the San Jorge Gulf Basin in southern Argentina. Results from spontaneous imbibition tests and mercury intrusion porosimetry (MIP) were integrated for 21 samples spanning a lithological range from coarse-grained tuffaceous sandstones to fine-grained tuffs. The sandstones exhibit porosities from 21 to 36% and permeabilities up to 10^{-13} m^2, whereas the tuffs exhibit porosities from 16 to 24% and permeabilities on the order of 10^{-17} m^2.

Spontaneous imbibition tests were used to track the evolution of saturation in each sample. Three parameters were derived from these curves: the initial absorption rate, the time to reach 50% saturation, and the total time to equilibrium. Simultaneously, MIP data were used to classify the pore throat size distribution of each lithotype into five classes, ranging from megapores to nanopores, following the scheme of Zhang et al. [3].

Coarse-grained tuffaceous sandstones exhibited rapid, homogeneous imbibition, reaching saturations of up to 72%, with 50% attained within the first 30 minutes (Figure 1a). This behavior is consistent with a pore network dominated by megapores and macropores (Figure 1b). This pore structure promotes early connectivity and rapid fluid transmission. In contrast, fine-grained lithologies display a three-stage kinetic pattern: a short initial stage, a prolonged intermediate stage, and a slow final stage (Figure 1a). Despite their slower kinetics, these lithotypes show a wider range of final saturations, reaching up to 90% in some samples, reflecting a heterogeneous network dominated by micropores and mesopores in which tortuosity delays fluid entry while enhancing overall retention (Figure 1b).

These results demonstrate that pore throat size distribution strongly controls imbibition kinetics and stabilization time, with direct implications for final saturation capacity and the hydraulic behavior of the reservoir-seal system. The integration of imbibition and MIP data provides a rapid predictive tool for assessing storage efficiency and seal integrity in underground gas storage scenarios within heterogeneous volcaniclastic media.

References

[1] Hawkes, C., McLellan, P. and Bachu, S. (2004). Geomechanical factors affecting geological storage of CO2 in depleted oil and gas reservoirs. Journal of Canadian Petroleum Technology, 44(10). http://dx.doi.org/10.2118/05-10-05.

[2] Lai, F., Li, Z., Zhang, T., et al., 2019. Characteristics of microscopic pore structure and its influence on spontaneous imbibition of tight gas reservoir in the Ordos Basin, China. J. Petrol. Sci. Eng. 172, 23-31. https://doi.org/10.1016/j.petrol.2018.09.020.

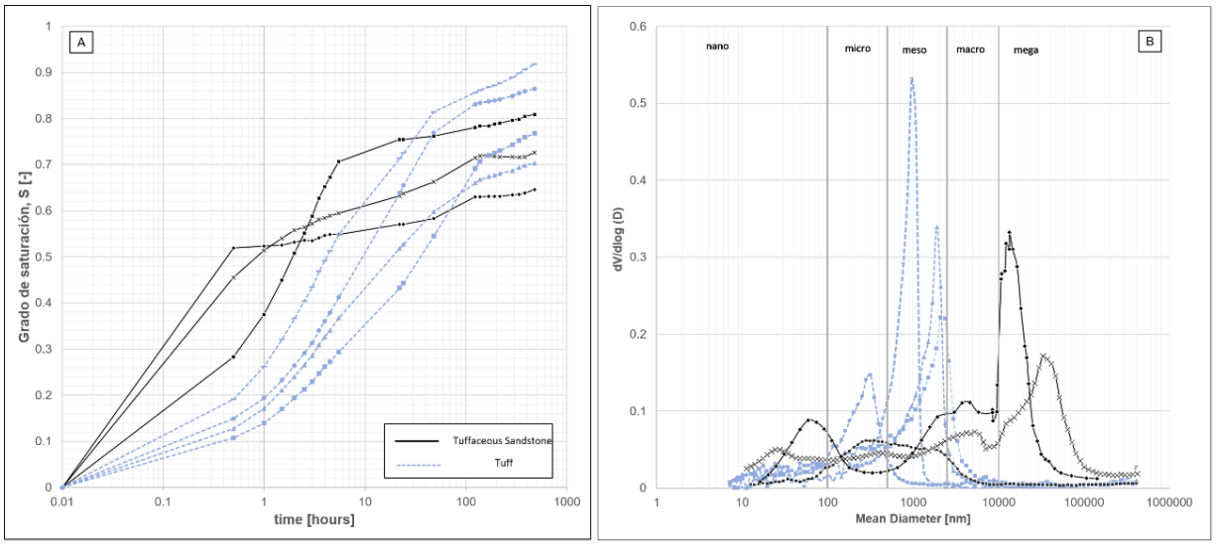


Figure 1: (A) Spontaneous imbibition curves for tuffaceous sandstone (black) and tuff (blue) samples. (B) Pore throat size distribution, classified

[3] Zhang, N., He, M., Zhang, B., Qiao, F., Sheng, H. Hu, Q. (2016). Pore structure and permeability of deep sedimentary rocks by MIP. J. Earth Sci., 27(4), 670-676. https://doi.org/10.1007/s12583-016-0662-z.

Adaptive Mesh Refinement for Phase-Field Fracture

Prince KITEMBO[1,2], Philipp BRAUN[2], Ana LOYOLA[2], Diego MANZANAL[1], Jean-Michel PEREIRA[2], Miguel STICKLE[1]

[1] UPM

[2] Navier ENPC

prince.kitembo@enpc.fr

The phase-field approach to fracture is a robust tool for modelling crack initiation and propagation without requiring discrete crack tracking [1], [2], [3]. However, its accuracy strongly depends on the spatial resolution of the damage localization zone. In practice, the characteristic element size must be sufficiently small with respect to the characteristic phase field length scale in the regions where damage localizes. As a consequence, reliable simulations usually require a sufficiently fine mesh surrounding the crack path.

This work presents the development and implementation of an adaptive local mesh refinement (AMR) strategy within the PhaseFieldX framework for phase-field fracture simulations [4]. Inspired by the AMR approach proposed by [5], the objective is to concentrate the computational effort only in mechanically relevant regions, while keeping the mesh size of the rest of the domain relatively coarse. The proposed approach is driven by an energy-based crack prediction criterion. Indeed, the active regions of the domain, where damage occurs, are determined via an energetic criterion which identifies cells where an elastic fracture energy threshold is exceeded by an elastic energy source. In addition, a history dependent marking strategy is introduced to update the fields state and to avoid repeatedly refining the same regions, while an additional surrounding zone is used to anticipate the evolution of the crack path. The refinement process is further limited by a mesh size condition, preventing element smaller than a fraction of the phase-field internal length scale. The adaptive algorithm is integrated directly into the staggered solution workflow of PhaseFieldX [1], [4], [6]. After each refinement event, the displacement field, phase-field variable, history variables, and marker fields are transferred to the new mesh in order to preserve solution consistency. Additional diagnostic outputs are introduced to visualize the active cells, refinement zones, and refined regions in ParaView.

We apply our framework to study the efficiency of AMR in 2D benchmark cases, such as the single notch, shear and three point bending tests. We compare crack path evolution, global stress-strain behavior, calculation time and local refinement. The AMR is able to significantly reduce computational time while providing accurate results. Then we investigate the influence of different strain-energy decomposition schemes, such as isotropic, spectral and volumetric-deviatoric splits, since they directly control the energy used in the criterion of the AMR.

References

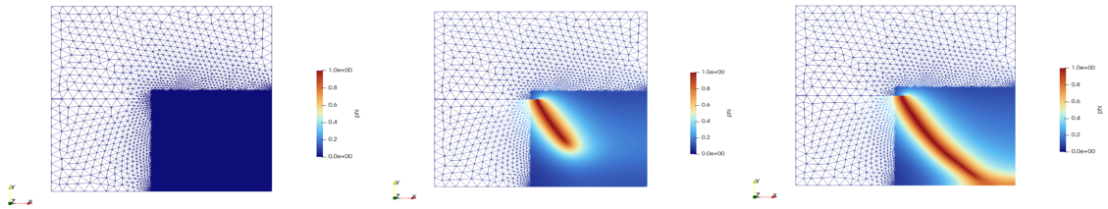
[1] C. Miehe, M. Hofacker, et F. Welschinger, "A phase field model for rate-independent crack propagation: Robust algorithmic implementation based on operator splits", Comput. Methods Appl. Mech. Eng., vol. 199, no 45, p. 2765-2778, nov. 2010, doi: 10.1016/j.cma.2010.04.011.

[2] B. Bourdin, G. A. Francfort, et J.-J. Marigo, "Numerical experiments in revisited brittle fracture", J. Mech. Phys. Solids, vol. 48, no 4, p. 797-826, avr. 2000, doi: 10.1016/S0022-5096(99)00028-9.

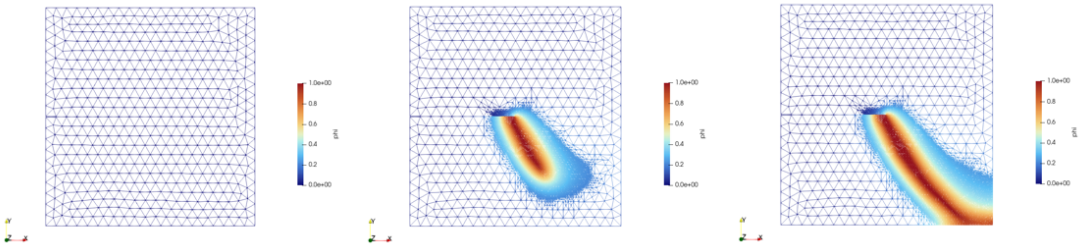
[3] B. Bourdin, G. A. Francfort, et J.-J. Marigo, "The Variational Approach to Fracture", J. Elast., vol. 91, no 1, p. 5-148, avr. 2008, doi: 10.1007/s10659-007-9107-3.

[4] M. Castillón, "PhaseFieldX: An Open-Source Framework for Advanced Phase-Field Simulations", J. Open Source Softw., vol. 10, no 108, p. 7307, avr. 2025, doi: 10.21105/joss.07307.

[5] F. Freddi et L. Mingazzi, "Adaptive mesh refinement for the phase field method: A FEniCS implementation", Appl. Eng. Sci., vol. 14, p. 100127, juin 2023, doi: 10.1016/j.apples.2023.100127.



(a) Reference refined configuration. A predefined refined zone is used to cover the possible crack trajectory



(b) Adaptive refinement. The refined zone evolves progressively and remains concentrated around the propagating crack

Comparison between the reference refined configuration and the adaptive local refinement strategy for the single-edge notched shear test. The phase-field variable ϕ is shown together with the mesh evolution during crack propagation.

[6] M. M. Stickle, D. Manzanal, P. Navas, et Á. Yagüe, "Phase field modeling of brittle fracture". Report Deliverable D7.2 Disco2Store.

Development and Verification of Coupled OpenFOAM–YADE CFD–DEM Solvers for Particle–Fluid Systems

Manikandan Valliappan[1], Eleni Gerolymatou[1]

[1] Chair for Geomechanics and Multiphysics Systems, Clausthal University of Technology, Germany

rammanish846@gmail.com

Coupled Computational Fluid Dynamics–Discrete Element Method (CFD–DEM) simulations provide a particle-scale framework for investigating fluid–granular interactions in geo-mechanical problems. However, their reliability depends strongly on the physical consistency of the interphase-force formulation, particle-to-mesh mapping, parallel particle localisation and time synchronisation between the CFD and DEM solvers.

This work presents the development and verification of three coupled OpenFOAM–YADE solvers: the point-force, PISO-based icoFoamYade; the Gaussian volume-averaged, PISO-based pisoFoamYade; and the Gaussian volume-averaged, PIMPLE-based pimpleFoamYade. The solvers were updated for OpenFOAM versions 10–14 and YADE 2024.08a. The developments include rank-aware particle localisation in decomposed domains, corrected Gaussian interpolation and normalisation, bounded fluid-volume-fraction mapping, semi-implicit momentum exchange, consistent separation of gravitational buoyancy, corrected hydrodynamic torque and strengthened parallel communication. The three formulations enable the effects of particle–mesh coupling and pressure–velocity solution algorithms to be examined separately under controlled conditions.

The implementations are verified using the settling of a single spherical particle in a quiescent incompressible Newtonian fluid at a terminal particle Reynolds number of approximately 0.048. In the Stokes regime, the analytical terminal velocity is given by

$v_t = \frac{(\rho_p - \rho_f) g d_p^2}{18 \mu_f}$,

and the corresponding transient velocity for a particle released from rest is

$v_p(t) = v_t \left[1 - \exp\left(-\frac{t}{\tau_p}\right)\right]$,

where

$\tau_p = \frac{\rho_p d_p^2}{18 \mu_f}$

is the particle relaxation time. Numerical particle velocities, trajectories, Reynolds numbers and hydrodynamic forces are compared with these analytical solutions. At terminal conditions, the additional force-balance criterion

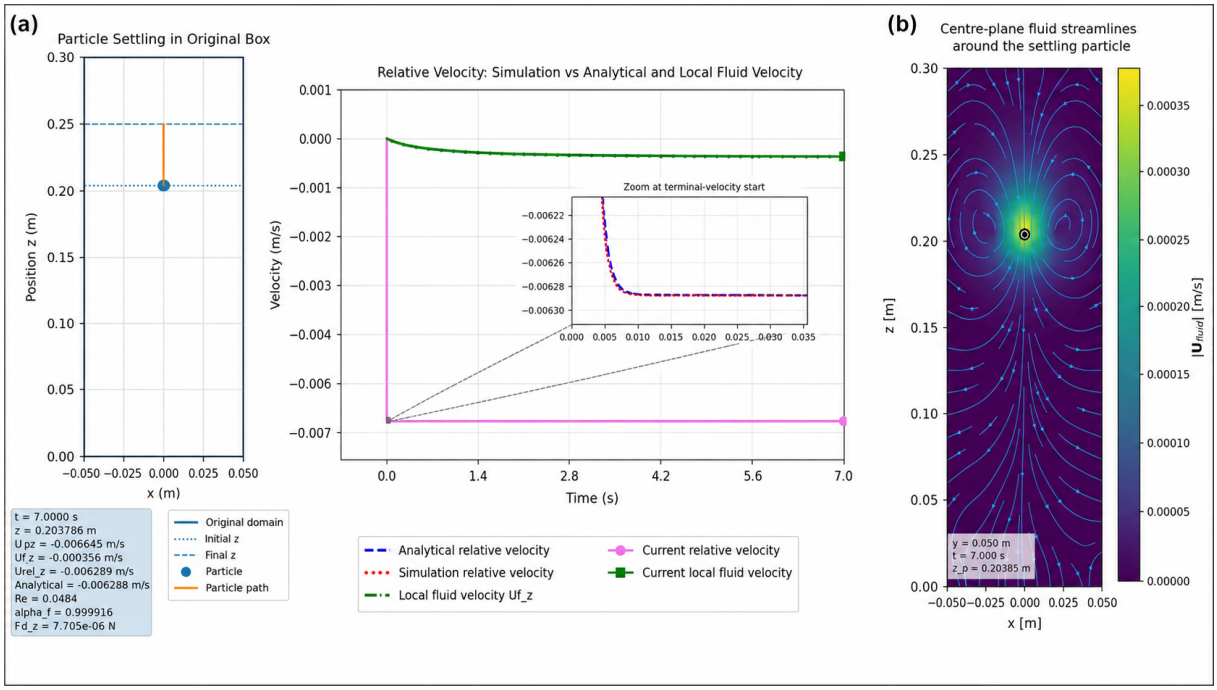
$|F_{\text{drag}}| = (\rho_p - \rho_f) V_p g$

is evaluated to verify consistency between drag, gravity and buoyancy.

All three solvers reproduce the analytical terminal response with high accuracy. The point-force solver gives a terminal-velocity error of approximately 0.021%, while the Gaussian-coupled solver achieves a terminal relative-velocity error of approximately 0.008% and a force-balance error below 0.001%. The PISO- and PIMPLE-based Gaussian solvers produce practically identical results for this dilute, weakly coupled benchmark, indicating that the pressure–velocity algorithm has negligible influence under these conditions. Time-step and mesh-sensitivity studies further demonstrate the numerical consistency of the implementation and confirm that the selected coupling parameters adequately resolve the transient particle response.

The results confirm that the revised OpenFOAM–YADE coupling provides an accurate, conservative and reproducible basis for simulations of more complex particle–fluid systems. The verified framework can support future investigations of hindered settling,

internal erosion, seepage-induced particle migration and saturated granular systems in which two-way and four-way coupling effects become important.



Single-particle settling verification: trajectory, analytical velocity comparison and terminal centre-plane streamlines using pimpleFoamYade.

References

[1] T. B. Anderson and R. Jackson, "A fluid mechanical description of fluidized beds," Industrial & Engineering Chemistry Fundamentals, vol. 6, no. 4, pp. 527–539, 1967.

[2] P. A. Cundall and O. D. L. Strack, "A discrete numerical model for granular assemblies," Géotechnique, vol. 29, no. 1, pp. 47–65, 1979.

[3] R. Clift, J. R. Grace and M. E. Weber, Bubbles, Drops, and Particles. New York: Academic Press, 1978.

[4] J. Zhao and T. Shan, "Coupled CFD–DEM simulation of fluid–particle interaction in geomechanics," Powder Technology, vol. 239, pp. 248–258, 2013.

[5] H. G. Weller, G. Tabor, H. Jasak and C. Fureby, "A tensorial approach to computational continuum mechanics using object-oriented techniques," Computers in Physics, vol. 12, no. 6, pp. 620–631, 1998.

[6] D. Kunhappan, B. Chareyre and P. Villard, "CFD–DEM coupled simulations with YADE and OpenFOAM," in Yade Documentation, 3rd ed., V. Šmilauer et al., Eds. The Yade Project, 2021. Available: https://yade-dem.org/doc/

Geomechanical Heterogeneity of a Volcaniclastic Formation: Potential Effects on Geological CO_2 Storage

Maximiliano Cortés[1], José Allard[2], Sandra Orlandi[2], Diego Manzanal[1]
[1] Universidad Politécnica de Madrid
[2] Universidad Nacional de la Patagonia
maximiliano.cortes@alumnos.upm.es

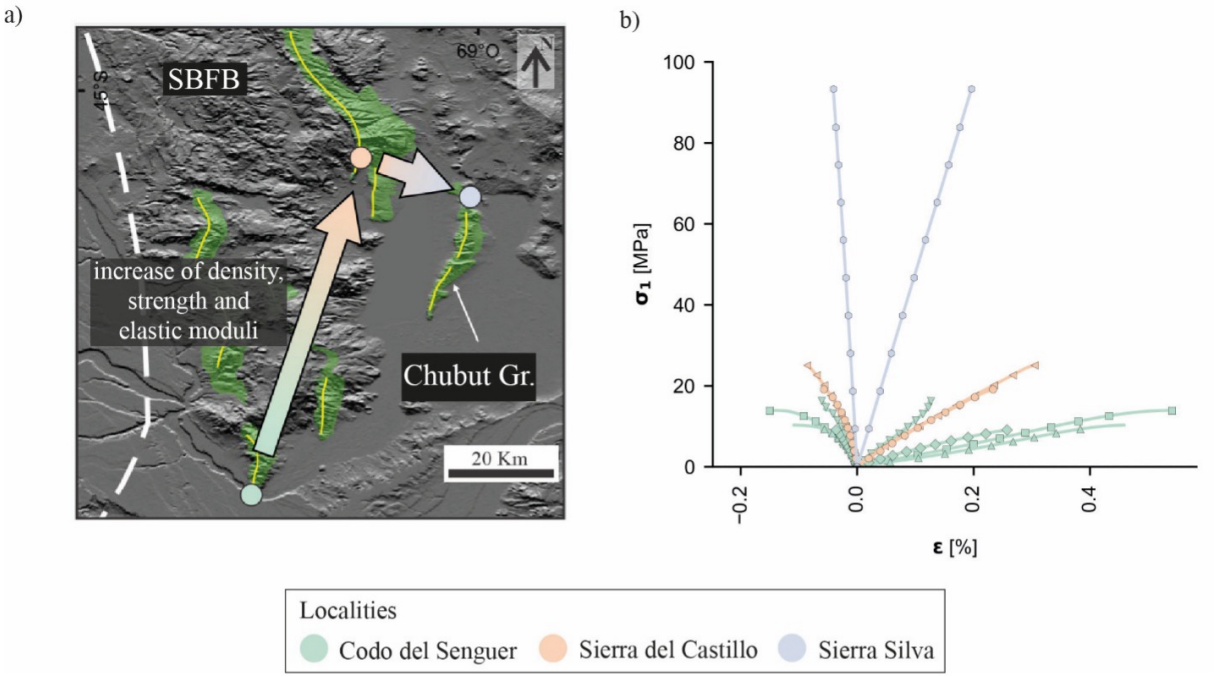
The increase in the Earth's surface temperature resulting from global warming has been one of the main drivers of the transition towards renewable energy sources. However, some energy-intensive industrial processes cannot yet be fully replaced by renewable alternatives. In this context, geological CO_2 storage represents a potential mitigation strategy for reducing greenhouse gas emissions. Depleted hydrocarbon reservoirs are widely regarded as suitable candidates for gas storage. Nevertheless, assessment of their physical and geomechanical properties is often constrained by the spatially limited nature of borehole-derived information, which is also confidential in many cases.

This study therefore investigates exposed reservoir analogs, as they provide an opportunity to characterize the intrinsic spatial variability of reservoir properties at the regional scale. The materials analysed comprise volcaniclastic rocks belonging to the same geological formation and exposed at three localities separated by approximately 25 to 80 km. Cylindrical specimens were used to determine dry density, total porosity, mercury intrusion porosity, uniaxial compressive strength, and static elastic moduli.

From a spatial perspective, the southern locality is characterized by the lowest dry density, uniaxial compressive strength, and static elastic modulus values. These properties reach intermediate values towards the north, whereas the highest values occur in the northeastern sector of the study area. In contrast, total porosity displays the opposite regional pattern, with higher values in the south and lower values in the northeast. Porosity determined by mercury intrusion follows the same general trend as total porosity. However, a decrease in pore-throat size is also observed towards the northeastern sector.

The regional heterogeneity observed within the studied formation appears to be associated with variations in mineralogical composition and diagenetic cementation. Previous studies have reported a strong predominance of volcaniclastic lithic fragments, together with marked spatial differences in cement type. In the northeastern sector, dawsonite cement is reported to fill pore spaces and reduce pore volume (Olazábal et al., 2025), consistently with the lower total and mercury intrusion porosities measured in this study. By contrast, clay-rich and zeolitic cements are more common in the southern and northern sectors. These cement types may preserve more favourable petrophysical properties but appear to be associated with poorer geomechanical performance than rocks containing dawsonite cement (Wang et al., 2024).

These results demonstrate that a single geological formation may exhibit substantial regional variability in its petrophysical and geomechanical behaviour. Mineralogical composition, particularly the type, exerts an important control on pore-system characteristics. In turn, the combined influence of mineralogical and pore-structure attributes affects the geomechanical response of the rock and may have important implications during supercritical CO_2 injection. Regional mineralogical differences are therefore expected to produce variable responses depending on the susceptibility of individual mineral phases and cements to CO_2-induced alteration, with potential consequences for the long-term geomechanical stability of the reservoir.



a) Location map of the study area showing the three investigated localities and the regional increase in dry density, uniaxial

References

[1] Olazábal, S., Tunik, M., Paredes, J., Allard, J. y Foix, N., 2025. The Chubut Group (Cretaceous, Golfo San Jorge Basin): A synthesis of its sedimentary petrography. Latin American Journal of Sedimentology and Basin Analysis, 32(1), pp. 44-56.

[2] Wang, W., Lin, C. y Zhang, X., 2024. Elastic rock properties analysis of diagenetic facies identification of deep tight sandstone in the Xihu Sag, China. Marine and Petroleum Geology, 160, 106661.

A proposed Tuffaceous Index (Gs-Z) for evaluating volcaniclastic reservoirs

Pablo Vidal[1], Jose Allard[2], Diego Manzanal[1]

[1] Universidad Politécnica de Madrid

[2] Universidad Nacional de la Patagonia

pa.vidal@alumnos.upm.es

Volcaniclastic reservoirs are heterogeneous systems in which conventional sandstone frameworks may incorporate variable proportions of ash-derived and volcanic components. These metastable constituents are prone to dissolution, alteration and diagenetic transformation, commonly producing clay minerals, zeolites, pseudomatrix and secondary porosity [2]. As a result, volcaniclastic sandstones and tuffs cannot be reliably interpreted using the same assumptions commonly applied to compositionally simpler siliciclastic sandstones, where porosity, sorting and cementation are usually considered the main controls on reservoir quality.

This study proposes a (GS-Z) Tuffaceous Index as an integrated framework to evaluate the geomechanical and petrophysical behaviour of volcaniclastic reservoir analogues. Solid specific gravity, (GS), is used as an indirect compositional indicator of tuffaceous influence, whereas acoustic impedance, (Z), calculated from dry bulk density and P-wave velocity, is used as a non-destructive predictor of the mechanical integration of the rock framework. The dataset includes GS, dry bulk density, P-wave velocity, Z, mercury intrusion porosimetry (MIP), air permeability Kair, uniaxial compressive strength (UCS) and static Young's modulus (E), supported by petrographic and mineralogical observations.

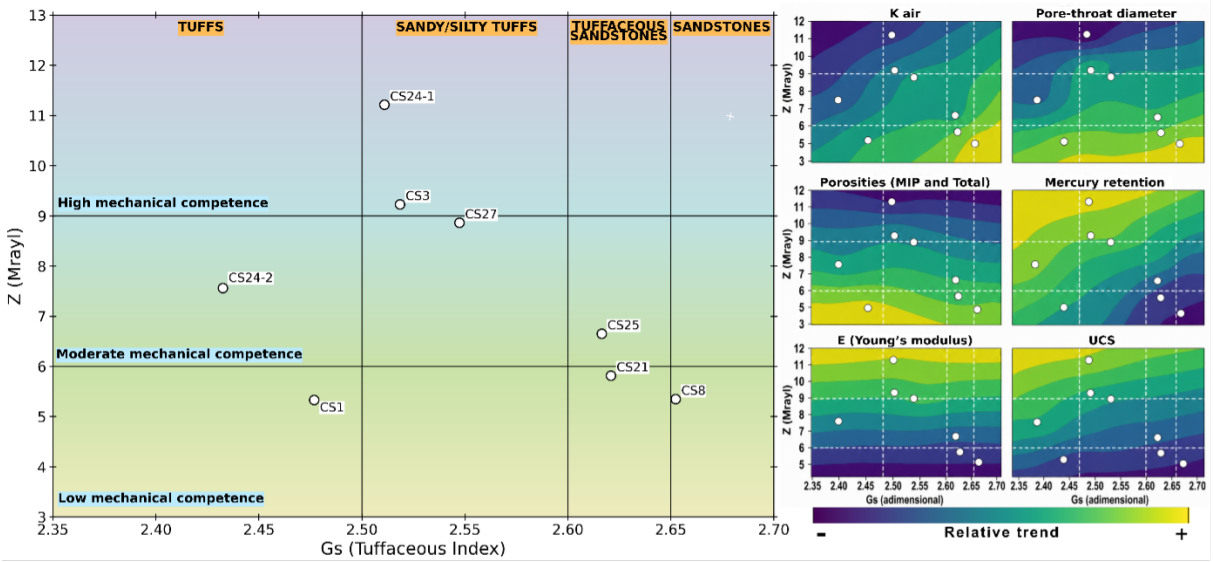
The analysed rocks belong to the Upper Cretaceous Bajo Barreal Formation, Golfo San Jorge Basin, Argentina. This unit represents one of the main fluvial reservoir intervals of the basin and is characterized by channelized volcaniclastic sandstones interbedded with tuffaceous floodplain deposits [3]. Outcrop samples from the Codo del Senguer area define a sandstone–tuff continuum, including volcaniclastic sandstones, tuffaceous sandstones, sandy tuffs and tuffs.

The results show that decreasing GS marks a progressive transition from siliciclastic sandstone-dominated compositions toward stronger tuffaceous influence. This interpretation is consistent with reported grain-density contrasts between reference sandstones and altered tuffs, such as Berea Sandstone and Neapolitan Yellow Tuff (e.g. [4]). Lower GS values are associated with finer pore-throat systems, lower air permeability and greater mercury retention, indicating reduced hydraulic efficiency. In parallel, increasing Z is associated with higher P-wave velocity, greater stiffness and higher uniaxial compressive strength, reflecting enhanced continuity and rigidity of the load-bearing framework.

The GS-Z space separates two complementary controls on reservoir behaviour. Composition and diagenetic transformation are mainly expressed by GS, whereas mechanical competence is mainly represented by Z. Total porosity alone does not reproduce the observed trends, confirming that pore volume is insufficient to explain the coupled response of these rocks. Instead, pore-throat architecture, cementation and framework continuity govern the transition from hydraulically efficient sandstones to mechanically competent tuffaceous rocks.

The proposed GS-Z Tuffaceous Index provides a simple and reproducible framework for organizing petrophysical and geomechanical variability in volcaniclastic reservoirs. This approach extends previous petrophysical classifications based on matrix density and

tuffaceous content [1] by incorporating acoustic impedance as a predictor of mechanical competence. It may support preliminary rock typing of sandstone–tuff systems and offers a transferable tool for subsurface reservoir characterization when calibrated with laboratory and well-log data.



Tuffaceous Index. Petrophysical quality is represented by inclined isolines, with higher quality toward the lower-right corner of the (GS-Z) space.

References

[1] Breda, E., Lucero, M. (2005). Caracterización de los reservorios de la Formación Bajo Barreal Inferior Arenas y Tobas (Sección Tobácea). VI Congreso de Exploración y Desarrollo de Hidrocarburos, Actas, 197–214.

[2] Limarino, C. O., Giordano, S. R., Rodríguez Albertani, R. J. (2017). Diagenetic model of the Bajo Barreal Formation (Cretaceous) in the southwestern flank of the Golfo San Jorge Basin (Patagonia, Argentina). Marine and Petroleum Geology, 88, 907–931.

[3] Paredes, J. M., Foix, N., Allard, J. O. (2016). Sedimentology and alluvial architecture of the Bajo Barreal Formation (Upper Cretaceous) in the Golfo San Jorge Basin: Outcrop analogues of the richest oil-bearing fluvial succession in Argentina. Marine and Petroleum Geology, 72, 317–335.

[4] Vanorio, T., Prasad, M., Patella, D., Nur, A. (2002). Ultrasonic velocity measurements in volcanic rocks: Correlation with microtexture. Geophysical Journal International, 149, 22–36.

[5] Vidal, P. A., Cortés, M., Allard, J. O., Manzanal, D. (2026). Definición de un Tuffaceous Index para la evaluación de análogos de reservorios de la Formación Bajo Barreal, Cuenca del Golfo San Jorge (Argentina). XII Congreso de Exploración y Desarrollo de Hidrocarburos, Actas, Mendoza, Argentina.

Normal–tangential coupling in elastoplastic contacts enables stress recovery in cyclically sheared granular materials

Min Deng[1,2], Yi Pik Cheng[2], Lianheng Zhao[1]

[1] Central South University, Changsha, 410075, China
[2] University College London, London, WC1E 6BT, UK

h.dengmin@csu.edu.cn

Typical elastoplastic contact laws predict zero normal force with a finite residual displacement upon complete normal unloading. When combined with the Coulomb friction law, they also predict zero tangential resistance in this residual state, implying unconstrained tangential motion that does not reflect actual contact behaviour. To address this limitation, we develop a thermodynamically consistent normal–tangential coupling framework for elastoplastic contacts under normal unloading. The framework assumes a decreasing degree of engagement during tangential motion relative to the persistent plastic contact patch to restore a repulsive normal force, whereas normal reloading restores engagement. Both the normal and tangential coupling forces are derived from a single free-energy potential scaled by a coupling participation factor β, allowing tangential motion to store recoverable energy until plastic-patch renewal. These coupling forces are then superimposed onto the host elastoplastic contact forces. The framework is then incorporated into the rough-surface contact model of Otsubo et al.

Independent asperity-resolved boundary element method (BEM) simulations of rough surfaces provide qualitative evidence for the assumption that tangential motion at a fixed unloaded normal displacement can recover normal force before further asperity yielding (Fig. 1). Across 15 rough-surface pairs unloaded to near-zero force (0.2% of preload), subsequent tangential loading recovers a normal force of 1.3%–6.1% of the preload before renewed asperity yielding.

At the assembly scale, the framework is applied to discrete element method (DEM) simulations using 5000 spherical particles in a periodic cell, with initial mean stress () of 100 kPa, cyclic deviatoric stress () amplitude of 40 kPa, interparticle friction coefficient of 0.3, root-mean-square (RMS) roughness of 0.223 μm, and coupling participation factor of $\beta = 0.05$. Both coupled and uncoupled contact models progressively lose mean stress during constant-volume cyclic loading (Fig. 2). As the mean stress approaches zero, the uncoupled elastoplastic rough-surface contact model accumulates axial strain beyond 20% without rebuilding shear resistance. In contrast, the coupled rough-surface contact model exhibits repeated stress recovery near zero mean stress, successfully reproducing cyclic mobility.

Decomposing the macroscopic stress into host and coupling components reveals that the coupling component triggers the onset of stress recovery, after which the host component carries most of the recovered stress (Fig. 3a, b). Near the local stress minimum around zero mean stress, almost vanishes while sustains a small but finite mean stress. At the micro-scale, as the mean stress approaches zero, the fraction of residual contacts exceeds 80%, but the coupling reactivates the majority of them into recovered contacts, preventing contact-network collapse (Fig. 3c). Tangential disengagement thus initiates stress recovery by maintaining finite contact forces as the host contribution approaches zero.

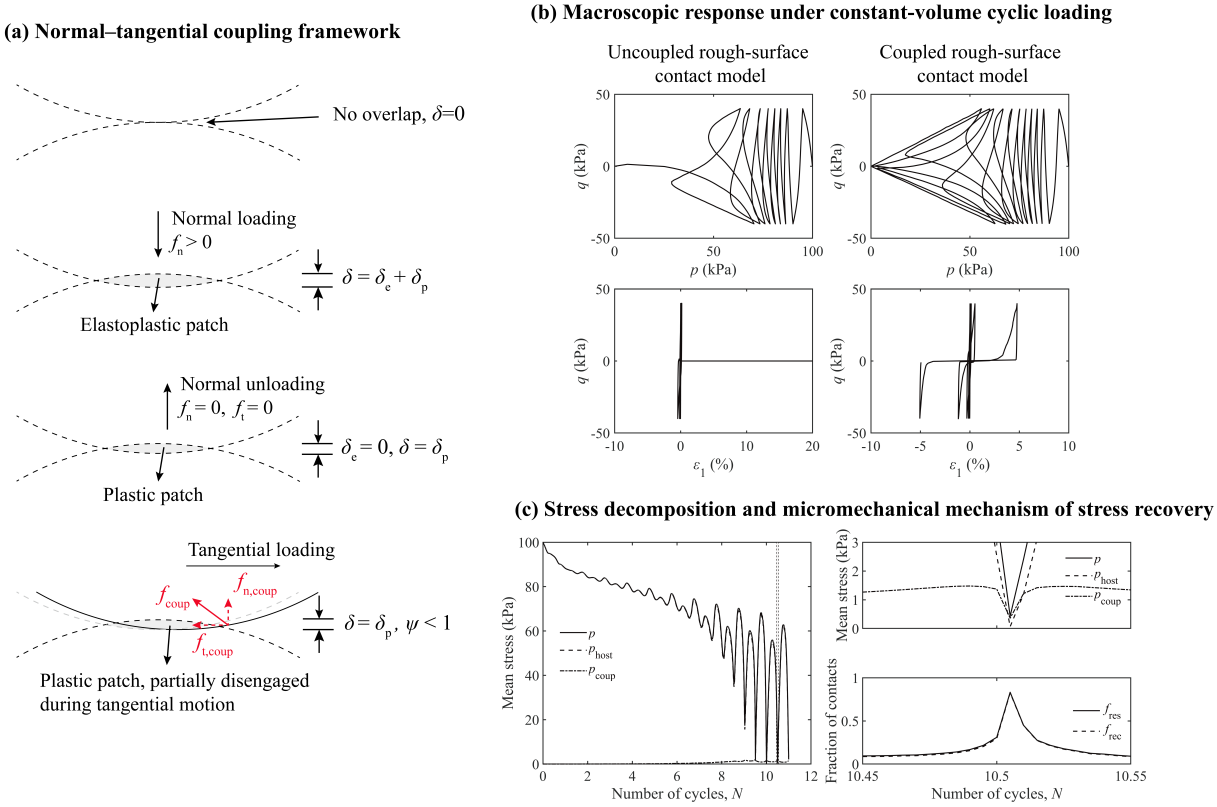


Figure 1. Normal–tangential coupling and multi-scale stress recovery

References

[1] Kadin, Y., Kligerman, Y., & Etsion, I. (2006). Unloading an elastic–plastic contact of rough surfaces. Journal of the Mechanics and Physics of Solids, 54, 2652–2674. https://doi.org/10.1016/j.jmps.2006.04.013

[2] Vu-Quoc, L., Zhang, X., & Lesburg, L. (2001). Normal and tangential force–displacement relations for frictional elasto-plastic contact of spheres. International Journal of Solids and Structures, 38, 6455–6489. https://doi.org/10.1016/S0020-7683(01)00065-8

[3] Brizmer, V., Kligerman, Y., & Etsion, I. (2007). Elastic–plastic spherical contact under combined normal and tangential loading in full stick. Tribology Letters, 25, 61–70. https://doi.org/10.1007/s11249-006-9156-y

[4] Otsubo, M., O'Sullivan, C., Hanley, K. J., & Sim, W. W. (2017). The influence of particle surface roughness on elastic stiffness and dynamic response. Géotechnique, 67, 452–459. https://doi.org/10.1680/jgeot.16.P.050

[5] Wang, G., Nie, J., Cui, Y., & Guo, J. (2025). Incorporating particle roughness and hardness into contact model to reproduce elastic behaviors of granular soils in DEM. Computers and Geotechnics, 179, 107054. https://doi.org/10.1016/j.compgeo.2025.107054

[6] Ishihara, K. (1993). Liquefaction and flow failure during earthquakes. Géotechnique, 43, 351–415. https://doi.org/10.1680/geot.1993.43.3.351

A Hydromechanical eTANN Macroelement for Translational Slides in Partially Saturated Slopes

Andres Macias-Gutierrez[1], Jean Vaunat[1], Yeudy Felipe Vargas-Alzate[1]
[1] Universitat Politécnica de Catalunya
andres.macias@upc.edu

Climate-driven variations in water content and suction are primary factors controlling the stability of partially saturated slopes. Classical limit-equilibrium methods provide efficient tools for engineering-scale screening [2,7], while unsaturated effective-stress formulations offer a rational framework for incorporating suction effects [3,1,4,11]. Nevertheless, these approaches do not explicitly capture deformation, hydromechanical path dependence, or the progressive localization of failure. More rigorous alternatives rely on fully coupled hydro-mechanical Finite Element analyses. However, their application within probabilistic frameworks for regional-scale hazard assessment – where thousands to millions of simulations may be required over multiple slope geometries, parameter sets, and spatial grid cells – remains computationally prohibitive.

To overcome these limitations, the present study develops a reduced-order hydromechanical macroelement for predicting the response of an unsaturated slope using 4 thermodynamically consistent state variables: the driving force, the resulting displacement, the water volume, and the work-conjugated suction. The proposed macroelement is implemented as a thermodynamics-based artificial neural network (TANN) and trained on a database of hydro-mechanical FEM simulations. Hydromechanical Macroelement Definition

At the scale of a Representative Elementary Volume, the work input of an unsaturated porous material ($\dot{w}$) is expressed as the sum of a mechanical and a hydraulic term [5,8]: $\dot{w} = \boldsymbol{\sigma}'' : \dot{\boldsymbol{\varepsilon}} + s\dot{\varepsilon}_w = \dot{w}_m + \dot{w}_h$

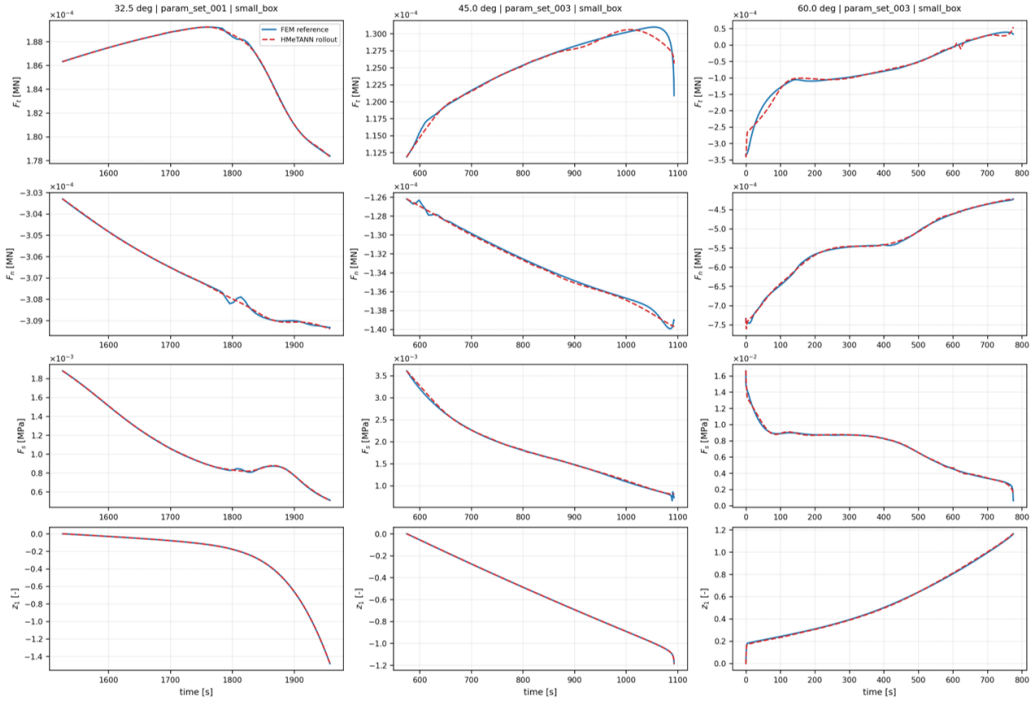
By integration, the work input along the shear band at the base of the failure mass ($\dot{W}$) is given by: $\dot{W} = F_t\dot{u}_t + F_n\dot{u}_n + F_s\frac{\dot{V}_w}{V_s} = \dot{W}_{m,t} + \dot{W}_{m,n} + \dot{W}_h$, where:
$F_t = B\int_{\Gamma_s}(\boldsymbol{\sigma}''\mathbf{n})\cdot\mathbf{t}\,d\Gamma$
$F_n = B\int_{\Gamma_s}(\boldsymbol{\sigma}''\mathbf{n})\cdot\mathbf{n}\,d\Gamma$
$\dot{V}_w = B\int_{\Gamma_s}\dot{\theta}_w(\Gamma)\,b_\Gamma(\Gamma)\,d\Gamma$

Accordingly, u_t and u_n are the displacements work-conjugated to the forces F_t and F_n, while F_s is the suction work-conjugated to $\dot{V}_w$. Thus, we will consider two pairs of work-conjugated vectors for the macroelement: $x = (\delta u_t, [\delta u]_n, [\delta V]_w)$ and $q = (F_t, F_n, F_s)$. Practically, F_t, F_n, δV_w, $\delta W_{m,t}$, $\delta W_{m,n}$ and δW_w, are directly computed by integration of the stress, strain and water content fields obtained in the FEM simulation. $[\delta u]_t$, $[\delta u]_n$ and F_s and then computed as their work-conjugated variables: $\delta u_t = \frac{\delta W_{m,t}}{F_t}$, $\delta u_n = \frac{\delta W_{m,n}}{F_n}$, $F_s = \frac{\delta W_h}{F_s}$

The eTANN constitutive map is derived from a Helmholtz free-energy potential $\psi(x, z, p)$, with internal state variables z and material parameters p, and constrained by the Clausius-Duhem inequality [6]. The model achieved R^2 values above 0.98 for all generalized forces over 18,552 samples. The potential is defined such that the conjugated-pairs consistency is maintained. $q = \frac{\partial\psi(\mathbf{x},\mathbf{z};\mathbf{p})}{\partial\mathbf{x}} = (F_t, F_n, F_s)$

Training trajectories are generated in CODE_BRIGHT [9] using the unsaturated CASM constitutive model. For each inclination and parameter set, shear localization and strain evidence are condensed into a reduced slip line for stress integration and work-conjugated macroelemental variable construction. Internal variables are represented by POD-reduced

coordinates [10] and advanced through a DMDc-type incremental operator, $z_(k+1) = Az_k + B\eta_k$, where η_k contains the current macrostate and conditioning inputs. Validation therefore focuses on autonomous rollouts against FEM trajectories rather than teacher-forced calibration errors. Parity and trajectory results show that the macroelement reproduces the evolution of tangential, normal and hydraulic generalized variables through a compact constitutive representation.



Temporal rollout for representative cases. Showing the capabilities of the HMeTANN macroelement to represent evolution of internal state and generalized

References

[1] E. E. Alonso, A. Gens, and A. Josa. (1990). A constitutive model for partially saturated soils. Geotechnique, 40(3), 405-430.
[2] A. W. Bishop. (1955). The use of the slip circle in the stability analysis of slopes. Geotechnique, 5(1), 7-17.
[3] A. W. Bishop. (1959). The principle of effective stress. Teknisk Ukeblad, 106(39), 859-863.
[4] D. Gallipoli, A. Gens, R. Sharma, and J. Vaunat. (2003). An elasto-plastic model for unsaturated soil incorporating the effects of suction and degree of saturation on mechanical behaviour. Geotechnique, 53(1), 123-135.
[5] G. T. Houlsby. (1997). The work input to an unsaturated granular material. Geotechnique, 47(1), 193-196.
[6] F. Masi, and I. Stefanou. "Evolution TANN and the identification of internal variables and evolution equations in solid mechanics." Journal of the Mechanics and Physics of Solids 174 (2023): 105245.
[7] N. R. Morgenstern, and V. E. Price. (1965). The analysis of the stability of general slip surfaces. Geotechnique, 15(1), 79-93.
[8] J. J. Nitao, and J. Bear. (1996). Potentials and their role in transport in porous media. Water Resources Research, 32(2), 225-250.
[9] S. Olivella, A. Gens, J. Carrera, and E. E. Alonso. (1996). Numerical formulation for a simulator (CODE_BRIGHT) for the coupled analysis of saline media. Engineering Computations, 13(7), 87-112.
[10] G. Piunno, I. Stefanou, and C. Jommi (2025). A POD-TANN Approach for the Multiscale Modeling of Materials and Macro-Element Derivation in Geomechanics. International Journal for Numerical and Analytical Methods in Geomechanics, 49(2), 700-719.
[11] Wheeler, S. J., Sharma, R. S., and Buisson, M. S. R. (2003). Coupling of hydraulic hysteresis and stress–strain behaviour in unsaturated soils. Géotechnique, 53(1), 41-54.

Multiscale Experimental and Analytical Validation of a DEM Framework for Compressibility of Rockfill

Cristian Maurer[1], Carlos Ovalle[2], Esteban Saez[3]
[1] Pontificia Universidad Catolica; Polytechnique Montreal
[2] Polytechnique Montreal
[3] Pontificia Universidad Catolica
comaurer@uc.cl

Grain crushing governs the compressibility of rockfills and mine waste materials, yet its macroscopic response is commonly represented using phenomenological constitutive models that provide limited insight into the underlying grain-scale mechanisms [1,5]. Although the Discrete Element Method (DEM) offers the possibility of investigating these mechanisms, the realistic representation of particle morphology, fragmentation and evolving grading remains a major challenge [3,4].

This study presents a multiscale DEM framework capable of reproducing the one-dimensional compressibility of crushable rockfill by calibrating only grain-scale mechanical properties while explicitly incorporating realistic particle geometries derived from X-ray micro-computed tomography (μCT) scans. Large-scale oedometer compression tests and single-particle crushing tests were performed to characterize the compressibility, grading evolution and statistical strength distribution of the material. Grain fragmentation was modeled through a hierarchical strategy combining the Bonded Cell Method (BCM) for primary breakage [3] with the Split-Cell Method for secondary fragmentation [4].

The DEM simulations successfully reproduced the experimental stress–strain response, the evolution of particle size distribution and the onset of yielding up to a vertical stress of 3200 kPa. The simulations further enabled tracking of breakage events throughout loading, revealing that yielding and subsequent compression are triggered by the onset of grain crushing, in agreement with previous experimental observations [2]. Microstructural analyses indicate that geometric and mechanical granular anisotropies evolve concurrently with particle breakage, compensating each other to maintain an approximately constant stress ratio during oedometric compression. As loading progresses, the increasing size contrast between the coarse and fine fractions leads to differentiated roles within the force network, thereby enhancing force anisotropy. Conversely, the generation of fine particles increases the number of contacts surrounding coarse grains, reducing contact anisotropy. This framework provides direct access to evolving microstructural descriptors and establishes a direct micro-to-macro link between grain fragmentation and the macroscopic compressibility of crushable geomaterials.

References

[1] Einav, I. (2007). Breakage mechanics—Part I: Theory. Journal of the Mechanics and Physics of Solids, 55, 1274–1297.
[2] Ovalle, C., Dano, C., Hicher, P.-Y., & Cisternas, M. (2015). Experimental framework for evaluating the mechanical behavior of dry and wet crushable granular materials based on the particle breakage ratio. Canadian Geotechnical Journal, 52, 587–598.
[3] Cantor, D., Azéma, E., Sornay, P., & Radjai, F. (2017). Three-dimensional bonded-cell model for grain fragmentation. Computational Particle Mechanics, 4, 441–450.
[4] Cantor, D., Estrada, N., & Azéma, E. (2015). Split-Cell Method for grain fragmentation. Computers and Geotechnics, 67, 150–156.
[5] McDowell, G. R., & Bolton, M. D. (1998). On the micromechanics of crushable aggregates. Géotechnique, 48, 667–679.

From Clay to Tailings: Evaluation of the Terracota Model for Liquefiable Iron Ore Tailings

Pablo Dos Santos Cardoso Coelho[1], Fangzhou Liu[2], Gordon Ward Wilson[1], Paul Simms[3], Gonzalo Zambrano Narvaez[1]

[1] University of Alberta
[2] Mcgill University
[3] Carleton University

pdossan1@ualberta.ca

Hydrodynamic constitutive models provide an alternative to classical elastoplasticity by describing the stress-strain behavior of soil as the result of energy transfer and dissipation processes occurring at mesoscopic and microscopic scales, rather than by modelling these effects through pre-defined yield surfaces and hardening laws. The Terracota model [1] is a relatively simple hydrodynamic model developed within the framework of two-phase entropy introduced by [2] with the Granular Solids Hydrodynamics model [3][4]. The state evolution in the Terracota model is modelled as a consequence of the evolution of mesoscopic elements (particles or clusters) motion, described by the mesoscopic temperature, and by Onsagerian transport equations controlling the rates of energy dissipation via viscous and plastic dissipative currents. The dissipative nature of the phenomena modelled by the Terracota model enables capturing strain-rate-dependent behavior, promising for modelling strain-rate dependent phenomena such as flow-slides.

This work investigates the applicability of the Terracota model to the iron ore liquefiable silty sandy tailings (AM1) published by [5]. The model is calibrated against conventional isotropic consolidation and drained and undrained triaxial compression tests. Emphasis is given to whether the original plastic transport structure proposed by the Terracota model can reproduce the mechanical behavior of materials that do not exhibit a unique isotropic consolidation line. The elastic energy equation originally employed, based on [6], is revisited, and a detailed calibration process of the elastic exponent, fixed at 6 in the Terracota model, is presented.

The original Terracota model formulation is unable to reproduce the experimental dataset consistently, with the plastic strain rates being strongly influenced by the preconsolidation stress. The introduction of a phenomenological plastic multiplier in the plastic transport equation substantially improves the reproduction of the undrained test data, whereas trends of viscous coefficients indicate that the evolution equation for the mesoscopic temperature – and consequently the equation of viscous transport – might need additional adjustment for this specific type of tailings.

The main contribution of this study is to identify limitations of the Terracota model when applied to the modelling of more complex materials such as the studied tailings, proposing targeted reviews – especially the Onsagerian transport equations.

References

[1] M. Wiebicke and I. Einav, "A simple hydrodynamic model for clay," Journal of the Mechanics and Physics of Solids, vol. 192, article 105789, 2024, doi: 10.1016/j.jmps.2024.105789.

[2] Y. Jiang and M. Liu, "Granular solid hydrodynamics," Granular Matter, vol. 11, pp. 139–156, 2009, doi: 10.1007/s10035-009-0137-3.

[3] Y. Jiang and M. Liu, "Why granular media are thermal, and quite normal, after all," The European Physical Journal E, vol. 40, no. 1, article 10, 2017, doi: 10.1140/epje/i2017-11497-4.

[4] S. Luding, Y. Jiang, and M. Liu, "Un-jamming due to energetic instability: statics to dynamics," Granular Matter, vol. 23, no. 4, article 93, 2021, doi: 10.1007/s10035-021-01119-0.

[5] S. C. Oliveira, "Influência do estado de tensão na obtenção dos parâmetros de estado crítico de rejeitos filtrados de minério de ferro," Universidade Federal de Ouro Preto, 2022. Available: http://www.repositorio.ufop.br/jspui/handle/123456789/16478.
[6] D. M. Riley, I. Einav, and F. Guillard, "A consistent derivation of soil stiffness from elastic wave speeds," Géotechnique, vol. 75, no. 13, pp. 215–224, 2025, doi: 10.1680/jgeot.23.00457.

Learning Thermo-Hydro-Mechanical Coupled Fracture Permeability Evolution via Physics-Informed Generative AI in Geotherma

Jiangmei Qiao[1], Mengwei Liu[2], Xi Hua[1], Shengzong Xu[1], Xuhai Tang[1]

[1] Wuhan University

[2] National Energy Technology Laboratory, U.S. Department of Energy, Morgantown, WV 26505, USA

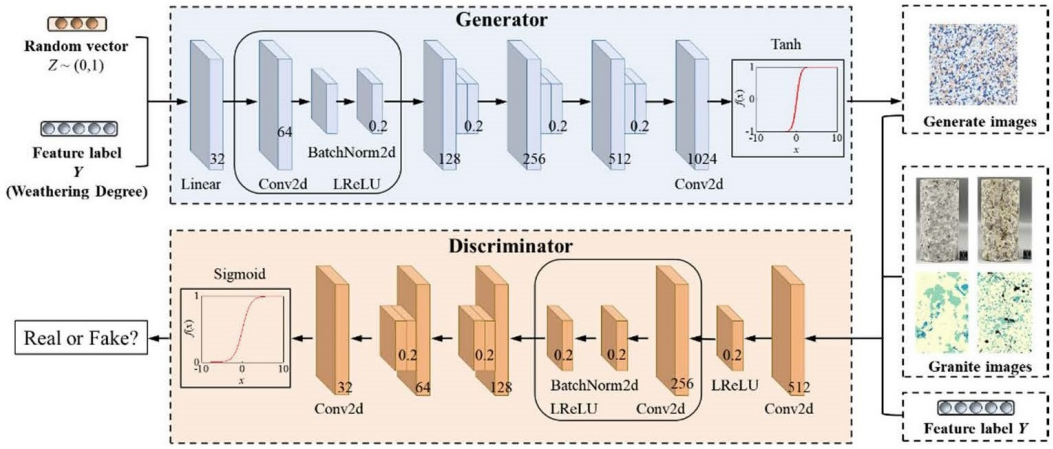
jiangmei_qiao@whu.edu.cn

Keywords: Geothermal; Altered granite; Conditional Generative Adversarial Network (CGAN); Fracture permeability

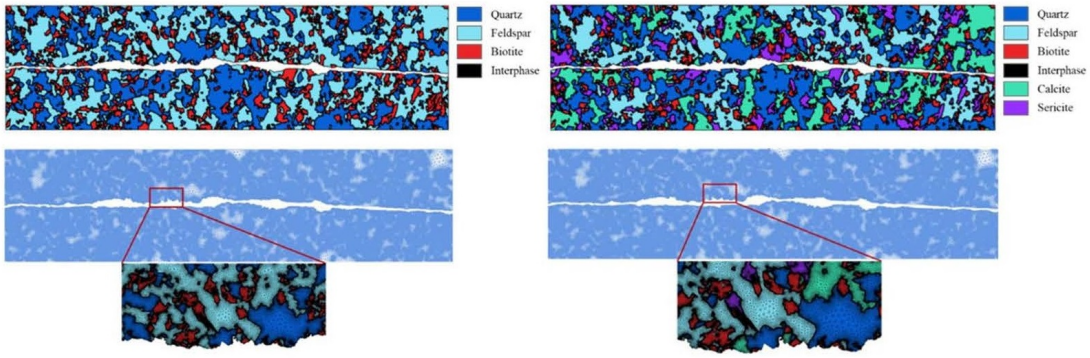
In enhanced geothermal systems (EGS), deep granite reservoirs are commonly subjected to prolonged hydrothermal alteration. However, it is difficult to obtain physically representative altered granite specimens from such depths for experimental testing. As a result, accurately evaluating the mechanical and hydraulic behavior of altered granite remains a major challenge.

In this work, we propose a Conditional Generative Adversarial Network (CGAN)-based method to generate high-fidelity microstructures of altered granites. This approach integrates extensive prior knowledge of mineral weathering with a limited amount of site-specific data. The generated microstructures successfully capture key alteration-induced features, including mineral transformations (e.g., feldspar to sericite, biotite to chlorite) and the development of microdefects. These AI-generated digital granite are then used to investigate the fracture permeability through accurate grain-based modelling under geostress conditions.

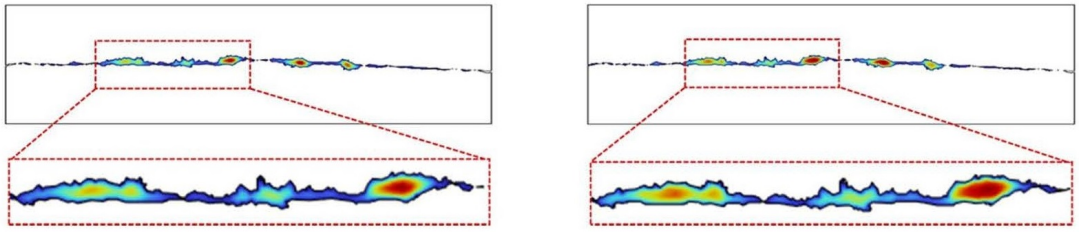
The main findings of this work are as follows: 1) Long-term geothermal production reduces the elastic modulus of granite while increasing its deformability. Consequently, altered granite exhibits greater fracture closure under compression, with fracture aperture decreasing by 6.75% relative to unaltered granite; 2) Permeability decreased by 3.21% in altered granite. This is because the mineral transformation and the proliferation of microdefects, both reduced the size and connectivity of flow pathways. This study demonstrates that physics-informed generative AI can provide a practical digital-rock approach for evaluating hydro-mechanical property evolution in altered geothermal reservoirs where representative core samples are scarce.



(a) CGAN framework



(b) AGBM before and after alteration



(c) Fluid in fracture before and after alteration

Geomechanical Characterization of Biopolymer-Treated Kaolinite: Plasticity and Undrained Shear Strength Evolution

Milad Jabbarzadeh[1], Arash Alimardani Lavasan[1]
[1] University of Luxembourg
milad.jabbarzadeh@uni.lu

The transition toward sustainable ground improvement has accelerated the investigation of biopolymers as low-carbon alternatives to traditional cementitious binders. Biopolymer-treated soils show significant promise across diverse geotechnical and geoenvironmental applications, including broad soil stabilization within the construction sector, erosion mitigation, desiccation cracking control, and the development of impermeable subsurface barriers. Among available biomaterials, Xanthan Gum (XG) has demonstrated considerable potential in altering the hydro-mechanical properties of clay-rich soils. However, optimizing its application in the field requires a precise understanding of the transitional behavior of the soil's index properties and mechanical strength across varying dosages and environmental curing conditions.

This study investigates the geomechanical behavior of kaolinite clay treated with XG biopolymer. To systematically evaluate the interaction between the biopolymer hydrogel matrix and the clay particles, an experimental program was conducted utilizing XG dosages ranging from 0% to 2% by dry weight. Specimen preparation utilized a dry mixing method to ensure homogenous polymer distribution prior to hydration. The temporal evolution of the mixture's structural integrity was captured by evaluating curing times ranging from a single day up to four weeks. The experimental regime focused on the relationship between plasticity evolution, determined via Liquid Limit (LL) tests, and the undrained shear strength profile, systematically captured using cone fall tests at varying moisture contents.

Preliminary results indicate a pronounced, proportional increase in the liquid limit as the XG dosage increases up to 2%. This progressive plasticity is attributed to the highly hydrophilic nature of the XG hydrogels and their capacity to fundamentally alter the water retention characteristics and pore fluid viscosity of the kaolinite matrix. Concurrently, the mechanical response exhibits distinct non-linear behavior. Analysis of the cone fall test data reveals the existence of a specific threshold dosage governing undrained shear strength. Beyond this critical XG concentration, the rate of strength improvement alters trajectory, suggesting a saturation point in clay-polymer cross-linking and the onset of hydrogel rheological dominance within the pore space. Furthermore, the varied curing periods highlight time-dependent strengthening mechanisms.

This presentation will discuss the experimental methodology, the qualitative trends linking plasticity and strength, and the underlying hydro-mechanical mechanisms driving the observed threshold behavior.

Experimental and Numerical Study of Erosion in Chalk Reservoirs

Tatsuki Komatsubara[1], Alexandre Lavrov[1], Euripides Papamichos[2], Roar Egil Flatebø[3]

[1] Norwegian University of Science and Technology, Trondheim, Norway
[2] SINTEF Industry, Trondheim, Norway; Aristotle University of Thessaloniki, Thessaloniki, Greece
[3] Aker BP, Stavanger, Norway

tatsuki.komatsubara@ntnu.no

Hydrocarbon production from chalk fields in the North Sea has been challenging due to well instabilities and massive chalk influx events. It has been reported that most chalk influx problems occur in weak and fluid-saturated chalk formations in the near-wellbore region. These problems can be triggered by arching failure near perforations. The objective of this study is to develop experimental and numerical models to investigate chalk erosion under hydro-mechanical conditions.

Arching experiments were performed on cylindrical chalk specimens with different perforation sizes and pore fluid types to evaluate the failure mechanisms. Also, permeability was measured during the experiments to investigate complex interactions between erosion and pore fluid flow. To replicate the experiments, an elasto-plastic model was developed as a user-defined subroutine in Abaqus. In addition, a coupled hydro-mechanical approach was implemented in the model. The failure of the rock was judged by the critical plastic strain limit while the failed elements were deleted in the numerical simulation to represent the arching failure. Also, a case study was performed evaluating erosion under various stress and pore pressure conditions.

The experimental results showed that the arching failure occurs near the perforation, where pore fluid flow induces material detachment from chalk samples and leads to outward propagation of the arching zone. Also, the parametric study results suggested that the effects of the perforation size and pore fluid type were significant for chalk influx problems. It was found that samples saturated with water fail more easily than those saturated with oil. In addition, the numerical study results showed that the poro-elasto-plastic model properly simulates the failure propagation experienced during the experiments and can be used to evaluate chalk erosion under drawdown conditions. The experimental and numerical approaches that evaluate chalk erosion allow engineers to determine appropriate perforation design and critical drawdown pressure, which contributes to preventing well instabilities and chalk influx problems during production.

New aspects of inclined surface flows of photoelastic disks

Fu-Ling Yang[1]
[1] Mechanical Engineering National Taiwan University
fulingyang@ntu.edu.tw

This work investigates steady inclined surface flows of photoelastic disks with additional aspects from the evolutoin of force network and associated grain rotation. From the time-lapsed photoelastic images, we discovered a penetration band that force network may grow from the frictional base, and the normalized band height (by the flow height) is found to decay with the flow Froude number. High-speed images are analyzed for the depth profiles of flow velocity, shear rate, granular temperature, and particle rotation and they all show distinctive trends acorss the fringe penetration band. In addition, the fringe is analyzed for indirect stress evaluation which will be discussed together with the direct forcing at the chute wall, to provide new aspects to the classic problem of steady granular flows down an incline.

References

[1] A. Riccardo and P. Richard, "Effective wall friction in wall-bounded 3D dense granular flows," Physical review letters 115.15: 158001, 2015
[2] F.-L. Yang and Y. T. Huang. "New aspects for friction coefficients of finite granular avalanche down a flat narrow reservoir," Granular Matter 18,1-13, 2016
[3] C. C. Lin, R. Artoni, F.-L. Yang and P. Richard, "Modelling the wall friction coefficient for a simple shear granular flow in view of the degradation mechanism," Journal of Fluid Mechanics, 969, A7, 2023

Enhancing the Soil–Anchor Interface of Screwed Pile Anchors in Loose Sand through MICP Treatment

Xuanyi Chen[1], Frank Mcdermott[2], Shane Donohue[1], Budi Zhao[1]
[1] School of Civil Engineering, University College Dublin, Ireland
[2] School of Earth Sciences, University College Dublin, Ireland
chen.xuanyi@ucdconnect.ie

Screwed pile anchors mobilise uplift resistance through complex interactions between the helix, shaft and surrounding soil. In loose sand, however, the volume of soil effectively engaged during pull-out may be limited by installation constraints and weak interface confinement. Post-installation microbially induced calcite precipitation (MICP) offers a potential route to modify the soil–anchor interface by forming a cemented transition zone around the anchor. The mechanical benefit of such treatment depends not only on the amount of calcium carbonate precipitated, but also on where precipitation occurs, how far it extends from the anchor, and whether the treated zone remains continuous along the soil–anchor interface.

This study investigates the influence of injection flow rate on the formation of MICP-treated soil around a model screwed pile anchor installed in loose sand. Bacterial and cementation solutions were delivered through a hollow anchor shaft to target the soil above and below the helix. The treatment programme consisted of a bacterial injection followed by multiple pulsed injections of cementation solution under different flow-rate conditions. After treatment, the anchor and surrounding soil were excavated to examine the size, shape, radial extent and continuity of the cemented soil mass formed around the anchor.

Preliminary observations show that injection flow rate strongly controls the morphology of the bio-cemented transition zone. Lower flow rates tend to promote localised precipitation close to the injection points and may induce near-anchor clogging, limiting the radial extent of treatment. Higher flow rates transport cementation solution further into the sand and can increase the overall cemented radius, but excessive flow rates may reduce precipitation close to the anchor and lead to partial separation between the anchor surface and the surrounding cemented soil mass. These observations suggest that injection protocols need to balance treatment radius, cementation continuity and interface bonding. A staged injection strategy, for example progressively reducing the flow rate from high to medium to low, may therefore provide a practical route to forming a larger, more continuous and mechanically effective cemented zone around screwed pile anchors. The findings provide insight into the hydraulic and chemical controls on bio-cemented soil–structure interface formation in loose sand.

A new interface shear method for investigation of the influence of lateral stress components

Sabine Gehring[1], Hans Henning Stutz[1]
[1] Institute of Soil Mechanics and Rock Mechanics, Karlsruhe Institute of Technology
sabine.gehring@kit.edu

Geotechnical projects include not only soil, but also structures like piles, foundations or retaining walls. In such systems, the interface behaviour between the structure and the neighbouring soil often governs the overall system's behaviour. For example, the shaft friction between piles and the surrounding soil is decisive for the loading capacity of piles. Therefore, many researchers investigated the interface behaviour and developed different laboratory tests to model in-situ contact shear behaviour. They identified several influencing factors, such as roughness and hardness of the contact surface, grain shape, density and normal stress on the contact surface [1,2,3].

The existing interface shear devices have one drawback in common: The lateral deformation of the sample is hindered by rigid frames (direct interface shear test) or rigid rings (simple interface shear test) [1,2,3]. Hence, the stress components on the planes orthogonal to the interface can not be measured or controlled. Therefore, the influence of these stress components and various 3D-stress states on interface shear behaviour have not yet been investigated. Few exceptions show devices which can control one stress component on a plane orthogonal to the contact plane [4,5,6]. Still, it is not possible to control independently from each other the normal stress on the contact plane and two different normal stress components on the planes orthogonal to the contact plane (Figure b).

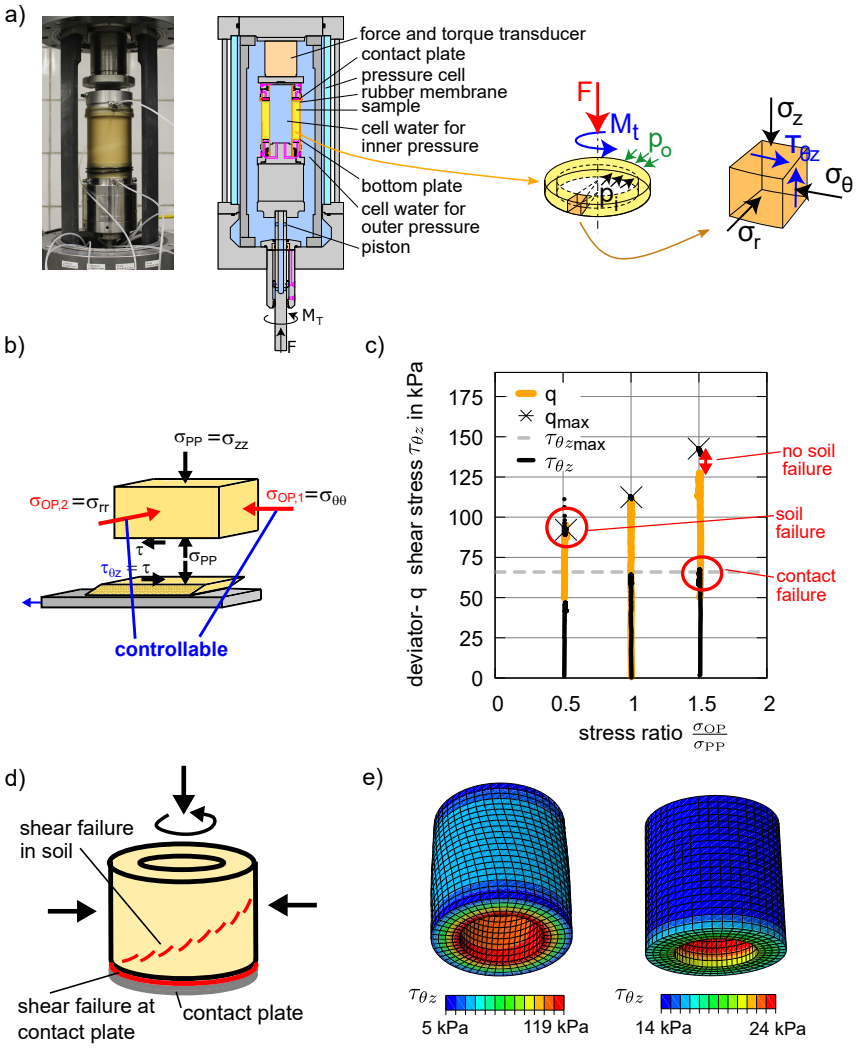
To overcome this shortcoming and create new research opportunities, a new test method is developed to enable investigations on the influence of different stress states on interface shear behaviour. A hollow cylinder device is modified with an interchangeable contact plate to conduct interface tests [7]. The top and bottom cap of a hollow cylinder shaped sample are rotated against each other to induce a displacement between the contact plate and the opposite sample end. With four independently controllable quantities (axial force F, inner cell pressure p_i, outer cell pressure p_a, torque M) it is possible to control three normal stress components in the soil above the contact surface (Figure a and b).

The measured test results (Figure c) are interpreted with two possible failure mechanisms: soil failure due to an exceeded shear strength (q_{critical}) and contact failure due to the attainment of the contact shear strength ($\tau_{\max}$), see Figure d. Figure c shows test results with an equal and constant normal stress on the plane parallel to the interface $\sigma_{\text{PP}}) = 100\,\text{kPa}$. The ratio between the normal stress on the planes orthogonal to the interface and the normal stress on the plane parallel to the interface $\frac{\sigma_{\text{OP}}}{\sigma_{\text{PP}}}$ influences the failure mode and also the value of the maximum shear stress $\tau_{\theta z}$. The failure mechanism hypothesis is plausibilized by modelling the test as a boundary value problem with the finite element method (Figure e).

The new interface shear method enables the realistic modelling of in-situ stress states at interfaces in laboratory and the systematic variation of stress components on the planes orthogonal to the contact plane. It enables to investigate the influence of different 3D-stress states on interface shear behaviour.

References

[1] M. Uesugi and H. Kishida, "Influential factors of friction between steel and dry sands", *Soils and foundations*, vol. 26, no. 2, pp. 33-46, 1986, doi: 10.3208/sandf1972.26.2_33



caption

[2] J.D. Frost, J.T. DeJong and M. Recalde, "Shear failure behaviour of granular-continuum interfaces", *Engineering Fracture Mechanics*, vol. 69, no. 17, pp. 2029-2048, 2002, doi: 10.1016/S0013-7944(02)00075-9

[3] E. Wernick, „Tragfähigkeit zylindrischer Anker in Sand unter besonderer Berücksichtigung des Dilatanzverhaltens", Veröffentlichungen des Institutes für Bodenmechanik und Felsmechanik am Karlsruher Institut für Technologie (KIT), Heft 75, PhD thesis, 1978

[4] J. Tejchman and W. Wu, "Experimental and numerical study of sand-steel interfaces", *International Journal for Numerical and Analytical Methods in Geomechanics*, vol. 19, no. 8, pp. 513-536, 1995, doi: 10.1002/nag.1610190803

[5] A. Corfdir, „A cylindrical shear apparatus", *Geotechnical Testing Journal*, vol. 27, no. 5, pp. 447-455, 2004, doi: 10.1520/GTJ11551

[6] S. Liu et al., „Shear rate and roughness effect on clay-steel interface strength properties in CU and CPD drainage conditions", *Ocean Engineering*, vol. 305, 2024, doi: 10.1016/j.oceaneng.2024.117956

[7] S. Gehring and H. H. Stutz, "Influence of anisotropic stress states on soil-structure interface behavior: a new experimental approach in a modified hollow cylinder apparatus", *Soils and Rocks*, vol. 48, no. 4, 2025, doi: 10.28927/SR.2025.003725

Effect of contact friction variability on granular behavior

Nabil Younes[1], Saeid Nezamabadi[1], Franck Radjai[1]
[1] LMGC, Univ Montpellier, CNRS, Montpellier, France
saeid.nezamabadi@umontpellier.fr

Understanding how microscale variability influences the shear strength of granular soils is essential for modeling natural hazards such as slope failures and debris flows. The mechanical behavior of granular materials emerges from grain scale interactions and the development of force and fabric anisotropy [1]. In this study, the Discrete Element Method (DEM) is used to investigate how spatial variability in interparticle friction affects the mechanical response of granular assemblies. Three dimensional triaxial compression tests are performed while systematically varying both the mean friction coefficient and the amplitude of its variability, starting from identical dense isotropic states. The macroscopic behavior is interpreted alongside micromechanical indicators including friction mobilization and fabric and force anisotropies [2].

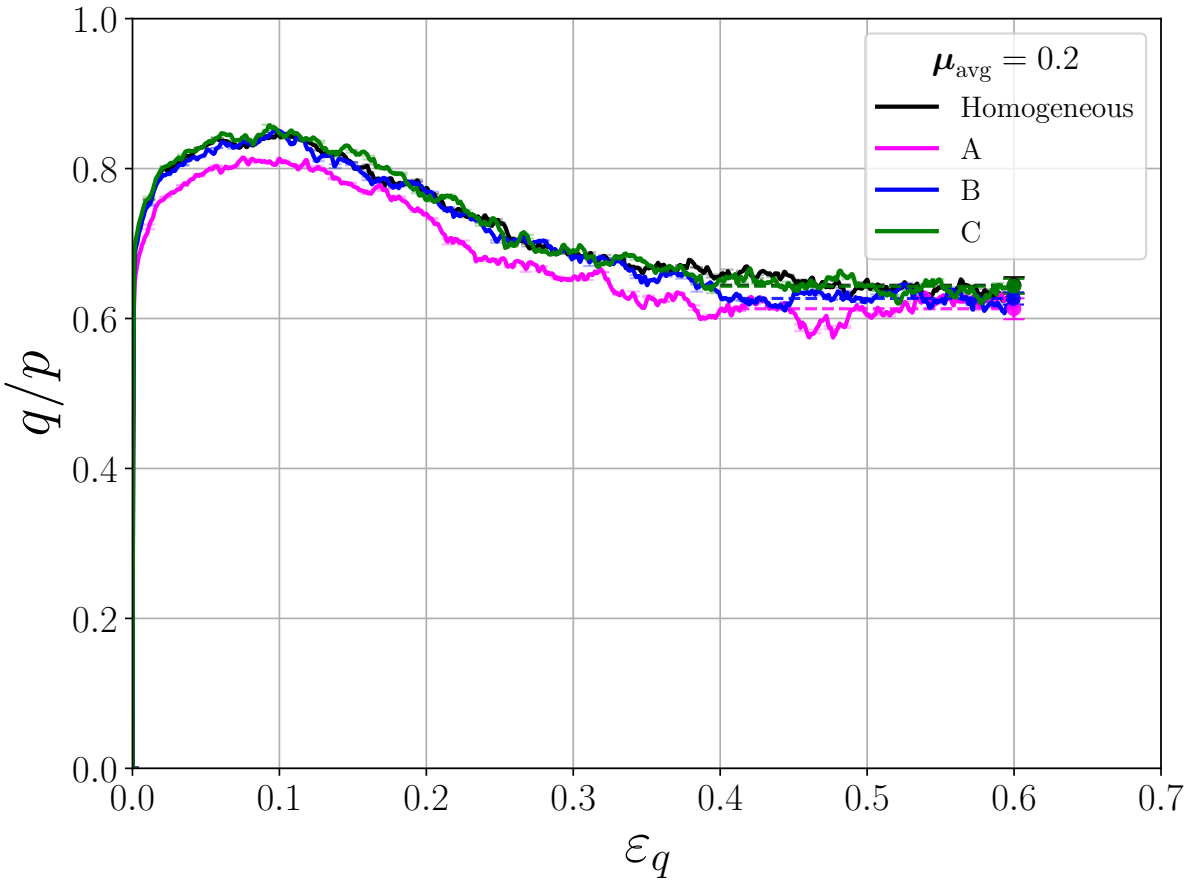
To characterize frictional heterogeneity, four configurations are considered: one homogeneous reference case, in which a single friction coefficient is assigned to all contacts, and three heterogeneous cases (Groups A, B, and C) as shown in Figure 1. In the heterogeneous cases, the contact friction coefficient is distributed over a prescribed interval with identical mean value but different variability amplitudes, with Group A exhibiting the largest variability, Group B an intermediate one, and Group C the smallest variability. This design allows isolating the effect of friction variability while keeping the average friction identical across all simulations.To characterize frictional heterogeneity, four configurations are considered: one homogeneous reference case, in which a single friction coefficient is assigned to all contacts, and three heterogeneous cases (Groups A, B, and C). In the heterogeneous cases, the contact friction coefficient is distributed over a prescribed interval with identical mean value but different variability amplitudes, with Group A exhibiting the largest variability, Group B an intermediate one, and Group C the smallest variability. This design allows isolating the effect of friction variability while keeping the average friction identical across all simulations.

The results show that friction variability has only a minor influence on peak shear strength and practically no effect on the critical state response, as illustrated in Figure 1. This agrees with previous DEM studies indicating that shear strength is mainly controlled by the mean friction coefficient and anisotropic force transmission, while also complementing recent stochastic DEM work [3], which reported that friction heterogeneity primarily broadens the macroscopic stress–strain response without fundamentally altering the deformation mode. Even large contact scale variability induces only limited deviations from the homogeneous case. In this work, micromechanical analysis confirms that the internal force–fabric structure remains nearly invariant across variability levels, explaining the insensitivity of the macroscopic response.

These findings suggest that granular materials retain stable shear resistance despite significant contact scale friction heterogeneity, supporting the reliability of friction based constitutive models used in hazard assessment, slope stability analysis, and debris flow simulations.

References

[1] Rothenburg, Leo, and R. J. Bathurst. "Analytical study of induced anisotropy in idealized granular materials." Geotechnique 39, no. 4 (1989): 601-614.



[2] Yang, Ming, Mahdi Taiebat, Patrick Mutabaruka, and Farhang Radjai. "Evolution of granular materials under isochoric cyclic simple shearing." Physical Review E 103, no. 3 (2021): 032904.
[3] Huang, Yu, Xiaolin Tan, Ying Luo, Pengpeng He, and Chongqiang Zhu. "The effect of inter-particle friction uncertainty on the shear behavior of granular materials: Insight from the discrete element method coupled with stochastic field theory." Journal of Geophysical Research: Earth Surface 131, no. 2 (2026): e2025JF008915.

DEM Modeling of Crack Formation and Propagation in Fine-Grained Soils

Zahra Mousavi[1], Arash Alimardani Lavasan[1]
[1] University of Luxembourg
zahra.mousavi@uni.lu

Desiccation cracking can significantly reduce the structural integrity and hydraulic performance of fine-grained soils used in geo-infrastructure systems [1]. Although surface crack patterns have been widely investigated, the three-dimensional evolution and internal propagation of crack networks remain difficult to characterize. This study uses the Discrete Element Method (DEM) to investigate shrinkage-induced cracking in cohesive soils.

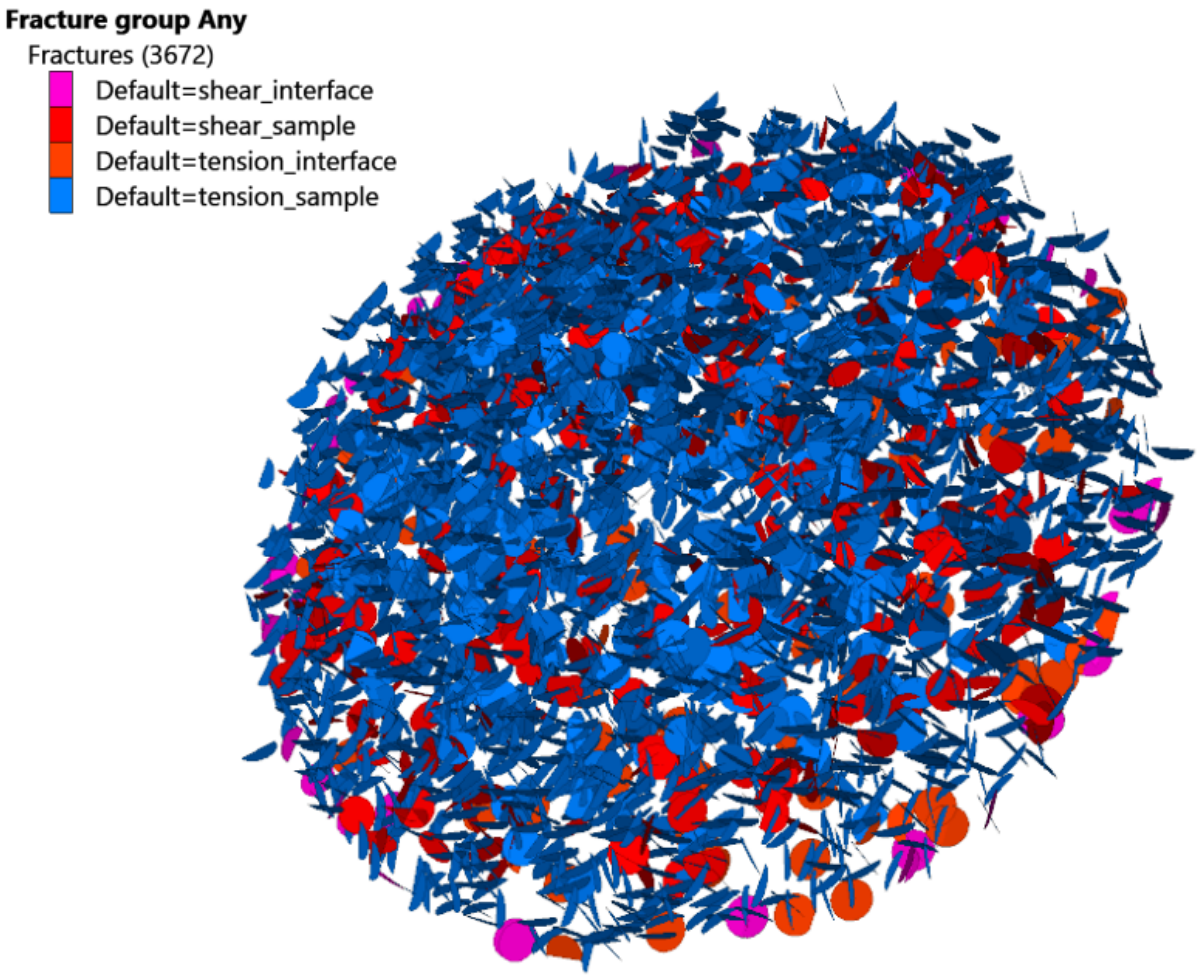
A three-dimensional, particle-based model of a cylindrical soil specimen was developed to simulate progressive volumetric shrinkage during drying. Each grain shrinks with decreasing water content according to an aggregate-shrinkage law, while inter-particle cementation is represented by a linear contact-bond model whose stiffness and strength degrade with water content, calibrated against benchmark desiccation-cracking data [2]. Cracking is represented through progressive bond breakage in tension and shear, distinguishing cracking within the sample interior from cracking at the sample-boundary interface, consistent with recent DEM studies of boundary-condition effects [3].

Preliminary simulations, in which the specimen water content is reduced from 60% to below 5%, already capture the expected transition from negligible early-stage bond breakage to a three-dimensional network of interconnected fractures penetrating the sample interior (Fig. 1), consistent with the initiation-to-propagation mechanism reported from DEM simulations elsewhere [4]. Both tensile and shear bond failures are captured, together with distinct interface-versus-interior cracking behavior.

The model is currently being refined ahead of the workshop: ongoing work focuses on quantitative calibration of the shrinkage and bond-degradation laws, validation of the simulated crack morphology against experimental and numerical benchmarks, and a parametric study of specimen geometry and interface strength. This refined model will form the basis for the next stage of this research, improving the understanding of the mechanisms governing three-dimensional crack development in fine-grained soils and their implications for the long-term degradation of soil barriers and earthen structures.

References

[1] H. Péron, T. Hueckel, L. Laloui, and L. Hu, "Fundamentals of desiccation cracking of fine-grained soils: experimental characterisation and mechanisms identification," Canadian Geotechnical Journal, vol. 46, no. 10, pp. 1177–1201, 2009.
[2] J. Sima, M. Jiang, and C. Zhou, "Numerical simulation of desiccation cracking in a thin clay layer using 3D discrete element modeling," Computers and Geotechnics, vol. 56, pp. 168–180, 2014.
[3] Z.-Y. Lin, Y.-S. Wang, C.-S. Tang, Q. Cheng, H. Zeng, C. Liu, and B. Shi, "Discrete element modelling of desiccation cracking in thin clay layer under different basal boundary conditions," Computers and Geotechnics, vol. 130, art. 103931, 2021.
[4] T. Wang, C.-S. Tang, W.-J. Liu, Q. Cheng, Z.-T. Shen, and X.-H. Pan, "Insight into the initiation and propagation mechanism of desiccation cracking in clayey soil from DEM simulations," Computers and Geotechnics, vol. 175, art. 106694, 2024.



Three-dimensional network of broken inter-particle bonds classified by failure mode (tension/shear)

Modelling Wetting–Drying Effects in Unsaturated Soils: The Role of Expressions in Predicting Relative Permeability.

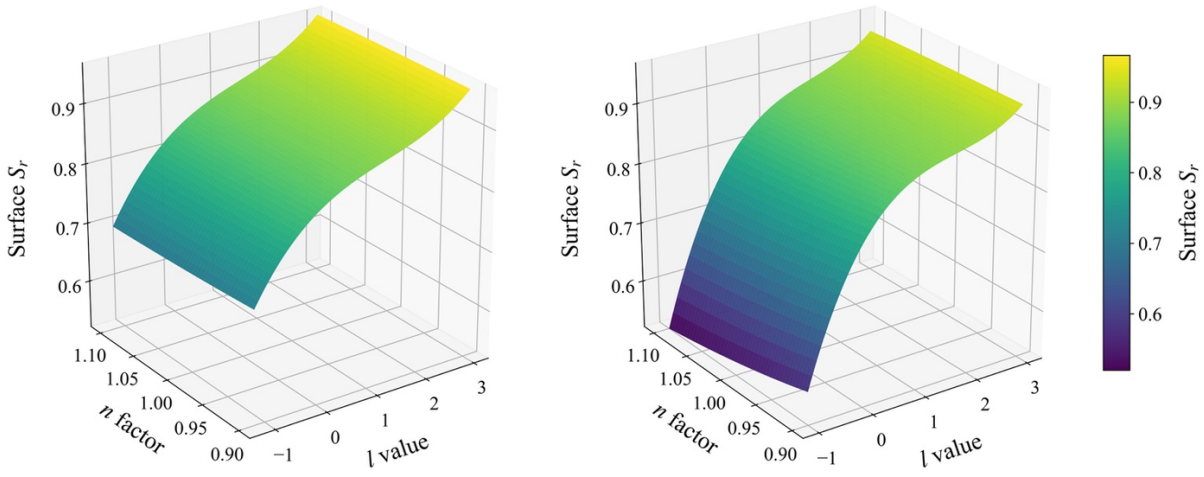
Qinghexing Kong[1], Catherine O'Sullivan[1], Katerina Tsiampousi[1], Hao Wang[1]
[1] Imperial College London, United Kingdom
qinghexing.kong21@imperial.ac.uk

Many slopes and engineered embankments are partly saturated (unsaturated) under normal operating conditions. Rainfall-induced instability is therefore important for natural hazard assessment and infrastructure management.management. The hydraulic response in unsaturated soil is governed by water storage and transmission within the soil; the unsaturated hydraulic conductivity controls the water flux under given boundary conditions. Unsaturated soil hydraulic conductivity is commonly quantified from the saturated hydraulic conductivity using the relative permeability (k_r), which is defined as the ratio of unsaturated to saturated hydraulic conductivity. Relative permeability depends upon the degree of saturation, and the soil pore structure including pore-size distribution, pore connectivity and tortuosity. The function that is adopted to predict k_r in stability analyses can significantly affect predictions of how the suction and degree of saturation evolve, as well as their steady-state distributions. These hydraulic states are important because they can directly influence the predictions of effective stress, shear strength and factor of safety in hydro-mechanical stability assessment.

Burdine [1] and Mualem [2] proposed two classical models to predict k_r using the soil water retention curve (SWRC). Van Genuchten [3] later combined his SWRC equation with the two relative permeability models, leading to the van Genuchten–Burdine (VGB) and van Genuchten–Mualem (VGM) expressions to predict k_r. The VGM expression is more widely used because of its convenient closed-form, and it is implemented in numerical software, such as PLAXIS [4] and HYDRUS [5]. However, the resulting widespread use of the VGM expression has generally evolved without significant critical analysis of the expression. Even with the same retention curve and saturated hydraulic conductivity, the choice between VGM and VGB can further lead to different suction and saturation profiles due to the different expressions.

Direct comparison between the VGB and VGM expressions is difficult using currently available numerical packages as they generally implement VGM as the default hydraulic conductivity model. In addition, the closed-form VGM and VGB expressions are associated with different coupling assumptions between the van Genuchten retention parameters m and n. It is not possible using PLAXIS or HYDRUS to independently assess sensitivity to the SWRC and the relative permeability model.

To isolate the effect of the k_r expression on predicted responses in-situ, a customised one-dimensional soil-column code was developed in Python. The code allows the retention curve, saturated hydraulic conductivity, initial condition and boundary conditions to be maintained constant while only changing the relative permeability expression. The code was validated against PLAXIS [4] using the VGM formulation. Then a controlled sensitivity analysis considered a 1.5 m sand column model with a closed bottom boundary and a constant top flux of 30 cm/day. Data for the final degree of saturation within the upper 0.5m of the soil column for different values of the van Genuchten shape parameter n and the tortuosity parameter l are given in Figure 1. The near-surface saturation varies substantially with the selected formulation and parameterisation. These data indicate the need for a critical appraisal of these models, including a re-evaluation of assumptions used in their original derivation.



caption

References

[1] N. T. Burdine, “Relative permeability calculations from pore-size distribution data,” *Journal of Petroleum Technology*, vol. 5, no. 3, pp. 71–78, doi: 10.2118/225-G.

[2] Y. Mualem, “A new model for predicting the hydraulic conductivity of unsaturated porous media,” *Water Resources Research*, vol. 12, no. 3, pp. 513–522, doi: 10.1029/WR012i003p00513.

[3] M. T. van Genuchten, “A closed-form equation for predicting the hydraulic conductivity of unsaturated soils,” *Soil Science Society of America Journal*, vol. 44, no. 5, pp. 892–898, doi: 10.2136/sssaj1980.03615995004400050002x.

[4] Bentley Systems, *PLAXIS 2D Reference Manual*. Seequent, Bentley Systems, 2024.

[5] PC-Progress, *HYDRUS Software Package for Simulating Water, Heat and Solute Movement in Variably Saturated Media*. Prague, Czech Republic: PC-Progress s.r.o., 2024.

The role of geological uncertainties in the modelling of deep-seated gravitational slope deformations

Maria Honisch[1], Barbara Schneider-muntau[1]

[1] University of Innsbruck, Department of Infrastructure Engineering, Unit of Geotechnical Engineering

maria.honisch@uibk.ac.at

Deep-seated gravitational slope deformations (DSGSDs) are a widespread phenomenon in the Alpine region and have recently become more important due to their influence on sensitive infrastructure. DSGSDs describe extremely slow (max. 16 mm/a) to very slow (max. 1.6 m/a) [1], long-lasting mass movements that are caused by rock weakening and typically affect an entire mountain slope. The characterization of these mass movements is not trivial, as deep outcrops are usually limited to the more accessible valley areas which are the focus of infrastructure projects. Using the example of the Padauner Berg in Tyrol / Austria, this contribution shows the importance of evaluating different geological scenarios for further numerical modelling, which result from the existing input parameters such as geophysics, borehole data and remote sensing data. The Padauner Berg mass movement is an excellent case study, as the slope foot area is well explored due to the current renewal of a prominent motorway bridge, the Lueg Bridge. Nevertheless, the results from the exploration raise new questions that provide fresh insights into the complexity of the subsurface.

Uncertainty analyses in numerical modelling capture the variability of soil parameters, but in most cases are based on a single geological model without including the uncertainties in the geological interpretation in the calculations.

Different geological models result not least from the geologist's experience and creativity in allowing different interpretations of the input parameters (such as geophysical profiles, drill core images, etc.) and not committing to a single, plausible explanation.

In the case of the Padauner Berg, the uncertainty begins with the formation of this profound mass movement, which could have been caused by a catastrophic failure [2] on the one hand, and by the deglaciation after the last ice glacial maximum (LGM) [3] on the other, whereby other phenomena such as seismic activity, the uplift of the Tauern Window [4] or weak layer boundaries must also be taken into account as triggers. This has an impact on the geological model, such as whether there are defined sliding horizons or whether the slope has a gradual disintegration, decreasing with depth.

Additionally, the interpretation of the drill cores and the seismic survey also leave room for the geological subsurface model. For example, drill core recordings are not always definite and strongly dependent on the assessment by the geologist. Also, seismic reflectors / refractors do not always correlate with the lithology change interpreted by the geologist from cores. For example, the seismic rock top can certainly deviate from the geological rock top, if weathering is present. To examine the impact of geological uncertainties on numerical models, we present potential scenarios for the formation of the DSGSD Padauner Berg, as well as an analysis of the uncertainties in a detailed section of the slope foot area where the Lueg bridge is situated.

References

[1] C. Zangerl, C. Prager, R. Brandner, E. Brückl, S. Eder, W. Fellin, G. Poscher, H. Schönlaub, 2008. „Methodischer Leitfaden zur Prozessorientierten Bearbeitung von Massenbewegungen.“, Geo.Alp 5, pp. 1–51.

[2] M. Ostermann, D. Sanders, 2017. „The Benner pass rock avalanche cluster suggests a close relation between long-term slope deformation (DSGSDs and translational rock slides) and catastrophic failure", Geomorphology, vol. 289, pp. 44–59, doi:10.1016/j.geomorph.2016.12.018.
[3] GeoSphere Austria, „Vergletscherung der Ostalpen in der Würm-Eiszeit.", https://www.geosphere.at.
[4] P. Sternai, C. Sue, L. Husson, E. Serpelloni, T.W. Becker, S.D. Willett, C. Faccenna, A. Di Giulio, G. Spada, L. Jolivet, P. Valla, C. Petit, J.M. Nocquet, A. Walpersdorf, S. Castelltort, S., 2019. „Present-day uplift of the European Alps: Evaluating mechanisms and models of their relative contributions", Earth-Science Reviews, vol. 190, pp. 589–604, doi:10.1016/j.earscirev.2019.01.005.

Characterisation of drying-induced cementation and shearing behaviour of biopolymer-treated sand using X-ray tomography

Mhlengi Khaya Luke Masango[1], Hui Zhang[2], Budi Zhao[1]
[1] University College Dublin
[2] University College Dublin and Université Gustave Eiffel (ENPC)
mhlengi.masango@ucdconnect.ie

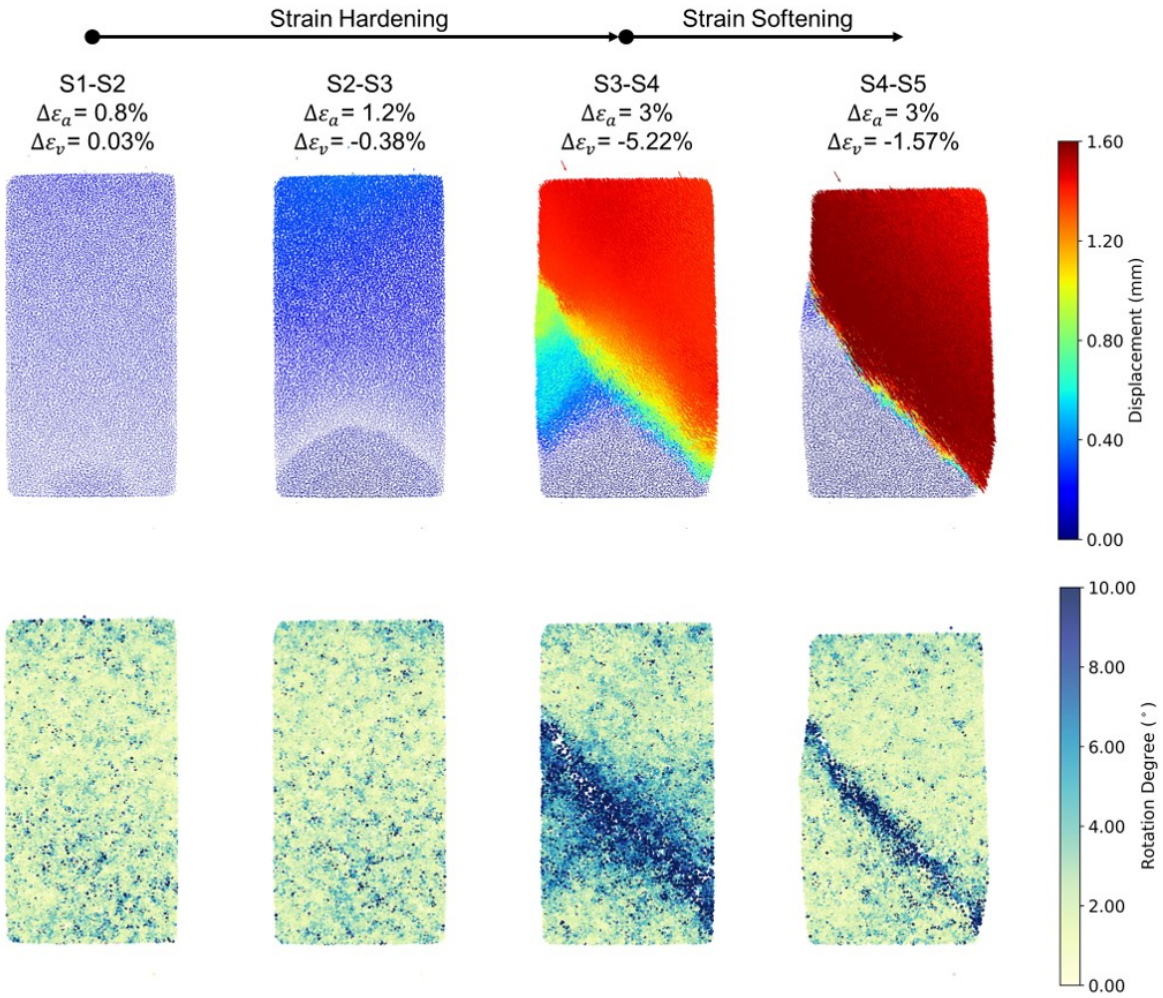
Bio-inspired soil improvement has gained traction because of the demand for sustainable solutions in geotechnical engineering. Biopolymer treatment has emerged as a promising stabilisation alternative. Studies show that biopolymers enhance soil strength, reduce erosion, suppress dust, and reduce permeability. Although several biopolymers have been investigated, xanthan gum has received attention because of its workability, water solubility, and reinforcing capability.

Previous studies have focused on laboratory testing of biopolymer-treated soils. However, the processes governing biopolymer bond formation during curing, and the influence of bond distribution on strength and failure mechanisms, remain poorly understood. Unlike lime or Portland cement treatment, which cures through hydration, biopolymer treatment is governed by drying. Drying conditions and initial fluid properties influence biopolymer cementation within the granular skeleton. These conditions produce cementation patterns that cause strength variability and conflicting results in the literature. Drying may influence bonding strength by promoting cracks within biopolymer bonds or delamination between bonds and sand particles. Few studies have explored the failure mechanisms of biopolymer-treated soils. Literature typically interprets failure phenomenologically by linking stress-strain responses, particularly peak strength, cohesion, and friction angle, to biopolymer type and content. Although valuable, these interpretations remain empirical correlations and offer limited insight into strength enhancement and microscopic failure mechanisms.

This study investigates curing in biopolymer-treated soil during one-dimensional drying using X-ray microtomography. We then link curing-controlled cementation patterns to mechanical response and failure mechanisms by coupling a miniature triaxial apparatus with in-situ X-ray microtomography. Leighton Buzzard sand was treated with xanthan gum at a mass ratio of 1%. Potassium iodide solution, equivalent to 10% moisture content, was added as a contrast agent to differentiate xanthan gum bonds in microtomography images. The treated sample was hand compacted into a cylindrical container, 20 mm diameter and 40 mm high, and oven-dried at 35°C. During drying, scans were acquired at moisture contents of 10%, 8%, 5%, 2%, and 0% to visualise internal drying and bond formation. After drying, the sample was tested under triaxial loading at a confining pressure of 50 kPa and a strain rate of 0.06% per minute. Additional scans were acquired at axial strains of 0%, 0.8%, 2%, 5%, and 8% to capture deformation.

The drying process showed diffusion-dominated behaviour, with an immediate decrease in drying rate. This process produced a vertical distribution of biopolymer cementation, with volume fraction increasing with depth. Near the drying surface, bonds were thinner and less extensive, whereas thicker and more continuous bonds persisted at the bottom. Preliminary results show that xanthan gum treatment increased shear strength to approximately 2.1 MPa, up to seven times that of untreated sand. X-ray microtomography images reveal that peak strength was mobilised while the bond network remained intact, whereas failure occurred through progressive bond breakage, particle rearrangement, and local dilation, which led to strain localisation (Figure 1). Ongoing research focuses on how

drying rate and initial fluid viscosity affect biopolymer distribution. Quantitative image analysis measures bond distribution, contact characteristics, and local strain distribution to elucidate strength enhancement and failure in biopolymer-treated sand.



caption

Integrated multi-method assessment of rainfall-induced debris flows

Giulia La Porta[1], Marina Pirulli[1], Giuseppe Bausilio[2], Diego Di Martire[2], Ascanio Rosi[3], Elisa Saler[3], Luca Badin[3], Andrea Gennaro[3], Francesca Da Porto[3], Carlo Esposito[4]

[1] Politecnico di Torino
[2] University of Naples Federico II
[3] University of Padova
[4] Sapienza University of Rome

giulia.laporta@polito.it

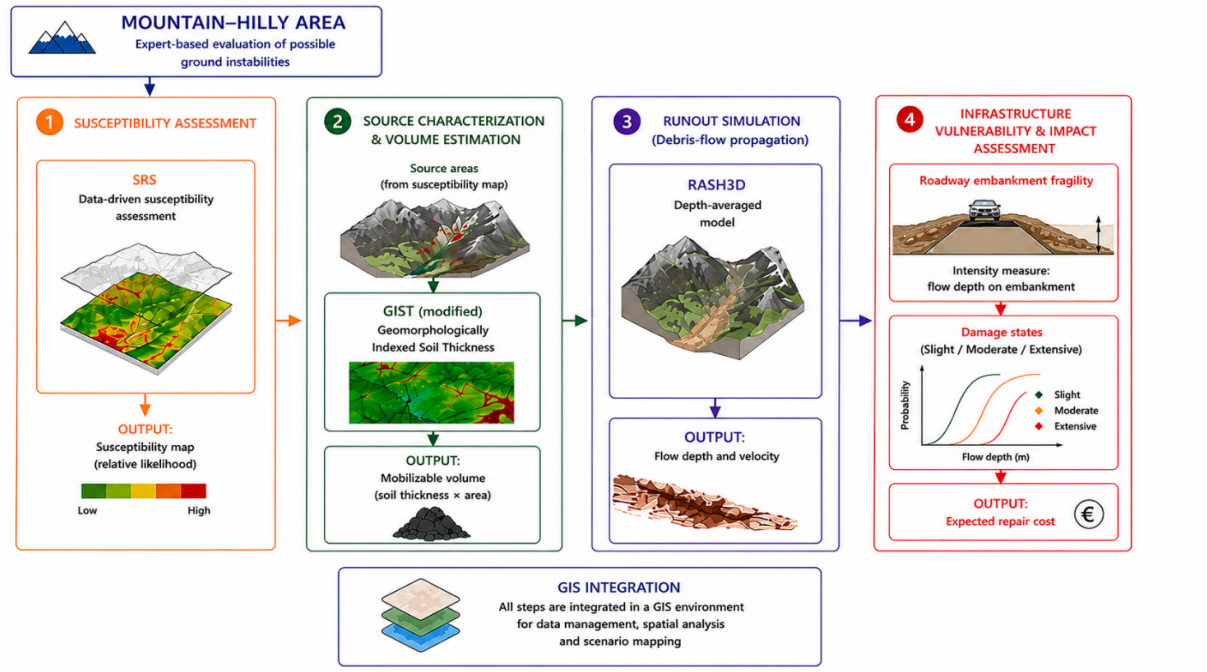
Rainfall-induced shallow landslides evolving into debris flows represent one of the major natural hazards affecting mountain transportation corridors. In Alpine environments, steep slopes and abundant unconsolidated deposits favour rapid flow-like processes capable of severely impacting road infrastructure and disrupting regional accessibility. Despite the increasing availability of susceptibility, propagation and impact models, integrated approaches are still limited, particularly in operational risk assessment frameworks.

This contribution presents a GIS-based integrated workflow developed within the RETURN (Multi-Risk Science for Resilient Communities under a Changing Climate) project, funded under the Italian National Recovery and Resilience Plan (PNRR), and applied to the Alpine Road Corridor in the Eastern Italian Alps, where debris flows constitute a major hydro-geomorphological threat for the roadway network. The proposed toolchain focuses on rainfall-induced shallow slope failures evolving into debris flows and combines data-driven susceptibility analysis, source characterization, runout simulation and infrastructure impact assessment within a modular and scalable framework.

Slope susceptibility is assessed using the Subaerial Regional Susceptibility (SRS) model, a data-driven tool developed within the RETURN project for the spatial identification of areas prone to shallow slope failure. The analysis relies on an ensemble modelling strategy combining the outputs of three complementary algorithms: Random Forest, Gradient Boosting Machine and Generalized Linear Model [3]. The highest susceptibility areas are subsequently retained as potential debris-flow source zones. Scenario building further integrates source-area characterization, soil thickness estimation and debris-flow propagation analysis. Soil thickness distribution is reconstructed through a modified GIST (Geomorphologically Indexed Soil Thickness) model [1], while debris-flow runout is simulated using the continuum-based depth-averaged numerical model RASH3D [5] in selected catchments directly connected to the road corridor. The workflow allows the identification of potential impact areas along the valley floor and provides a first-order evaluation of the interaction between debris-flow propagation and exposed transportation infrastructure. Runout intensity measures are further coupled with roadway embankment fragility relationships for debris-flow impact assessment [4], enabling the definition of preliminary infrastructure damage scenarios. Expected repair costs associated with debris deposition on roadway pavement layers are also evaluated according to the framework proposed by [2].

The application highlights the capability of the proposed workflow to consistently link debris-flow susceptibility, source characterization, flow propagation and infrastructure impact within a complex Alpine environment. The modular structure of the toolchain allows adaptation to different data availability conditions and territorial contexts, while maintaining methodological consistency across the different analytical steps. At the same time,

the application emphasizes the importance of expert judgement in the selection of input parameters and in the critical interpretation and validation of modelling outputs. The proposed approach provides a flexible framework for supporting risk-based assessment, mitigation planning and infrastructure risk management in mountain regions.



caption

References

[1] Catani, F., Segoni, S., and Falorni, G. (2010). An empirical geomorphology-based approach to the spatial prediction of soil thickness at catchment scale. Water Resources Research, 46(5).

[2] Ferlisi, S., Marchese, A., and Peduto, D. (2021). Quantitative analysis of the risk to road networks exposed to slow-moving landslides: a case study in the Campania region (southern Italy). Landslides, 18, 303–319. https://doi.org/10.1007/s10346-020-01482-8

[3] James, G., Witten, D., Hastie, T., and Tibshirani, R. (2021). An Introduction to Statistical Learning: With Applications in R. Springer US. https://doi.org/10.1007/978-1-0716-1418-1

[4] Nieto, N., Chamorro, A., Echaveguren, T., Sáez, E., and González, A. (2021). Development of fragility curves for road embankments exposed to perpendicular debris flows. Geomatics, Natural Hazards and Risk, 12(1), 1560–1583.

[5] Pirulli, M., Bristeau, M.-O., Mangeney, A., and Scavia, C. (2007). The effect of the earth pressure coefficients on the runout of granular material. Environmental Modelling & Software, 22(10), 1437–1454.

Author Index

Abimaje
Faith, 30
Acary
Vincent, 68
Ahmadi
Ali, 78
Akbar
Ali, 38
Akbulut
Suat, 2
Al-Subari
Lutf, 38
Alcantara Fuentes
Marcopolo, 24
Alimardani Lavasan
Arash, 112, 124
Allard
Jose, 100
José, 98
Alrifai
Alissar, 56
Anbazhagan
P, 26
Ari
Abdulmuttalip, 2
Asanza-Izquierdo
Enrique, 42
Aubry
Jérôme, 60
Aversa
Stefano, 8
Azizi
Mahsa, 62
Azéma
Emilien, 18, 36

Bacquaert
Goustan, 64
Badin
Luca, 132
Bausilio
Giuseppe, 132
Bhattacharya
Debayan, 80, 84, 86
Biene
Gimena, 92
Bisht
Mukesh Singh, 22
Bleyer
Jérémy, 64
Braun
Philipp, 14, 94
Brochard
Laurent, 70

Caballero-Ezquerro
Mario, 42
Cabrera
Miguel, 30
Calvello
Michele, 24
Castro-Malaver
Carolina, 36
Chen
Xuanyi, 118
Cheng
Helen, 72
Hongyang, 46
Yi Pik, 102
Ciaglia
Rita, 8, 10, 12
Coelho
Pablo Dos Santos Cardoso, 108
Conil
Nathalie, 88
Cortés
Maximiliano, 98
Cuomo
Sabatino, 8, 10, 12
Cárdenas-Barrantes
Manuel, 36

Da Porto
Francesca, 132

Dangla
Patrick, 70
Dantas
Ana Karine Santos, 40
Dardé
Benjamin, 34
Datta
Manoj, 80
Deng
Min, 102
Dhanai
Prity, 84
Di Donna
Alice, 56, 66
Di Martire
Diego, 132
Di Perna
Angela, 10, 12
Donius
Corentin, 48
Donohue
Shane, 118
Druette
Ludovic, 64

Escudero-Merino
Diego, 42
Esposito
Carlo, 132

Fabbrini
Edoardo, 68
Fellin
Wolfgang, 32
Ferdik
Manuel, 32
Flatebø
Roar Egil, 114
Frost
David, 86
Fuentes
Raul, 38

Garza
Mattia, 66
Gehring
Sabine, 120
Gennaro
Andrea, 132
Gerolymatou
Eleni, 96
Ghabezloo
Siavash, 64
Guayacan Carrillo
Lina Maria, 88
Guigonnet
Vincent, 60
Guillard
François, 62
Gupta
Ritesh, 66
Gutiérrez-Oribio
Diego, 58

Hadrien
Rattez, 82
Han Ming
Lai, 6
Herle
Ivo, 4
Honisch
Maria, 128
Hua
Xi, 110

Jabbarzadeh
Milad, 112
Jeong
Juyeon, 24
Jitsangiam
Peerapong, 18

Khandelwal
Amrisha, 80
Kirby
Matthew, 6
Kitembo
Prince, 94
Komatsubara
Tatsuki, 114
Kong
Qinghexing, 126
Kurugodu
Harsha Vardhan, 86
Kwon
Tae-Hyuk, 24

La Porta
Giulia, 132

Laanaiya
Majdouline, 56
Laina Gómez
Carlos, 42
Laue
Jan, 44
Lavrov
Alexandre, 114
Leng
Jingyi, 70
Li
Guangzhi, 74
Liu
Fangzhou, 108
Mengwei, 110
Loyola
Ana, 94
Luding
Stefan, 46

Macias-Gutierrez
Andres, 104
Magnanimo
Vanessa, 46
Maiorano
Rosa Maria Stefania, 8
Manzanal
Diego, 92, 94, 98, 100
Martinelli
Mario, 8, 10, 12
Masango
Mhlengi Khaya Luke, 130
Masi
Filippo, 68
Matsushima
Takashi, 74
Maurer
Cristian, 106
Maurice
Christian, 44
Mcdermott
Frank, 118
Mishra
Govind, 46
Mladý
Tomáš, 28
Moniaci
Rosario Mattia, 28
Moscariello
Mariagiovanna, 10, 12
Mousavi
Zahra, 124
Mugele
Luis, 30, 54

Neuner
Matthias, 50
Nezamabadi
Saeid, 122
Niclaes
Jens, 82
Nicot
François, 60

O'Sullivan
Catherine, 126
Olarte-Garzon
Maria, 14
Orazzo
Raffaele, 8
Orlandi
Sandra, 92, 98
Ovalle
Carlos, 36, 106

Papamichos
Euripides, 114
Pereira
Jean-Michel, 14, 88, 94
Pierre
Delmelle, 82
Pirulli
Marina, 132
Potts
David, 6
Prommarin
Jitinun, 18

Qiao
Jiangmei, 110
Quinten
Tristan, 30

Radjai
Franck, 122
Raja
Yogarish Narasinga, 26
Renouf
Mathieu, 18, 36

Rey
Clément, 20
Ribeiro-Santos
Alan, 34
Richefeu
Vincent, 22
Riley
David, 16
Rognon
Pierre, 62
Rosi
Ascanio, 132

Saafan
Abdalla, 44
Sac-Morane
Alexandre, 14
Saez
Esteban, 106
Saler
Elisa, 132
Sarkar
Sourav, 26
Scaringi
Gianvito, 28
Schneider-Muntau
Barbara, 128
Scovazzi
Guglielmo, 16
Secades
Alejandro, 32
Shahu
J.T., 80
Simms
Paul, 108
Stathas
Alexandros, 50
Stefanou
Ioannis, 16, 58, 90
Stickle
Miguel, 94
Stutz
Hans, 30
Hans Henning, 54, 120
Sulem
Jean, 88

Tang
Anh-Minh, 34
Xuhai, 110
Tarullo
Angelo Giuseppe, 24
Thomas
Poulet, 82
Toromanovic
Jasmina, 44
Tsiampousi
Katerina, 126

Ullmann
Sebastian, 4

Valliappan
Manikandan, 96
Vandamme
Matthieu, 70
Vangla
Prashanth, 86
Vargas-Alzate
Yeudy Felipe, 104
Vaunat
Jean, 104
Vidal
Pablo, 100
Villanueva Zavala
Fernan, 88

Wang
Bowen, 52
Hao, 126
Wilson
Gordon Ward, 108

Xu
Shengzong, 110

Yang
Fu-Ling, 116
Yi
Zhiqiang, 76
Younes
Nabil, 122

Zambrano Narvaez
Gonzalo, 108
Zdravkovic
Lidija, 6
Zhang
Hui, 130

Xinran, 72
Zhao
Budi, 118, 130
Lianheng, 102
Zhou
Yubao, 90
Zürn
Jochen, 54